

**School of Molecular and Life Sciences**

**Investigating the impact of different organics on  
calcium oxalate crystallization in a synthetic urinary  
environment**

**Odin Bottrill**

**0000-0002-9172-0657**

**This thesis is presented for the Degree of**

**Masters of Research (Chemistry)**

**of**

**Curtin University**

**February 2021**

**School of Molecular and Life Sciences**

## Declaration

To the best of my knowledge and belief this thesis contains no material previously published by any other person except where due acknowledgment has been made.

This thesis contains no material which has been accepted for the award of any other degree or diploma in any university.

Signature: .....

Date: 11/02/2021

# Abstract

Kidney stones affect approximately 12% of the world's population. In the majority (60-80%) of cases these kidney stones are made primarily of calcium oxalate. In this research 16 additives are tested in a synthetic urinary medium using a variety of analysis methods to determine their impact on the growth and development of calcium oxalate crystals. The long-term goal of this study is to find treatments that inhibit the growth and development of kidney stones. This research builds on previous research by looking at new molecules for calcium oxalate growth. These new molecules are amino acid functionalised calix[4]arenes and are compared to their respective amino acids. This project involved the use of many instruments and methods including the analysis of the morphological changes and alterations to size as well as information on the likelihood of aggregation and the overall rate of nucleation. In addition, further investigation was undertaken on some additives to determine the method of interaction. This involved looking at the incorporation of the additive into the crystal, determining if adsorption occurred and measuring the impact the additive had on the growth rate of the crystal in the  $\langle 001 \rangle$  and  $\langle 010 \rangle$  directions. Interesting results were observed for some multiple carboxylic acid containing additives and the macromolecules. Tartaric acid and EDTA were found to be potent inhibitors producing significant changes to the morphology of crystals. The propyl resorcin[4]arene functionalised with aspartic acid significantly altered the potential for aggregation as well as stabilising calcium oxalate dihydrate. The propyl calix[4]arene functionalised with lysine showed a very interesting effect on the morphology and requires more research. There is much research to be done with the calixarene scaffold and this work begins to investigate the results from these large molecules.

## Abbreviations

CaOx	Calcium oxalate
COM	Calcium oxalate Monohydrate
COD	Calcium oxalate dihydrate
COT	Calcium oxalate trihydrate
FT-IR	Fourier transform infrared
NMR	Nuclear magnetic resonance
SEM	Scanning electron microscopy
CRM	Confocal Raman microscopy
AFM	Atomic force microscopy
CA	Citric acid
SUM	Synthetic urine medium
TA	Tartaric acid
EDTA	Ethylenediamine tetraacetic acid
MA	Maleic acid
LA	Lactic acid
SA	Succinic acid
ASA	Acetylsalicylic acid
Fru	Fructose
Gal	Galactose
Glu	Glucose
NaG	Sodium Gluconate
AA	Aspartic Acid
Lys	Lysine
Pro	Proline
PRAA	Propyl resourcin[4]arene functionalised with aspartic acid
PCLys	Propyl Calix[4]arene functionalised with lysine
CPro	Calix[4]arene functionalised with proline

# Table of Contents

1. Introduction .....	9
1.1.  Biom mineralisation and Kidney stones .....	9
1.1.1.  Stone formation mechanism.....	9
1.1.2.  Kidney stone risk factors.....	11
1.1.3.  Treatment options .....	12
1.1.4.  Economic burden .....	13
1.2.  Crystallization growth .....	13
1.2.1.  Crystallization process .....	13
1.2.2.  Particle growth .....	17
1.2.3.  Growth of stones .....	17
1.3.  Growth modifiers .....	18
1.3.1.  Growth modifier mechanism .....	18
1.3.2.  Growth modifier threshold inhibition .....	19
1.4.  Calcium oxalate .....	19
1.4.1.  Calcium oxalate hydrate forms .....	19
1.4.2.  Calcium oxalate morphology .....	20
1.5.  Inhibition mechanism and previous studies .....	22
1.5.1.  Method of inhibition .....	22
1.6.  Small molecule additives (<500 g/mol) .....	23
1.6.1.  Literature .....	23
1.7.  Macromolecules additives (>500 g/mol).....	24
1.7.2.  Literature .....	25
1.8.  Scope .....	26
2. Methods .....	27
2.1.  Preparation of SUM.....	27
2.2.  Analysis of nucleation rate and zeta potential.....	28

2.3.	Calcium oxalate morphology analysis .....	28
2.3.1.	Morphological tests .....	29
2.3.2.	Crystal size measurements .....	30
2.4.	Investigating the mode of additive interaction .....	30
2.4.1.	Additive adsorption onto COM.....	30
2.4.2.	The impact of additives on the crystal growth of COM .....	30
2.4.3.	Raman analysis of COM crystals.....	31
2.5.	Materials.....	33
3.	Results and discussion.....	35
3.1.	Complexation Constants of additives used .....	35
3.2.	Zinc ions in SUM .....	37
3.3.	Nucleation rate of COM.....	38
3.3.1.	Nucleation rate of Sugar Additives .....	38
3.3.2.	Nucleation rate in the presence of Single Carboxylic acid containing additives.....	40
3.3.3.	Impact of additives with multiple carboxylic acids on nucleation rate.....	42
3.3.4.	Nucleation rate of Macromolecular additives .....	46
3.4.	Crystal Morphology .....	48
3.4.1.	COM and COD morphology in SUM.....	48
3.4.2.	Impact of sugar additives on Morphology .....	50
3.4.3.	Impact of Single Carboxylic acid containing additives on Morphology .....	53
3.4.4.	Impact of Multiple Carboxylic acid containing additives on Morphology.....	56
3.4.5.	Impact of Macromolecular additives on Morphology .....	60
3.4.6.	Impact of additives on crystal size.....	65
3.5.	Aggregation potential .....	70
3.5.1.	Effect of sugar additives on zeta potential .....	71
3.5.2.	Effect of single carboxylic acid containing additives on zeta potential.....	71
3.5.3.	Effect of multiple carboxylic acid containing additives on zeta potential .....	73
3.5.4.	Effect of macromolecular additives on zeta potential.....	74

3.6.	Adsorption to the surface of COM.....	77
3.6.1.	Adsorption tests in SUM.....	77
3.6.2.	Adsorption tests in deionised water .....	78
3.7.	Incorporation to the crystal.....	80
3.8.	2D Nucleation and Growth analysis.....	82
4.	Synthesis Methods.....	85
5.	Overall conclusion and further work.....	88
5.1.	Sugars .....	88
5.2.	Single Carboxylic acid containing additives .....	89
5.3.	Multi-Carboxylic Acid containing Additives.....	89
5.4.	Macromolecular additives .....	91
5.5.	Further work .....	92
6.	References .....	94
7.	Appendix .....	99

# Acknowledgments

I would like to acknowledge my supervisor, Franca Jones, and her group for the guidance and suggestions associated with this project and the thesis. Without this assistance and encouragement, I would not have been able to produce this research. As well I would like to acknowledge Matthew Boon for his assistance and advice with the data processing for this thesis.

I would also like to acknowledge Laura Clayson for her assistance editing and improving my English and grammar throughout this thesis.

I would like to thank both Peter Chapman and Tom Becker for their assistance and training when using the instruments for the analysis in this research.

Finally, I would like to thank all the staff and research members at Curtin University for making the research space so welcoming and enjoyable. I would also like to thank my friends and family for supporting me through these years.

# 1. Introduction

## 1.1. Biomineralisation and Kidney stones

Biomineralisation is a fundamental process by which an organism forms inorganic minerals. The purpose of this is varied and can be for beneficial structures such as shells or skeletons as seen in various living organisms. Approximately 50% of all known biominerals are calcium based; and of those the most abundant calcium based biomineral is calcium carbonate. (1) Within the body the biomineralisation process is typically controlled by some chemicals in the environment. (2) There has been significant research into this control, although the specifics of this process is still relatively unknown. (3)

Unfortunately, biomineralisation isn't always a controlled process, with solids forming where they are not required. For example, many people suffer from a condition called urolithiasis; where inorganic minerals are formed in the bladder or urinary tract.

Kidney stones (calculi) are an example of urolithiasis. These mineral concretions can be found either free or attached to the renal papillae. The kidney stones formed typically consist of calcium oxalate in 60-70% of cases, with the remaining percentage being phosphate, uric acid, cysteine, magnesium, ammonia or drug induced stones. (4-8) For those unfortunate to have kidney stones they tend to struggle with constant abdominal pain, blood in the urine and internal damage from the stone(s). These symptoms can also have cascading effects, with the person having interrupted sleep and quality of life. (4)

It is estimated that this could affect between 4 and 15% of the world's population. Additionally, of those who form stones the likelihood of forming stones again after the initial stone increases by 31 to 50 % after 10 years. (9-13) Studies by hospitals (based on patient's medical records) show that there is an increase in the incidence of kidney stone disease and the recurrence of formation as well. (6, 14)

### 1.1.1. Stone formation mechanism

While kidney stones have been an ongoing issue for many centuries the full mechanism for their formation is still unknown. However, there are some processes which are confirmed to occur in the formation pathway of kidney stones. Figure 1 shows the overall series of events for stone formation.

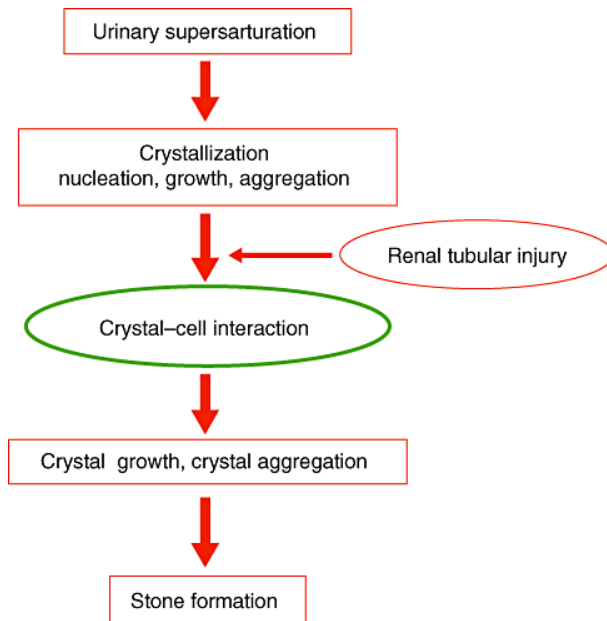


**Figure 1. Accepted major events for kidney stone development (6)**

Whilst there have been a number of hypotheses as to the initial mechanism of the growth and development of the stone forming solids, there are three prominent theories within published literature that are considered likely. These are:

- Heterogeneous nucleation/epitaxy theory (15, 16)
- Matrix theory (17)
- Inhibitor theory (18)

Heterogeneous nucleation refers to nucleation on a foreign substance/surface. Here, heterogeneous nucleation/epitaxy theory bases itself around the idea that urine naturally contains a number of pre-existing solids. In cases where the supersaturation within the urine is sufficient, the CaOx will crystallise over the existing solids. Epitaxy refers to the fact that this overgrowth often has some register with the underlying crystal structure. This theory has some limitations as it implies that urate solids should therefore cause kidney stones; however, in many cases this has not been identified. (19)

Matrix theory (17) is based on the hypothesis that organics within urine such as macromolecules take part in the crystal forming process, joining in what would otherwise be an inorganic matrix. This theory has some merit as analysis has shown that around 2.5% of the matrix of the mostly

inorganic urinary stones consists of organic material. This theory suggests that these macromolecules are responsible for the promotion of growth and aggregation of stones within the urine. Furthermore, the macromolecules exist in higher concentrations within the urine of people who form stones; however, the nature of the interactions between macromolecules and CaOx is unknown at this time.

Lastly, there is inhibitor theory. (18) Inhibitor theory proposes that in typical humans there is a chemical or chemicals present in urine that prevents the over-growth or aggregation of CaOx. It is believed, however, that stone formers have a lower concentration or absence of these chemicals; resulting in homogenous or heterogeneous nucleation that then leads to urolithiasis. It is also found that lower pH also results in some promotion. This theory appears to be possible due to the presence of inhibitory low and high molecular weight chemicals found within urine, however, there is still conflicting evidence for this theory, as noted in the above paragraphs.

### 1.1.2. Kidney stone risk factors

Kidney stone formation can be influenced by a range of conditions, from diet to ambient temperature. (20) Additionally, some pre-disposition to forming kidney stones is genetic (Figure 2). Treatment of the condition is therefore difficult as it has a large variety of risk factors.

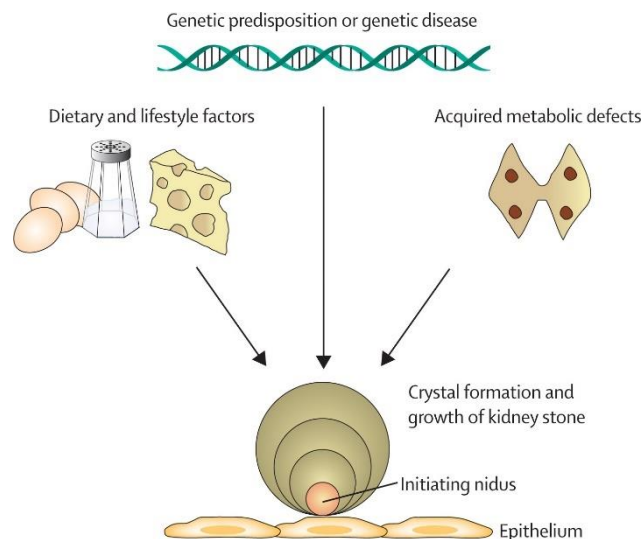


**Figure 2.** Associated risk factors that can cause a tendency of kidney stone formation (20)

One such factor is a monogenetic complication; causing an excessive urinary excretion of oxalate that can often result in the formation of calcium oxalate stones. This condition is called hyperoxaluria and is a result from gene mutation which makes proteins unable to process glyoxylate properly resulting in oxalate waste production. (21)

There have been a number of studies that relate obesity to increased formation of kidney stones, but the mechanism by which this would lead to kidney stones was not understood until a paper was published in 2018. (22, 23) This paper investigated the mechanism of the hyperoxaluria in obese mice. (24) The study found that a large percentage of the urinary oxalate concentration was introduced through consumption, but when under a controlled oxalate diet there was still significant evidence of oxalate in the urine. The reason for this was hypothesised as being due to the lowered transcellular intestinal oxalate secretion. (24)

Another condition which has been linked to the formation of stones is diabetes. The increased stone forming risk from diabetes comes from the increased acidity of the urine produced by affected people which specifically increases the risk of uric acid stones, and generally, for all kidney stones. (25)

One final factor shown to impact kidney stone development is increased temperature. (26) Scientists equate this increase to be due to the increased concentration of urine and sunlight exposure, which results in more vitamin D production. (26) This means hotter climates and hotter times of the year will increase the chance of developing kidney stones. As a result, some areas are being noted as the stone belt, which includes parts of America and Thailand (5, 27, 28)

### 1.1.3. Treatment options

Throughout the years there have been a variety of treatments for kidney stones, though many just involve the removal of stones; and removal can be difficult and high risk. This operation was considered of such high concern that Hippocrates made comment about leaving the removal of the stones to experts in his famous Oath of Medical Ethics. (29) While technology has significantly increased over time, there has been limited advancement in the treatment of kidney stones. There are currently three treatments for kidney stones: removal through surgery; passing the stone through the urethra; or shockwave lithotripsy.

Surgery was a mainstay for many years. This involves incision and physical removal of the stone. Whilst this technique has advanced significantly and now uses small tools and a camera to view and remove the stone, surgical options still result in a number of issues. Unless there is an immediate need for removal, non-surgical options are therefore preferred. (30)

One alternative method involves inserting a tube into the urethra to provide a removal pathway for the stone. However, urethral insertion causes significant discomfort.

Lastly, shockwave lithotripsy whereby a shockwave at the stone causes mechanical stress on the structure, causing fragmentation. Though this is the preferred treatment, research into chronic issues arise from this treatment as it causes renal damage. (30, 31) Additionally, due to the nature of the treatment it is not applicable to some patients. (30) This treatment also doesn't work with stones composed primarily of calcium oxalate monohydrate, the main component of most stones.

#### 1.1.4. Economic burden

Kidney stones not only effect patients physically, they are also a financial burden due to treatment costs.

In 2005, the American Urological Association published a paper which established that the costs of Urolithiasis are increasing based on data collected from 1990 to 2000. This study showed that in the year 2000 the costs associated with inpatient, outpatient, and emergency services, was \$2 billion US. (32) Since that publication the costs have increased; in 2014 the costs were up to \$3.79 billion US, due to increased population and the increasing proportion of people suffering obesity and diabetes. (33)

## 1.2. Crystallization growth

### 1.2.1. Crystallization process

Crystallisation is the process of depositing and forming a solid. In this project, aqueous crystallisation is of particular interest. Crystallisation begins with nucleation, where the solute undergoes a phase change from the aqueous phase to the solid.

There are two main types of primary nucleation; namely:

- Homogenous nucleation
- Heterogeneous nucleation

Homogenous nucleation is where a homogenous solution is supersaturated with certain ions and these ions then spontaneously nucleate into a solid. In contrast, heterogeneous nucleation is where some solid or surface (that is not the solute) exists, which allows the nucleation of the solid to occur. (34) Heterogeneous nucleation does still require the supersaturation of the

solution but the process will occur more readily than homogenous nucleation provided there is a favourable interaction between the solute and the surface. (35)

#### 1.2.1.1. Gibbs free energy

The first step of crystallization (and therefore stone formation) is the nucleation of a solid from a supersaturated liquid. This can be described by the relationships defined in classical nucleation theory. This theory was developed from the work of Josiah Willard Gibbs when he described the condensation of water droplets from vapour. (36) The theory was then expanded to encompass the nucleation of solids from liquids. To evoke the change from the bulk solution into the solid, the sum of the solution's free energy must be greater than the sum of the crystalline free energy. (36)

Equation 1.1 shows the method to calculate the change in Gibbs Free Energy of the phase change ( $\Delta G$ ). This value can then be used to determine if the phase change will occur spontaneously. When the solution is supersaturated sufficiently the nucleation reaction will be spontaneously driven.

$$\Delta G = G_b + G_i = -\frac{4\pi}{3}r^3\left(\frac{\Delta\mu}{\Omega}\right) + 4\pi r^2\alpha \quad \mathbf{E1.1}$$

Where:  $\Omega$  is volume per molecule

$\alpha$  is interfacial free energy

$\Delta\mu$  is the free energy of the phase change of molecules

$r$  is the radius of the product

$G_b$  is Gibbs bulk free energy

$G_i$  is interfacial free energy

It is noted that in supersaturated solutions: the higher the value of  $\Delta\mu$ , the greater the driving force of the phase change; and  $G_b$  and  $G_i$  will be of opposite signs. This is due to the interfacial free energy requiring energy to form the surface, making it positive. In contrast the lattice energy is negative and dominates the free energy for the bulk.

### 1.2.1.2. Supersaturation

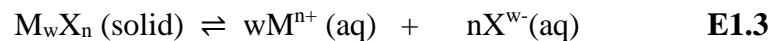
Equation 1.2 shows the relationship between the temperature, the ion activity product (IAP) and its influence on the free energy of the phase transition.

$$\Delta\mu = k_B T \ln(IAP) - \Delta G_{sol} = k_B T \ln\left(\frac{IAP}{K_{SP}}\right) \quad \mathbf{E1.2}$$

Where: IAP is ion activity  
K<sub>sp</sub> is the solubility constant  
k<sub>B</sub> is Boltzmann constant  
T is the temperature of the solution  
ΔG<sub>sol</sub> is Gibbs free energy of the solution

The solubility product is defined by the following equilibrium:

For an inorganic solid containing cation, M<sup>n+</sup> and anion, X<sup>w-</sup>



$$K_{sp} = a_M^w a_X^n \quad \mathbf{E1.4}$$

because  $a_{M_w X_n} = 1$  (a= activity)

The important aspect of this equation is the definition of supersaturation, given in Equation 1.5 with the IAP relating to the system's 'position' away from equilibrium. Using this definition, the solution is undersaturated if  $\sigma$  is less than 1 and when it is >1 the system is identified as supersaturated.

$$\sigma \equiv \ln\left(\frac{IAP}{K_{SP}}\right) \quad \mathbf{E1.5}$$

Where:  $\sigma$  is supersaturation  
IAP is the ion activity product  
K<sub>sp</sub> is the solubility constant

Equation 1.4 defines the homogenous nucleation rate (*J*) which is the nuclei formed per volume (m<sup>3</sup>) per second. As can be seen, there is a strong relationship between nucleation rate and the

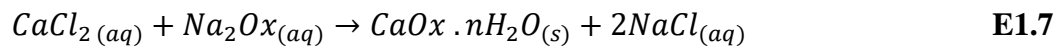
supersaturation and/or the interfacial free energy. The nucleation rate can be seen to increase with increasing supersaturation and decrease with increasing interfacial energy.

Lowering supersaturation leads to the lowering of the nucleation rate (Equation 1.6). The alteration of supersaturation within urine can occur through complexation with calcium and/or oxalate. (37) A lower supersaturation reduces the likelihood of subsequent nucleation and growth of CaOx. Adsorption of some species can also reduce nucleation rate without lowering the supersaturation. This is due to the increase in the interfacial free energy of the nuclei.

$$J = A \exp\left(\frac{-\Delta G_{ex}}{k_B T}\right), \quad \Delta G_{ex} = B \frac{\alpha^3}{\sigma^2} \quad \mathbf{E1.6}$$

Where: J is nucleation rate  
 $\Delta G_{ex}$  is excess free energy  
 $k_B$  is the Boltzmann constant  
T is the temperature of the solution  
B is a constant depending on the shape and density of the nucleating solid  
 $\alpha$  is interfacial free energy  
 $\sigma$  is supersaturation

In this research a solution will provide the ions necessary for crystallisation at a driving force that should result in nucleation. Solutions will be supersaturated by mixing two soluble salts; at which point nucleation will occur to form sparingly soluble CaOx crystals according to the following reaction: (34, 38)



Using Equation 1.5 and the literature value of the solubility of CaOx, the supersaturation of CaOx for the concentration used in this research, whilst in a pure water solution is calculated to be 18.2. (39). However, this value may change if chelation or complexation occurs. This change would not significantly alter the value to the point where the medium would be undersaturated.

### 1.2.2. Particle growth

On a microscopic level the growth of crystals is described by the incorporation of a *growth unit* on the two-dimensional existing surface of the crystal. The flat part of the surface is called the terrace. The raised portion is called a step and this step can have a kink on it, defined as the incomplete growth of the step. This kink is the main growth site as the solute molecule or growth unit will attach and fill that position creating a new kink for the process to repeat. (40) This growth is depicted in Figure 3. Growth at the kink site is the main growth mechanism (except at very low supersaturations) and can be followed and analysed *in-situ* by sensitive instruments such as an atomic force microscope (AFM).

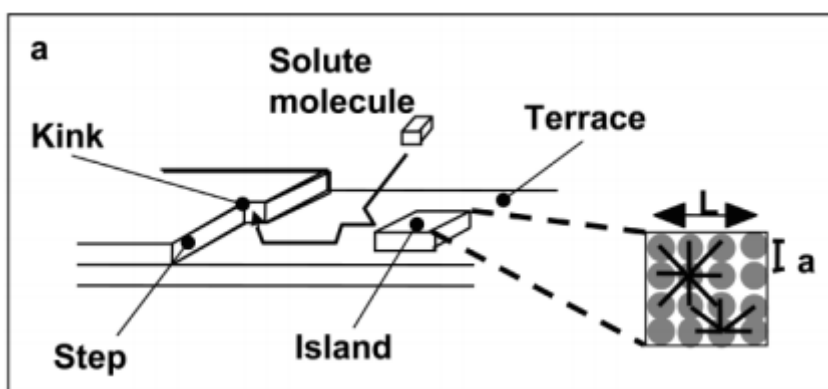


Figure 3. Depiction of growth on a crystal surface, showing the position of the kink, step and terrace (40)

### 1.2.3. Growth of stones

When supersaturation of calcium and oxalate ions has been reached in the kidneys the solid calcium oxalate may begin to form. In some scenarios there is exposed cell tissue from injury to the outer wall and this exposed area can result in a nucleation site for the initial formation.(6) Stones form on the cells of the damaged tube and this creates an “anchor” for the deposition of the stone over multiple urine secretions from the body. In turn, this allows this stone to continue forming until it is removed.

This anchored crystal also acts as a seed crystal making it more likely that further precipitation will occur in this area. Additionally, there may be aggregation of preformed solids onto the anchored crystal resulting in a further increase in size. (41) Aggregation is a mechanism where multiple pre-existing crystals bind with each other to form a larger crystal. When particles form in the urine they can be attracted to each other based on the charge around the surface of the

particle or they may be ‘cemented’ together by the supersaturation of the urine. This then can result in the formation of a larger stone overall.

It is believed that the charge around the solids (the zeta potential) may be affected by the organics present in the urine assisting in aggregation. (42, 43)

### 1.3. Growth modifiers

Growth modifiers of kidney stones can come in many different structures and functionalities, though to date the chemicals discovered all have similarities to oxalate. They all have one or more carboxylic acid groups. It was also noted multiple times that those chemicals with more carboxylic acid groups typically have the largest effect on the growth of the crystals.

#### 1.3.1. Growth modifier mechanism

Additives (or growth modifiers) can impact all stages of crystallization, even possibly leading to a stabilisation of a different hydrate or polymorph form. (44) Crystal growth modifiers can function in many ways. They can promote or prevent aggregation, growth, and/or nucleation. ‘Inhibitors’ inhibit these processes. Some inhibitors can constrain specific functions; one example is prevention of aggregation whilst not preventing nucleation. For all types of inhibition, the adsorption or binding of the organic onto the crystal nuclei or the crystal surface is an important step.

The presence of organics can also lead to chelation. This alters the supersaturation of the solution and may *appear* to be an inhibition effect. To invoke a change in the supersaturation there must be some sort of interaction between an ion and the organic. Possible ways in which this can be achieved are: (a) complexation between the calcium ion in solution with a ligand that then lowers the activity of the calcium ion in solution; or (b) complexation of the oxalate and a metal ion in solution lowering the oxalate activity in solution.

Adsorption of the organic impurity can change the surface chemistry or surface charge, possibly making the crystal more or less likely to aggregate. Adsorption can also result in the blocking of growth sites which will prevent or reduce the rate of the formation of solids onto the surface of the formed crystal; thereby altering the growth of the crystal. Substitution/incorporation of impurities into the crystal matrix can also occur, which impacts the solubility of the solid formed.

There have been a number of studies investigating the species that are naturally present in human urine. There are three main categories of inhibitors that have been explored, these are:

- Low molecular weight organics (45-47)
- High molecular weight organics (47-49)
- Metal ions. (37, 50)

### 1.3.2. Growth modifier threshold inhibition

A threshold inhibitor is able to inhibit crystallisation at very low concentrations; implying that supersaturation within the solution is not impacted.

Raistrick (1949) investigated the nucleation of calcium carbonate in the presence of phosphate and hypothesised that adsorption of the phosphate on calcium carbonate occurs in the early stages of nucleation, which in turn results in the stunted growth of crystals. This leads to sub-microscopic crystals. (51) Elliot (1970) took an alternative approach and theorised that the phosphate serves to increase the number of nucleation sites on the embryo crystals. (52) This results in the formation of multiple small crystals, as opposed to a smaller number of larger crystals.

More recent developments suggest that the additive doesn't need to adsorb to all faces of the crystal but in fact it is only required to adsorb onto the growth site of the crystal. (53, 54) This growth site is typically identified as the kink site.

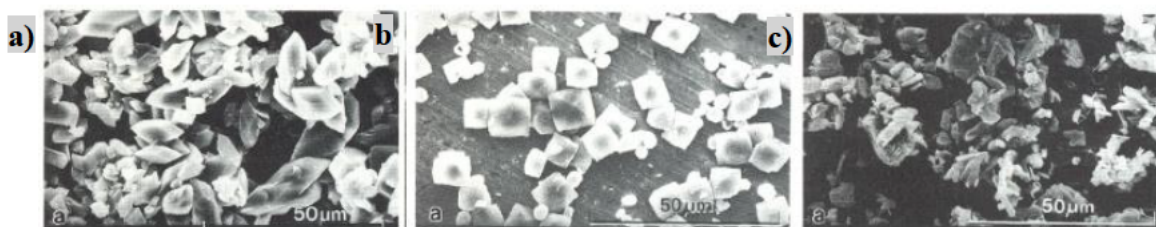
## 1.4. Calcium oxalate

### 1.4.1. Calcium oxalate hydrate forms

There are three hydrate forms of CaOx that have been found; these are:

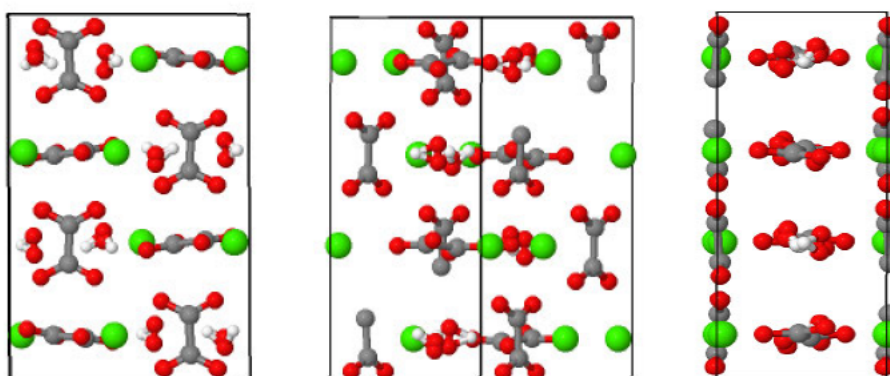
- Monohydrate (calcium oxalate monohydrate, or 'COM')
- Dihydrate (calcium oxalate dihydrate, or 'COD')
- Trihydrate calcium oxalate trihydrate, or 'COT')

Figure 4 shows these three forms. COT is metastable and will not form in standard urinary environments, thus is not typically found in kidney stones. (55) COD is the kinetically favoured form of the crystal and is more stable at lower temperatures, but at temperatures such as the standard human body temperature, COM it is more likely to form. As such, the COM is the most common form of CaOx found within stones.



**Figure 4.** *Different morphologies associated with the different hydrate crystals of CaOx*  
*a) COM, b) COD and c) COT (55)*

In the early stages of nucleation all three hydrate forms are present. Then due to stability COT and COD tend to redissolve into solution resulting in predominately COM observed after a period of time. (44) However, when there are specific chemicals present, such as the ones found in urine, there is the possibility that the COD is stabilised and remains. This may also be due to the organic molecule inhibiting the crystallization of COM, therefore increasing the amount of COD observed as it is still more stable than the COT form. (56) Figure 5 illustrates the unit cell of COM. (57)



**Figure 5.** *Unit cell of the monoclinic Calcium Oxalate Monohydrate (57)*

#### 1.4.2. Calcium oxalate morphology

The morphology of the two common hydrates (COM and COD) are quite dissimilar, with the ideal crystals of COM appearing as hexagonal prisms (Figure 6) and the COD taking a bipyramidal shape (Figure 7). (35, 58) Unlike the COD, the non-twinned COM crystals are not symmetrical. As such, it is important to note that some of the monohydrate crystals will grow on their side and will provide a different appearance under a microscope though no chemical change is happening.

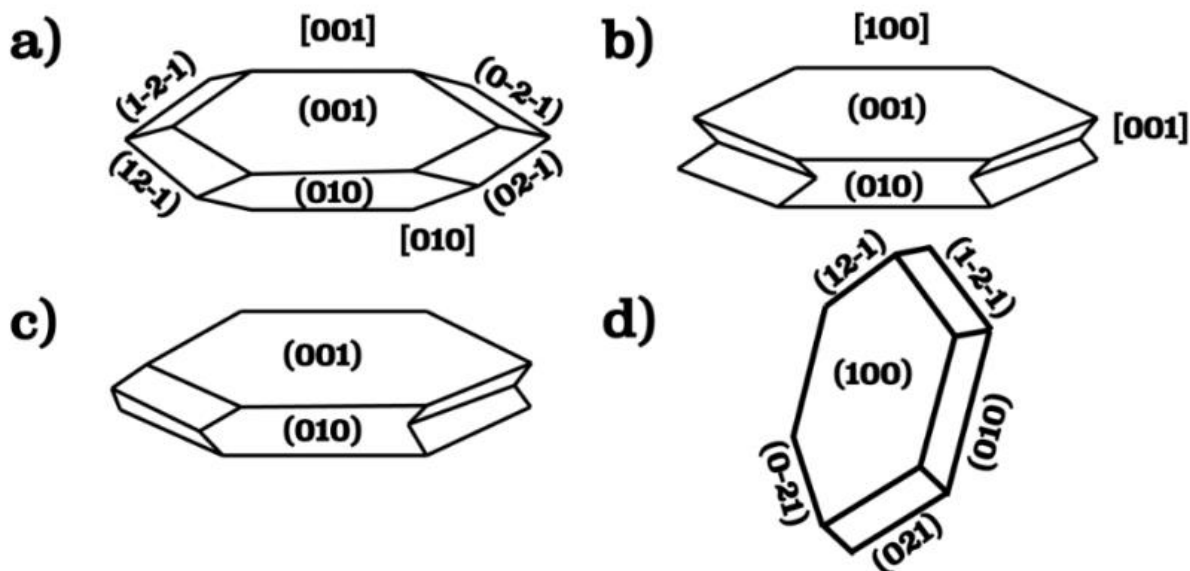


Figure 6. COM morphology a) single crystal (59) b) contact twin c) penetration twin (60) d) expected morphology in the presence of citric acid (61) (Depictions by Matthew Boon)

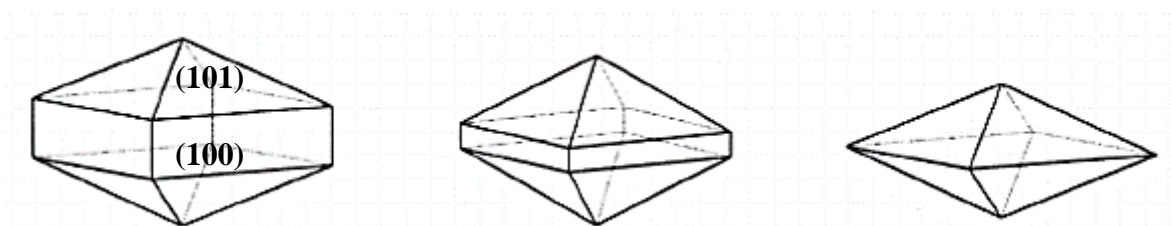
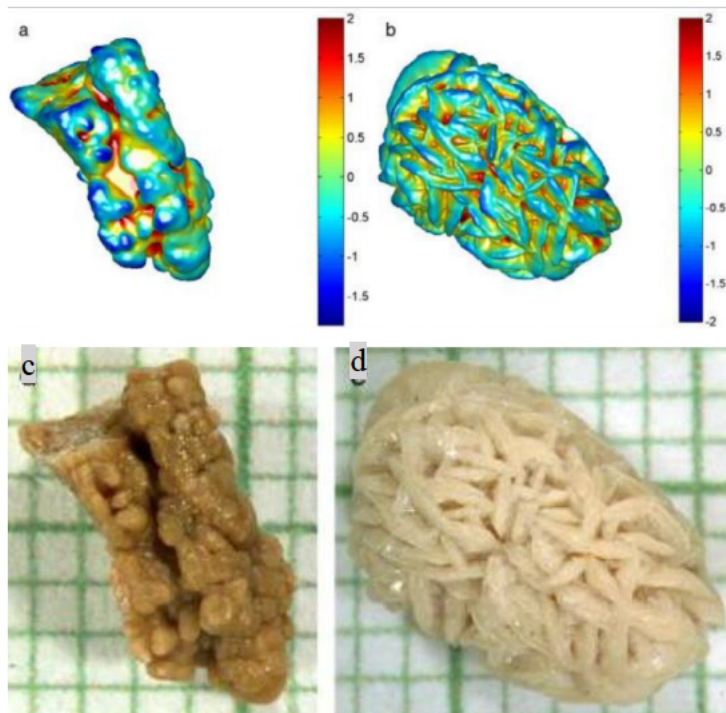


Figure 7: Variation in COD shape from the elongation of the (100) face(62)

Differentiation can sometimes be achieved by examining the morphology through visual inspection. However, in many cases, the morphology may be significantly different than what is expected (particularly when additives are present). An example of this difficulty can be seen in Figure 8. The morphology of these samples does not give any indication of the hydrate form. Both types of crystals (COM and COD) can be found in kidney stones and so it is important to differentiate between the two. In these instances, Raman Spectroscopy can be used to differentiate between them as there is an indicative doublet around  $1500\text{ cm}^{-1}$  that can confirm the COM form.



*Figure 8. Images of a COM and COD kidney stone: a) & c) COM stones, and b) & d) COD stones (63)*

## 1.5. Inhibition mechanism and previous studies

### 1.5.1. Method of inhibition

There are multiple mechanisms by which additives can inhibit the formation of kidney stones, as there are multiple steps involved in the production of these stones (Figure 1). Firstly, any chemical that reduces the supersaturation of calcium and oxalate in solution, either by chelating or in some way preventing the interaction between these ions is one impact. (64)

Further, chemicals which prevent the aggregation will significantly impact the overall ability for stone production as stones can pass through the body without forming larger particles. (65, 66) This is due to the particles forming and then attaching to each other which results in the overall stone shape similar to that in Figure 8. If the surface is surrounded in a chemical (making the surface no longer preferable for nucleation), the average size of the stones will be lowered, allowing relatively painless passing and removal of the stones. In the case of chemicals which inhibit the overall shape and size of the crystal, the typical method is to adsorb to the surface of the crystal resulting in a change of appearance. This binding can be face-specific changing the dominant face by slowing down the growth of a specific face.

## 1.6. Small molecule additives (<500 g/mol)

Many small molecules have been investigated in literature. This study will investigate some new chemicals as well as revisiting some that have previously been investigated in less complex media. The small molecules used in this research are broadly separated into three groups: sugars; chemicals containing one carboxylic acid functional group; and chemicals containing more than one carboxylic acid functional group and macromolecules.

### 1.6.1. Literature

A growing number of published research studies show that having increased vitamin D intake may increase the urinary calcium concentration, though the exact mechanism isn't known. (67) Though many studies show that in realistic concentrations there is no statistical increase in kidney stone formation. (68, 69)

One study (in pH-adjusted water), found that asparagine and TA significantly inhibited the size of COM. The research also found that zinc ions inhibited the nucleation rate and posited that this was likely through competitive chelation with the oxalate ions present. MA was also assessed in this study and showed some nucleation rate inhibition but no significant effect on the morphology or size.

In another study zinc ions were found to inhibit the nucleation (generating smaller particle sizes), while increasing the aggregation of these particles. (70) Addition of TA was found to inhibit the nucleation of the crystals formed, resulting in fewer particles as well as a mild increase in the surface charge and slight decrease in the particles' aspect ratio. (71) Addition of MA was noted to have mild inhibitory properties but reduced the magnitude of the surface charge making aggregation more likely. (71)

It has been shown in some studies that EDTA inhibits the production of COM and the mechanism of this inhibition was investigated. This research found that the inhibition was likely though an adsorption mechanism, (72) though EDTA is also a well-known chelator and the chelating effect is most likely to result in inhibition. There was also another study into the effect of other chelating agents such as a pyrophosphates, which also had a significant impact in the activity of calcium ions in solution. (64)

## 1.7. Macromolecules additives (>500 g/mol)

Large molecule inhibitors are defined for the purpose of this project as molecules that have greater than 500 g/mol total molecular weight. There has been research into larger molecules as inhibitors such as proteins, macrocycles, organic polymers and other compounds. (46, 73)

### 1.7.1.1. Calixarenes

Calixarenes (Figure 9) and other cyclophanes have been useful in a large number of fields since their discovery in 1979 by Gutsche. (74)

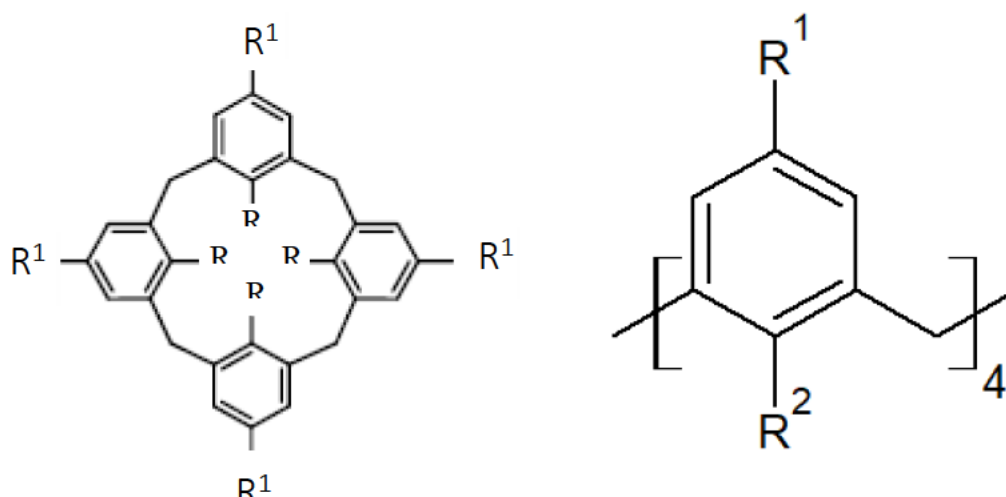


*Figure 9. Alternative depictions of calix[4]arene full depiction shown (left) and the simplified illustration (right)*

Following from this initial discovery alternative structures of similar compounds were also made, with the functionalised components being on different parts of the ring (Figure 10). This compound was named a calix[n]resorcinarene or simply a resorcinarene. This also allowed a lipophilic chain to be added on the bond between the benzene rings and allows even further control of the final molecular solubility. Additionally, the compound can be functionalised symmetrically or asymmetrically increasing even further its flexibility of being functionalised.

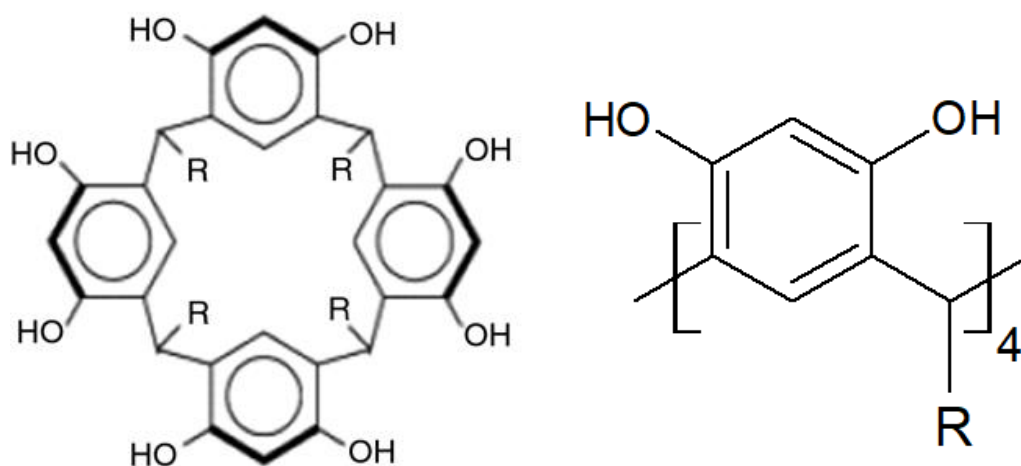


*Figure 10. Alternative depictions of calix[4]resorcinarene full depiction shown (left) and the simplified illustration (right)*

Medicine is one of the key areas for which calixarenes are researched. The theory is that by having more sites to functionalise, the chemical can have a stronger activity relationship with the target. (75) In addition, by editing the R groups the solubility and reactivity can also be edited making this base structure very versatile. There has been some research into amino acids being functionalised onto the calixarenes and their impact on the crystallisation of other chemicals. (76)

### 1.7.2. Literature

In a morphological study it was found that asymmetrical resorcinarenes functionalised with aspartic acid with varying carbon chain lengths (C3, C7, C11) significantly altered the morphology of CaOx. (76) However, this work was performed in pure water. From this it was found that the C3 carbon chain resulted in an inhibition to the growth of the (010) face. There was also a large number of needle-like aggregates present at higher concentrations. When a longer chain was present (C7 or C11) there was a noticeable roughening of the surface (76) with the greatest effect being the C3 functionless aspartic acid resorcinarene, likely due to the increase in water solubility and higher concentration achievable of the compound in solution.

There is also contradictory information where in some cases proteins have been seen to promote growth for subjects, (77) whilst other studies have identified that the same protein can inhibit growth of stones. (78)

Other research synthesised two amino acid functionalised calix[4]arenes, one with proline and another with aspartic acid. (79) This work looked at the impact of those molecules on calcium carbonate where they showed significant impact on the crystal's morphology. Since this impact

was recorded against another calcium containing compounds, it is theorised that this would relate to an impact on CaOx too.

Peptides have also been investigated, leading to some notable impacts from amino acids chained into larger molecules. This has shown that some specific peptides and proteins have either a negative or positive effect on the production of calcium oxalate. The polymerised Tamm-Horsfall protein has a promotion effect, (73) while the unpolymerized version has been observed to inhibit the production of calcium oxalate. (80) Though, there does appear to be a blind spot where there is no comparison to the amino acids themselves.

## 1.8. Scope

The first stage of this research is analysis of molecules that have been previously been investigated in water and study them within the more complex synthetic urinary medium. From these results, other additives are chosen or synthesised based on notable signs of inhibition or interesting structural chemistry. These molecules were subjected to analysis for their effect on morphology, nucleation rate and zeta potential. In addition, investigation into the mechanism of interaction was attempted by looking at whether adsorption, incorporation and complexation were occurring. Ultimately, this project is searching for prospective additives to inhibit or prevent kidney stones as well as further investigating the growth and development of kidney stones.

Due to the onset of the COVID-19 global pandemic the synthesis component of this research was impacted, resulting in fewer synthetic molecules being obtained than initially planned. As a result, some chemicals of similar functionality and base structure from other researchers were utilized for analysis.

## 2. Methods

### 2.1. Preparation of SUM

One litre of urinary medium stock solution was prepared at 10 times the desired concentration (Table 1). This solution is used to mimic standard urine properties in humans such as the pH. The SUM also has some species such as sodium chloride, at similar levels to human urine, which also results in a similar ionic strength to urine. Potassium phosphate monobasic stock solution was stored separately to avoid phosphate precipitation. Sodium azide (1% w/w) was added to the medium to prevent bacteria from growing. The final solution was adjusted to a pH of 6.5 with hydrochloric acid.

Sodium azide is a dangerous chemical that is highly toxic; refer to the material safety data sheet before use. Appropriate personal protective equipment should be worn at all times, including gloves when handling sodium azide.

Stock solutions of calcium chloride and sodium oxalate were made using deionised water (0.1 M concentrations).

**Table 1.** *Synthetic urinary medium stock solution (81)*

Species	Concentration (mM)
Sodium Citrate	3.21
Sodium Chloride	105.5
Potassium Chloride	63.7
Ammonium Chloride	27.6
Magnesium Sulfate	3.95
Potassium Phosphate monohydrate	3.23

Zinc ions are also a well-known inhibitor and are also present in urine. As such the interaction of zinc ions with SUM was tested by adding zinc chloride. The SUM with zinc ions is also a more physiologically comparable SUM. This also allowed the assessment of the interaction that

additives would have with ions such as zinc should they also be present in urine. The zinc chloride solution stock solution (0.1M) was kept separate from the SUM solutions and was added into the medium such that the final concentration was 1 mM, which is within the normal ranges for human urine. (82)

## 2.2. Analysis of nucleation rate and zeta potential

The determination of particle counts versus time through dynamic light scattering was used to assess the impact of additives on the nucleation rate. Similarly, the propensity of particles to aggregate was inferred by way of the magnitude of the measured zeta potential.

A 19.6 mL SUM solution was prepared by combining filtered deionised water and the urinary medium (2 mL), followed by potassium phosphate (2 mL, 32.3 mM), the zinc chloride (if required) and/or additive stock (depending on the test) solution. Sodium oxalate (0.4 mL, 0.1 M) was then added in a Teflon beaker and stirred constantly.

An aliquot of the solution (approximately 2 mL) was placed in a disposable cell and analysed using the Zetasizer Nano-ZS (Malvern) at 25 °C. Measurements were recorded using a DPSS laser with an excitation wavelength 633 nm. The standard operating procedure was set with an integration time of 10 seconds, taking 10 measurements. After the baseline analysis of the solution, stoichiometric calcium chloride was added, and analysis was undertaken every 5 minutes. The aliquot of the solution that was removed for these analyses was then returned to the solution. This was then repeated until 20 minutes had passed (where nucleation was typically observed to peak). For each analysis the time and the derived counts (in kilocounts per second, kcps) were recorded

Finally, 25 minutes after the addition of the calcium chloride three subsequent zeta potential measurements (in the same instrument) were taken from the same experiment. These tests use a using a folded capillary cell, containing ~1 mL, which undergoes a maximum of 100 subsequent tests which would end after concordant results were measured. The above sequence was repeated in triplicate and the values were averaged to provide a final measurement for each additive. This methodology was utilised for various additives and concentrations.

## 2.3. Calcium oxalate morphology analysis

### 2.3.1. Morphological tests

A 20 mL solution was prepared by using deionised water, 2 mL of the SUM stock solution and 2 mL of phosphate monobasic stock solution. Sodium oxalate solution 0.4 mL, 0.1 M was then added. A clean glass disk of 0.5 cm radius was added to the vial to allow for analysis of the solids formed. The additives (Table 1) for each test were then added, as required. Additives were tested at concentrations of 20, 10 and 1 mM. Water was added to make the final volume 20 mL. The mixture in the vial was left for 15 to 20 minutes until the temperature equilibrated to 37 °C before adding 0.4 mL, 0.1 M of calcium chloride to commence the crystallization process. This solution was left for 18 to 24 hours after which the glass disk was collected, washed gently with deionised water, and dried.

In the cases where zinc ions were added to the medium, zinc chloride was present at a 1 mM concentration in the SUM for all tests and added prior to the calcium chloride addition. This concentration was chosen as it is within the normal concentration range for human urine. (48) When zinc ions were present the concentrations for the additives investigated were 10, 5 and 1 mM. As per the above method, the mixture in the vial was left for 15 to 20 minutes until the temperature equilibrated to 37 °C before adding 0.4 mL, 0.1 M of calcium chloride to commence the crystallization process. This solution was left for 18 to 24 hours after which the glass disk was collected, washed gently with deionised water, and dried.

The recovered glass disks were then analysed using the Bruker supplied WITec alpha 300SAR to view the morphology of the crystals formed and determine if they are significantly different from the standard. In addition, the WITec alpha 300SAR was used to determine the hydrate form through the Raman spectrum. The Raman functionality utilises a frequency-doubled NdYAG laser of wavelength 532 nm (green) of 50 mW power with silicon being used as the reference material.

After observing the effects of the additives on the crystals using the optical microscope and Raman spectroscopy, a selection of glass disks were chosen for additional analysis. Those selected showed noticeable interaction and/or inhibition.

The disks were placed on carbon coated scanning electron microscope (SEM) stubs and carbon paint was applied to the circumference to avoid charging effects. The SEM stubs were sputtered with Platinum with a thickness of 2 to 20 nm and analysed with Neon focused ion beam – scanning electron microscope operating at 15 keV with a secondary electron detector. The SEM was operated by Dr Franca Jones or Matthew Boon.

### 2.3.2. Crystal size measurements

The particles on the glass disk were analysed by optical microscopy and images were taken to measure the area of COM crystals. Measurements were only undertaken in cases where the whole face was unobscured by other crystals. For all of the crystals meeting this criterium, regardless of size, a minimum of 60 crystals from each optical image were measured giving the area and the aspect ratio (length/width) with 10 % error. This was processed using ImageJ.

## 2.4. Investigating the mode of additive interaction

Results from the morphology of crystals and particle nucleation rates were used to select a subset of additives to examine the mechanism by which they affected the crystallisation process.

### 2.4.1. Additive adsorption onto COM

Adsorption onto the COM surface was investigated by the following procedure. The additive was at 0.1 M in 25 mL of the SUM, and COM (AR grade, 50 mg) was added. The solids were acquired from the solution by vacuum filtration, gently washed with deionised water and dried using vacuum filtration before being analysed with FTIR (4 cm<sup>-1</sup> resolution, Nicolet iS50 FTIR fitted with a dedicated single-bounce diamond ATR) and Raman spectroscopy (WITec alpha 300SAR, using both depth and single spectrum analysis with 100 accumulations and 0.250 s integration time). These spectra were subtracted from the baseline control (i.e. the CaOx in the urinary medium without additives) using analysis software. The presence of infrared or Raman bands that were assignable to the organic after this procedure implies that the organic has adsorbed onto the surface of the solid (COM in this instance).

### 2.4.2. The impact of additives on the crystal growth of COM

When the additive was found to have significant impact on the COM crystal nucleation rate, this additive was then tested for how it impacted the growth. Other additives were chosen based on their capability to alter the crystal's development assessed in the previous morphology tests. Atomic force microscopy (AFM) allows a crystal surface to be monitored *in-situ* in solution and so this method was used to monitor the impact of organics on COM growth on the basal face in the <001> and <010> directions. The Bruker Dimension FastScan® is built on a separate concrete slab to the rest of the building to reduce vibrations. The room is also sound proofed and has double doors to further prevent noise from being produced due to outside sources.



**Figure 11.** *In situ AFM set up, with the liquid pumping in on the right and out on the left*

The solutions were designed to have the calcium present in the SUM and oxalate to be present with the phosphate to allow for long term storage. The calcium and oxalate were present in solution at 1.2 mM so when introduced and mixed these would be present at 0.6 mM when in contact with the crystal and cantilever. The solutions were filtered through PALL® Life Sciences 0.2 µm Acrodisc syringe filter prior to combining with a T-junction. Initially, slightly acidic water was added to clean and remove the top few layers of the particles. The solutions were then mixed at a ratio of 1:1 with using a KDS 200 Legacy Syringe Pump. Solutions were pumped at 0.5 mL/min into a Teflon tray where there was a puck glued down with carbon paint with the glass slide on top, as shown in the above figure. The excess solution was removed using a peristaltic pump which was constantly pumping during the tests.

The images were processed using Gwyddion by measuring the width of etch pits that were isolated. (83) This was then used to measure the width change over time, and this was then used to determine the growth rate.

#### 2.4.3. Raman analysis of COM crystals

The organic molecules tested may adsorb onto the COM surface or they may be incorporated into the crystal. The Raman spectroscopic instrument (WITec alpha 300SAR) is able to be focussed at different heights and this allowed investigation of the where the additive is located with respect to the COM.

Analysis of the surface of the crystal was undertaken using single spectrum analysis with 100 accumulations at 0.1 second integration. In addition, the entire particle was analysed by focusing the laser at different depths, whereby line scans were undertaken resulting in a map of

signals across the z and y axis (Figure 12). From this the internal signals of the crystal can be observed to ascertain differences between the external and internal spectra.

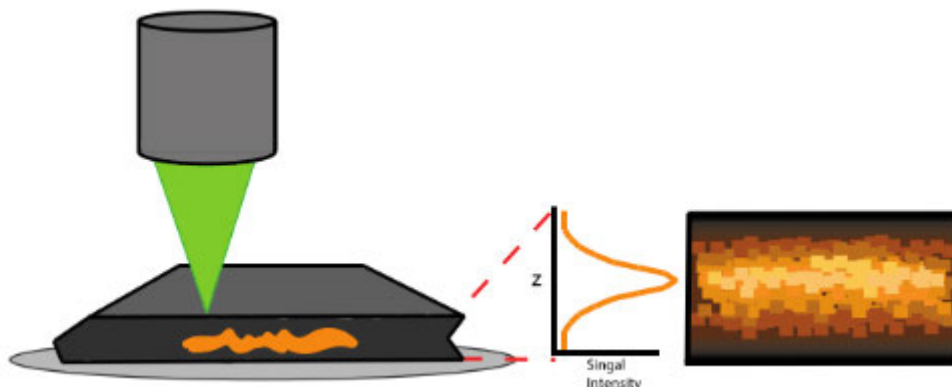
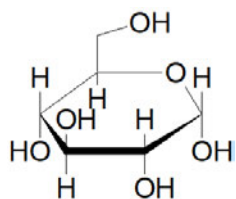


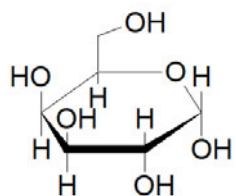
*Figure 12. The laser of the Raman scans down and across the crystal giving a map of intensity through the crystal. (84)*

## 2.5. Materials



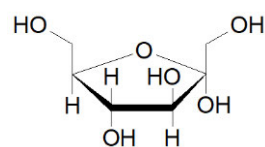
D- Glucose (Glu)

Supplied by Ajax  
Chemicals  
Purity >99%



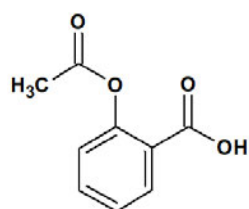
D-Galactose (Gal)

Supplied by Ajax  
Chemicals  
Purity >99%



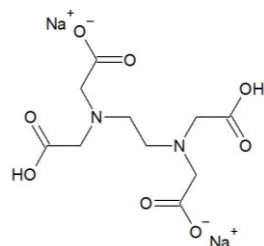
D-Fructose (Fru)

Supplied by Fluka  
Biochemika  
Purity >98%



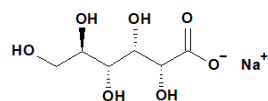
Acetyl Salicylic Acid  
(ASA)

Supplied by Scharlau  
Purity >99.5%



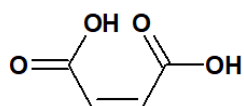
Disodium ethyl diamine  
tetra acetic acid (EDTA)

Supplied by APS  
Chemicals  
Purity >99%



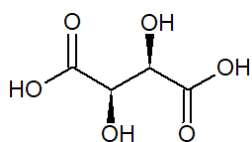
Sodium Gluconate (NaG)

Supplied by GPR  
Chemicals  
Purity >99%



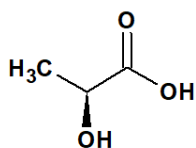
Maleic acid (MA)

Supplied by Sigma  
Aldrich  
Purity > 99%



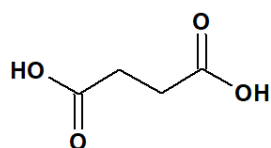
(+)-Tartaric acid (TA)

Supplied by Ajax  
Chemicals  
Purity >99%



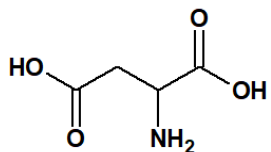
Lactic acid (LA)

Supplied by BDH  
Chemicals  
Purity >98%



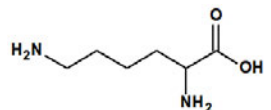
Succinic acid (SA)

Supplied by Ajax  
Chemicals  
Purity >98%



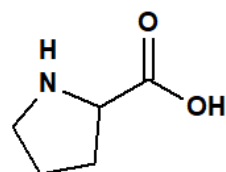
Aspartic acid (AA)

Supplied by Acros  
Organics  
Purity >98%



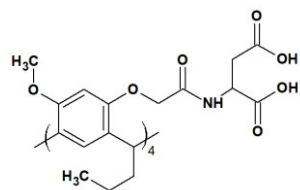
Lysine (Lys)

Supplied by BDH  
Biochemical  
Purity >98%



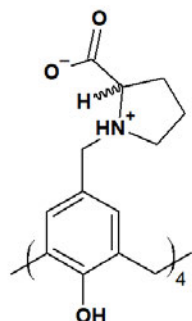
Proline (Pro)

Supplied by Sigma  
Aldrich  
Purity >99%



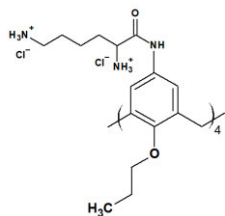
Aspartic acid  
functionalised propyl  
resorcin[4]arene (PRAA)

Synthesised by Odin  
Bottrill  
Method in Section 4  
Purity by NMR (>95%)



Proline functionalised  
calix[4]arene (CPro)

Synthesised by Ching  
Yong Goh  
Purity by NMR (>95%)



Lysine functionalised  
propyl calix[4]arene  
(PCLys)

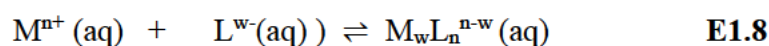
Synthesised by Caitlin  
Duncan  
Purity by NMR (>95%)

## 3. Results and discussion

### 3.1. Complexation Constants of additives used

The general relationship for the complexation between a metal and an ion can be given by a series (since more than one ligand or ion can complex) of the following reactions:

For a metal cation,  $M^{n+}$  and ligand,  $L^{w-}$



$$K_{\text{complexation}} = [M_wL_n]^{n-w} / [M^{n+}]^n [X^{w-}]^w \quad \text{E1.9}$$

As mentioned in section 1.1.3, one possible method the organic additive can inhibit is the through chelation, so through the use of the Murdoch JESS database (85), the theoretical complexation constants were obtained. This can give an insight to the possible interactions of these chemicals with and without the presence of the zinc ions in the solution. To obtain this the ionic strength is calculated which allows the accounting of some of the influence of the SUM.

*Table 2. Complexation constants of calcium ions with additives or relevant organics from the SUM acquired from JESS database (value in parenthesis is ligand charge)*

Metal	Ligand	Complexation Constant (log K)
<b>Calcium ion</b>	ASA (-1)	4.14
	EDTA (-4)	10.0
	NaG (-1)	1.17
	LA (-1)	1.34
	MA (-2)	1.38
	SA (-2)	1.03
	TA (-2)	1.74
	CA (-3)	3.13
	Ox (-2)	2.32
	Phosphate (-3)	4.92

In Table 2 the interaction of the calcium with the additives is presented. This will then allow the comparison between the interactions that the calcium ion will have with the other organics compared to the interaction with oxalate and citric acid. From this it can be seen that the citric acid has a higher complexation constant than the oxalate ion for calcium ions, which likely results in the interaction with the COM that is observed in literature. (37) Other chemicals of note are ASA and EDTA which both present a significantly higher tendency to complex with the calcium ions than oxalate. This means that it is highly likely for these molecules that any *inhibition* that is observed will be due to the decrease in calcium ion activity. It is also of interest to note the high value for the phosphate, though this is present at low concentration in comparison to the oxalate. This suggests some of the phosphate will interact with calcium ions preferentially to the oxalate, but this will not likely be noticeable.

**Table 3.** Complexation constants of zinc ions with additives or relevant organics from the SUM acquired from JESS database (value in parenthesis is ligand charge)

Metal	Ligand	Complexation Constant (log K)
<b>Zinc ion</b>	ASA (-1)	7.30
	EDTA (-4)	15.8
	NaG (-1)	1.65
	LA (-1)	1.75
	MA (-2)	1.99
	SA (-2)	1.58
	TA (-2)	2.52
	CA (-3)	4.61
	Ox (-2)	3.86
	Phosphate (-3)	2.01

Overall, the complexation constants of the additives were observed to be higher with zinc ions than calcium ions. This means that interaction with zinc ions will likely occur preferentially, especially in cases where the complexation constant with zinc ions is much higher. For those where the complexation constants are not so different there should be minimal competition between the two ions.

### 3.2. Zinc ions in SUM

Throughout the project there were a few instances where a gel like precipitate formed in solution. This included concentrations of zinc exceeding 1 mM as well as ASA tests above 5 mM. The Raman spectrum (Figure 12) attempted to identify one of these precipitates (zinc ions in SUM). This spectrum is distinctly different from that of the standard reference CaOx spectra (appendix figure 2), missing the characteristic doublet peak at approximately 1500  $\text{cm}^{-1}$ . In place of the doublet there is a triplet-like peak at approximately 1000  $\text{cm}^{-1}$ . This is similar to that of the  $\text{PO}_4^{3-}$  stretching peak recorded from phosphates such as hopeite ( $\text{Zn}_3(\text{PO}_4)_2 \cdot 4\text{H}_2\text{O}$ ) (86). As phosphate is present in SUM at 3.23 mM, it is possible that this is the compound that is being formed. The complexation constant for zinc and phosphate is listed in Table 3, showing a strong relationship between the two. Phosphate solids are known to generally have low solubility and so a zinc phosphate solid is highly possible. In addition, the precipitation reaction may be taking some of the calcium ions into its matrix.

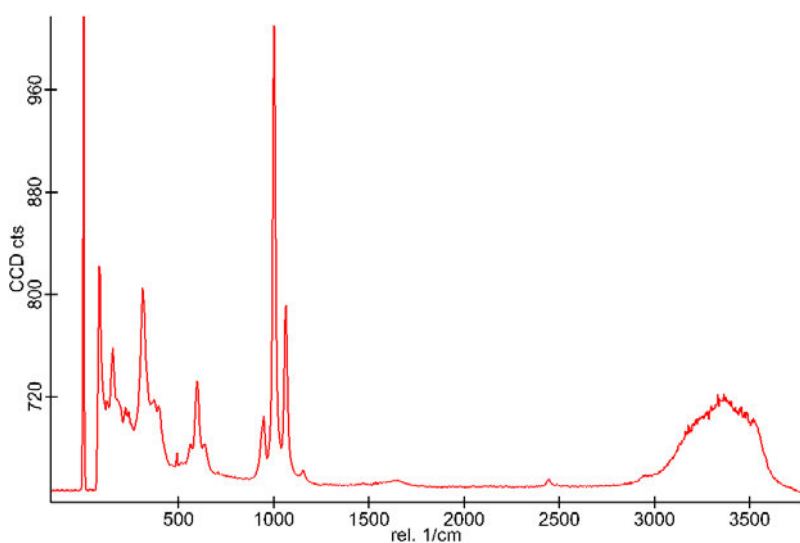


Figure 13. Raman spectrum of unknown gel-like compound from high concentration zinc ions in SUM

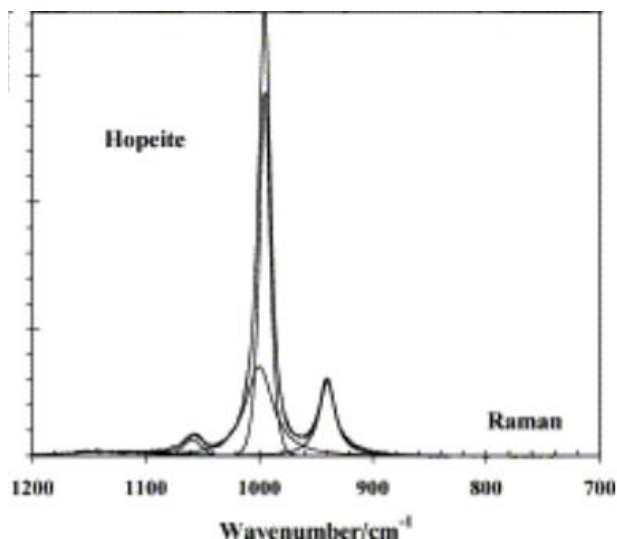


Figure 14. Literature reference Raman spectrum for Hopeite (86)

### 3.3. Nucleation rate of COM

The DLS was used to determine the particle counts (in kilocounts per second, kcps) versus time under different conditions. The counts can be used to infer the nucleation rate behaviour of the system over time. If the system is homogeneously nucleating, the counts will start low and then increase quickly. If processes such as aggregation or settling are absent the particle counts will be stable (assuming a single nucleation event). Particle count information from DLS, however, does have a high variability as shown by the tolerance bars in the following figures. As such, only significant differences in particle counts (outside the tolerance bars) are used to confirm whether a compound/molecule is a promoter or an inhibitor. In each graph there is the standard (std) (where nucleation of CaOx is in SUM) and when zinc ions (Zn) are present in the SUM to compare to. Any data that is significantly above the particle counts (~1000 kpc) can be indicated as a nucleation promoter, conversely any with a signal significantly below that of the standard will be denoted as an inhibitor of nucleation.

#### 3.3.1. Nucleation rate of Sugar Additives

##### 3.3.1.1. Effect of sugar additives in pure SUM

Observing the impact of sugars on the nucleation rate of CaOx (Figure 15) it can be seen that both galactose and fructose result in a significant increase in particles formed at the end of the 20 minute period. The presence of glucose appears to have little impact as the results are approximately that of the standard, with the deviation overlapping often with the values of the test with SUM.

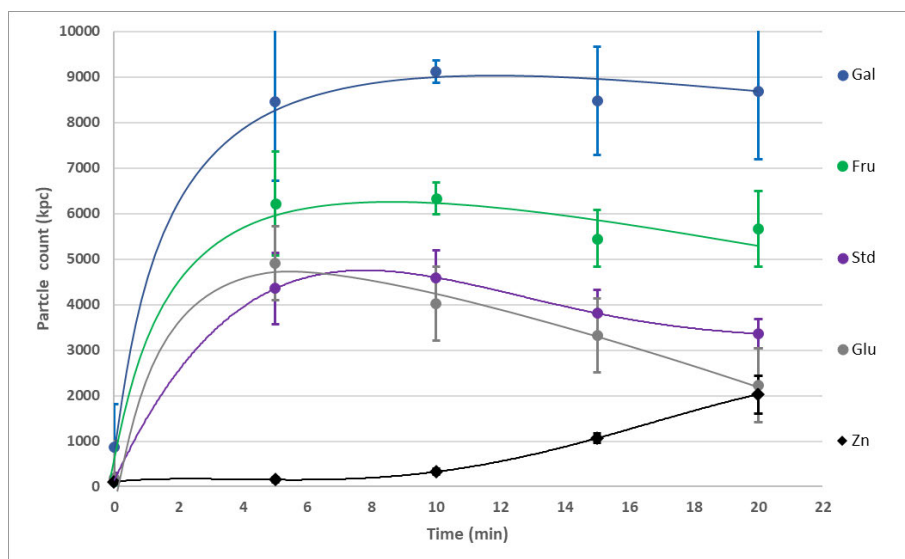


Figure 15. Impact of sugars additives on nucleation rate of CaOx in SUM

The promotion effect of Gal and Fru may be due to an interaction occurring with the other inhibitors present in the SUM, such as citric acid. One possibility is that this may happen through a reaction, or perhaps an intermolecular interaction that prevents the interaction of CA from inhibiting the formation of a nuclei. (87) Alternatively, the additives could be acting to lower the activation energy barrier, resulting in the catalysis of the nucleation reaction. (88, 89) A common activation energy barrier in crystallisation is the dehydration of the cation. Therefore, these molecules may bind weakly to calcium ions and aid de-watering, lowering this activation energy barrier.

As for Glu there is very little difference between this and the overall standard as the errors overlap it can be seen that there is no noticeable promotion or inhibition from Glu in SUM.

### 3.3.1.2. Effect of sugar additives in SUM with zinc ions present

Figure 16 shows the effect that these sugars have with zinc ions present in the SUM. Here it can be seen that galactose still has a significant promotion effect in the number of particles formed in the solution. Though the overall trend of the graph is different, the data continues rising without having a noticeable decrease in the count as the analysis continued. In comparison to SUM+Zn<sup>2+</sup> the Gal is a significant promoter while Fru is only a moderate promoter. Glu achieves final particle numbers similar to SUM+Zn<sup>2+</sup> and is considered neither a promoter or inhibitor.

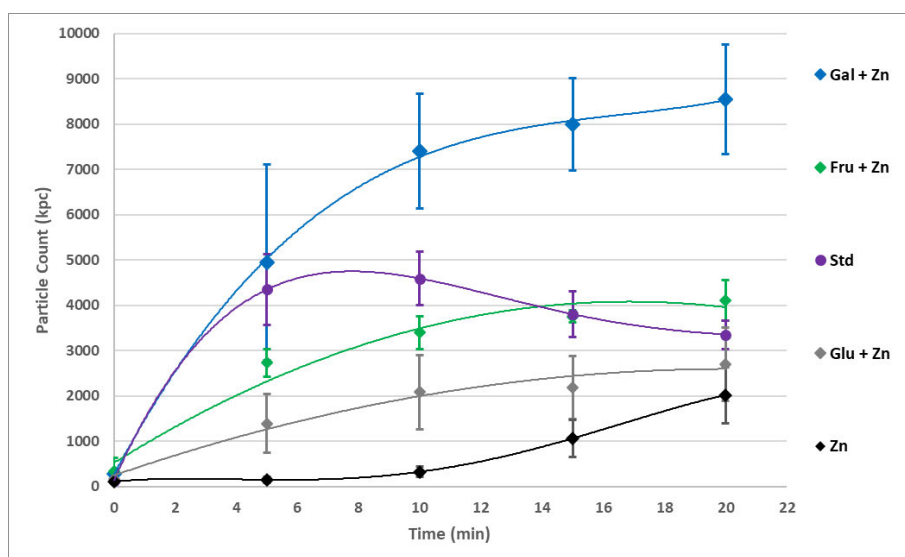


**Figure 16.** *Impact of sugars additives on nucleation rate of CaOx in SUM with zinc ions present*

Gal's interaction with CaOx is not known, while the Fischer projection has an aldehyde that may interact more strongly with the metal ion. Sugars may also exist in the Haworth projection where all the oxygens would have two different bonds to them. There has been some research into the complexation of Ca ions with sugars, but it is unlikely that the sugars will complex in a situation with so many species present that have higher likelihood of complexation. (90) There has been research into the interaction between zinc ions and sugar absorption though there has been no established connection at this time. (91) However, based on these results and the promotion in nucleation when zinc ions and Gal are present, it would appear that the zinc ions are interacting with galactose molecules in some unknown way(s).

For Fru and Glu the effects are largely similar to that recorded without zinc ions present. Thus, the impact of zinc ions in the presence of these sugars is negligible.

### 3.3.2. Nucleation rate in the presence of Single Carboxylic acid containing additives

#### 3.3.2.1. Effect of single carboxylic acid additives in pure SUM

Figure 17 shows the effect of single carboxylic acid containing additives on the nucleation rate of particles. It can generally be seen that these chemicals are nucleation promoters of CaOx. This is likely to be due to an impact on the interfacial free energy because there is no significant formation of complexes expected with these molecules, as the constants (Table 2) are significantly lower than that of oxalate and even citric acid in the solution.

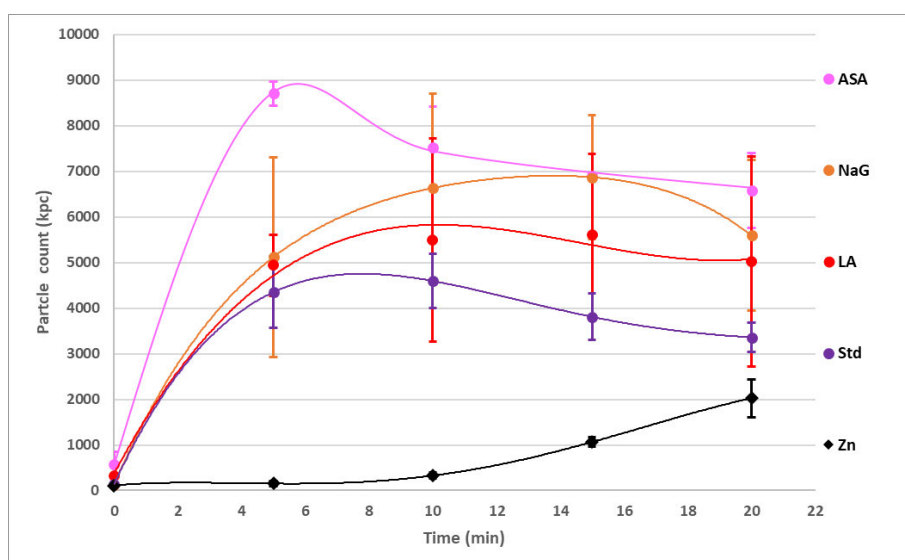
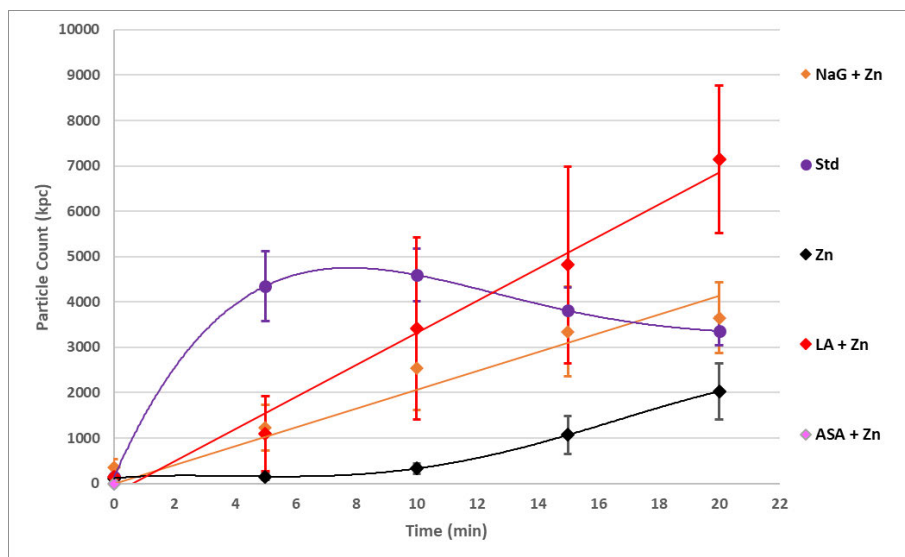
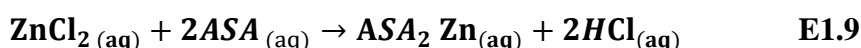


Figure 17. Impact of additives containing a single carboxylic acid on nucleation rate of CaOx in SUM

ASA has a significant impact on the overall nucleation rate, initially having a major production of crystals, that then sediment or aggregate despite ASA having a higher complexation constant to calcium ions than that of oxalate. This suggests that either some  $\text{Ca}(\text{ASA})_2$  precipitate is being produced in the early stages before formation of COM or there is an effect on interfacial free energy. The other organics appear to have a mild promotion effect on nucleation. The LA is very close to the standard when taking into account the standard deviation. NaG has a mild promotion effect in comparison to the other additives.

### 3.3.2.2. Effect of single carboxylic acid containing additives in SUM with zinc ions present

Figure 18 shows the impact of the single carboxylic acid additives on nucleation rate when the zinc ions are present in the SUM. Results for ASA were omitted from the following figure due to the precipitate that was formed from that solution. This precipitate was likely zinc salicylate, due to its complexation constant (Table 2, E1.9) but also means that it has exceeded the solubility of zinc salicylate in SUM.



**Figure 18.** Impact of additives containing a single carboxylic acid on nucleation rate of  $\text{CaOx}$  in SUM with zinc ions present

Whilst zinc ions are present the presence of LA resulted in particle counts noticeably higher after 20 minutes than SUM or  $\text{SUM} + \text{Zn}^{2+}$ . Additionally, LA and NaG have a very different trend to the standard but similar to the zinc ions in SUM albeit at higher particle counts. They

seem to have a linear relationship over time which could be related to the same trend as the zinc ions. Despite this, the NaG and La still have a higher nucleation rate than zinc ions in SUM; which is similar to these additives in SUM alone (in that they promote nucleation). This suggests that these additives are not impacted on by the presence of zinc ions. Another interesting thing of note is that nucleation seems to increase continuously, meaning that these additives may promote over a longer period of time given the linear trend.

### 3.3.3. Impact of additives with multiple carboxylic acids on nucleation rate

#### 3.3.3.1. Effect of multiple carboxylic acid containing additives in pure SUM

The impact on the nucleation behaviour in SUM by additives having multiple carboxylic acids is shown below in figure 19.

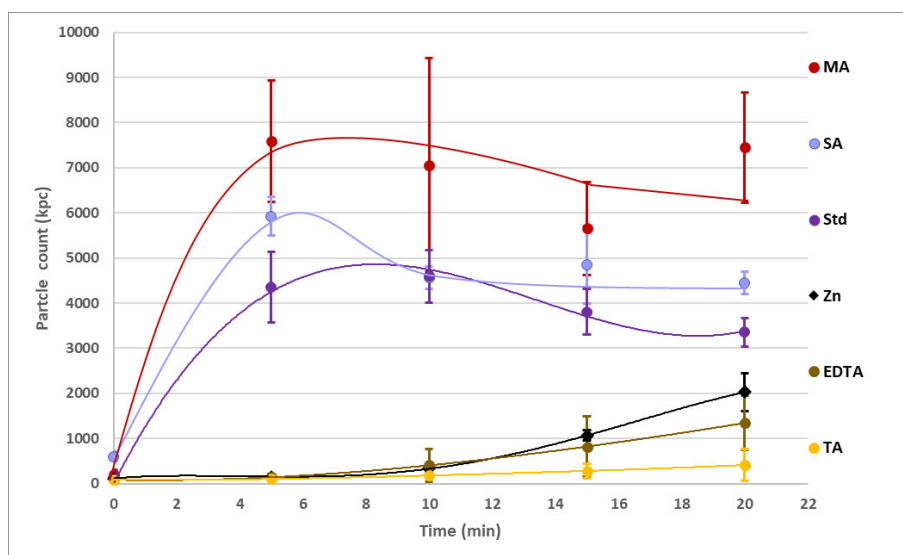


**Figure 19.** *Impact of additives containing multiple carboxylic acid on nucleation rate of CaOx in SUM*

TA, MA and SA share similar structures with each being a 4 carbon, dicarboxylic acid, and yet the differences in the compounds' behaviour is quite profound. While TA is the most potent inhibitor in this system even when compared to zinc ions, the other two are both promoters. This suggests that the two additional alcohol groups in TA are important, whereas the rigidity of MA results in promotion. SA shows only mild promotion compared to MA.

The inhibition mechanism of TA appears to be different to EDTA. TA has a lower complexation constant than that of oxalate with calcium ions (Table 2). This suggests the impact of TA is not to change the activity of calcium ions. Instead, adsorption is likely the mechanism of inhibition for this additive and/or an increase in interfacial free energy. An increase in interfacial free

energy of the particle would make nucleation less likely to be spontaneous. This would involve the adsorption of TA to the surface of nuclei.

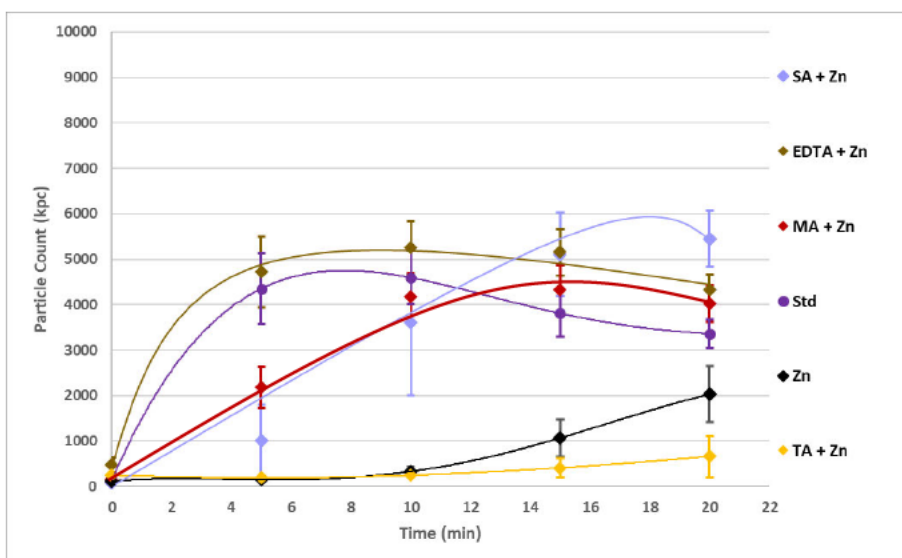
EDTA was significantly better as an inhibitor than the others in Figure 19, that is because the plotted data for EDTA is at 20 times less than the concentration of TA, as higher concentrations resulted in complete inhibition of crystallization. The mechanism for this inhibition is likely to be due to the chelation reaction between the EDTA and the Ca ion. This reaction follows E1.10 and forms a soluble compound at the end resulting in lower calcium ion activity. The strong complexation relationship is also shown in table 2 by the large complexation constant.



### 3.3.3.2. Effect of multiple carboxylic acid containing additives in SUM with zinc ions present

Figure 20 shows the impact the presence of zinc ions has on the overall nucleation rate of COM when multiple carboxylic acid containing additives are present as well. It can be seen that overall, the promoters have become less potent, this is likely due to the zinc ions and the additives interacting with each other. As the additive and zinc ions are now interacting with each other there is now less present to inhibit CaOx.

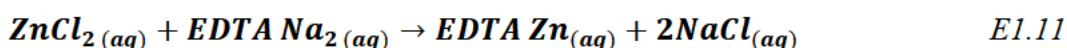
There is a significant change with the MA when zinc ions are present. Where before the MA is a significant promoter, it is now approximately equivalent to the behaviour of the standard, but it peaks at approximately 15 minutes instead of between 5 and 10 minutes. This change to the trend may be a positive interaction, as the slower rate may result in the stones forming slower overall. However, the presence of MA in SUM+Zn<sup>2+</sup> has a higher particle count than SUM+Zn<sup>2+</sup> alone. This suggests that MA is still a nucleation promoter in this case. Though now, the SA is promoting to an even greater extent than in SUM alone (where it was not as potent a promoter as MA).



**Figure 20.** *Impact of additives containing multiple carboxylic acid on nucleation rate of CaOx in SUM with the presence of zinc*

Very interesting is that the TA is not impacted significantly by the presence of the zinc ions. This means that the interaction that the TA has with COM is completely independent and is significantly preferred over the zinc ion interaction. Which is interesting considering the expected effect from the complexation constant. The fact that this is not impacted by zinc ions gives a lot of promise to TA being applied as an inhibitor for the formation of calcium oxalate particles in the urine.

Figure 21 shows the marked difference in nucleation rate of COM between EDTA in SUM and EDTA with zinc ions in SUM. In this situation the zinc ions and the EDTA were both present at concentrations of 1 mM. It is hypothesised that the nucleation rate is perhaps returning to the standard rate because the zinc ions in the solution forms a soluble complex with the EDTA; effectively removing the EDTA and the zinc ions from impacting the nucleation process and allowing the nucleation rate to revert to that seen in the standard solution. The zinc ions and EDTA are very likely to form a complex (Table 3) as the complexation constant is significantly higher for the reaction between zinc ions and EDTA than with calcium ions (Table 2).



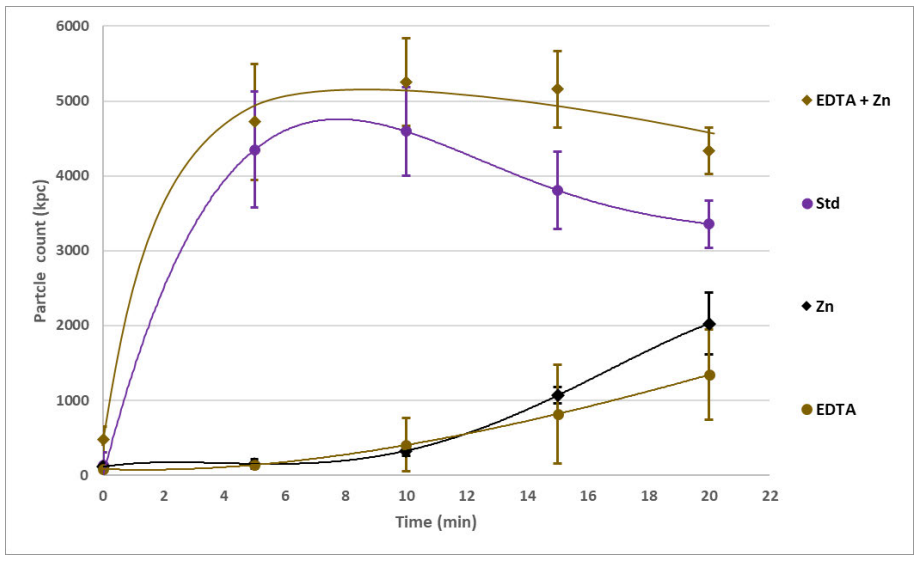


**Figure 21.** Comparison between the particle counts from nucleation with EDTA additive in pure SUM and SUM with zinc

### 3.3.4. Nucleation rate of Macromolecular additives

#### 3.3.4.1. Effect of macrocyclic additives in pure SUM

Figure 22 shows the trends of the macrocycles functionalised with amino acids Pro and AA at 1 mM. This graph also shows the amino acids at a comparative four times the concentration (4 mM) as the macrocycles contain four of the amino acids in their structure.

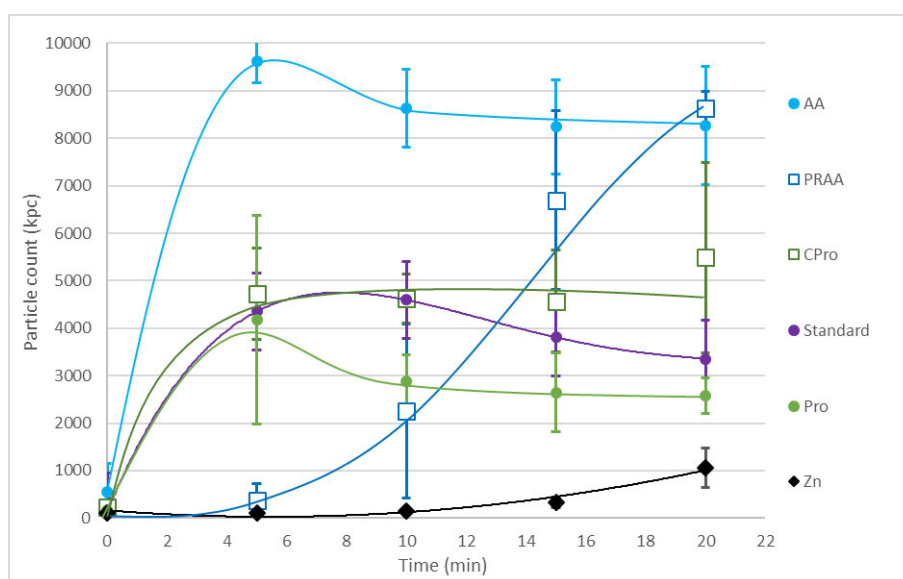


**Figure 22.** *Impact of additives containing multiple carboxylic acid on nucleation rate of CaOx in SUM*

When comparing the overall trend of when AA and macrocycle PRAA is present in the SUM there is a very slow increase in particle counts when PRAA is present but eventually reaches the same particle counts as when AA is in solution. This could mean that the macrocycle somehow slows down the interaction or in some way prevents the early interaction but ultimately effects the formation of CaOx in a similar fashion to AA. Overall, these both promote significantly above the standard.

In contrast when considering the macromolecule CPro and the amino acid Pro, both are at approximately the same particle count as the standard. The resulting effect of the additive on nucleation is very mild if present at all; with the Pro perhaps being a mild inhibitor compared to the standard. This suggests that the rigid Pro held in place on the macrocycle cannot interact in the same way as when Pro is in solution.

### 3.3.4.2. Effect of macromolecular additives in SUM with zinc ions present

When zinc ions were added to the system the general trend is that the total particle counts in figure 23 is lower than that in SUM.

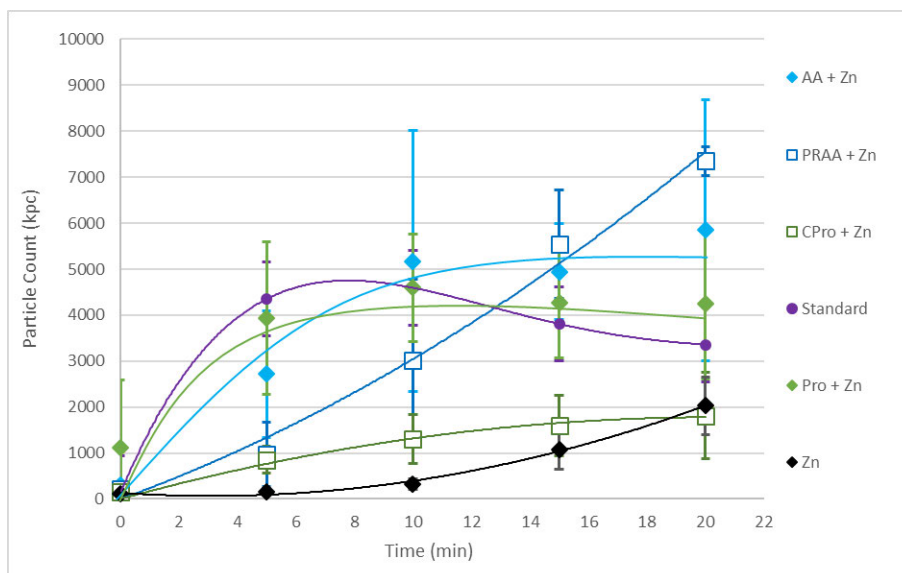


**Figure 23.** *Impact of additives containing multiple carboxylic acid on nucleation rate of CaOx in SUM with the presence of zinc ions*

Comparing the effect of AA to that of PRAA when zinc ions are also present it appears that both again are promoters (when comparing to  $\text{SUM}+\text{Zn}^{2+}$ ). However, the final particle counts are higher by a larger amount for PRAA when zinc ions are present. The presence of PRAA still seems to be slowing down the nucleation of CaOx as it doesn't reach the peak of 9000 kpc until 20 min. Similarly with the other amino acid, the Pro shows nucleation promotion while there is very minimal change to the particle count for from CPro compared to  $\text{SUM}+\text{Zn}^{2+}$ .

Overall, it seems that the effect of zinc ions is minimal with the macrocycles. This is interesting as the increase of the coordination sites should theoretically increase any interaction with a metal ion, but the result is the opposite as the interaction with zinc ions is much stronger with the free amino acids. This could mean that the interaction is hindered if stereochemical constraints are introduced (such as making the amino acids more rigid by attaching them to a macrocyclic scaffold). When the amino acids are tethered to a macrocycle the nitrogen may not be able to interact in the same way.

### 3.4. Crystal Morphology

#### 3.4.1. COM and COD morphology in SUM

Figure 24 depicts the COM and COD expected morphology with labelled faces. Figure 25 shows the experimentally obtained COM and COD crystals in the presence of the SUM.

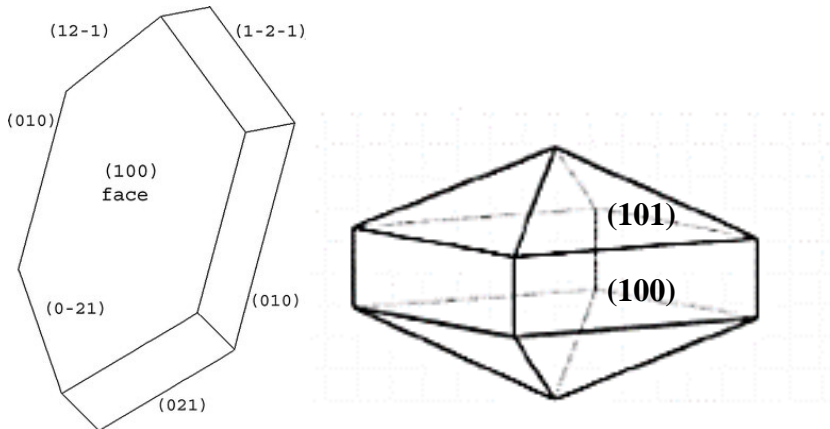


**Figure 24.** Drawn depictions of COM (left) (61) and COD (right) (62)

It can be seen that in the COM the SUM has a rounded appearance with the faces being less defined. This rounding is especially notable on the (0-21) faces. The key differences between the observed and expected morphology are that the corners have become rounded and the (010) face has become less prominent. This gives the crystal a more circular appearance than that created in pure water. This inhibition is due to the presence of citrate, which is a well-known morphological inhibitor of CaOx. (92)

The morphology of crystals grown using the various compounds are then compared to the morphology of these control crystals. By comparing the differences, one can determine what faces are present within the crystal, and how the organic has affected its growth. For example, if an inhibitor binds to a specific face, there should be a notable change in the morphology whereby that face is expressed.

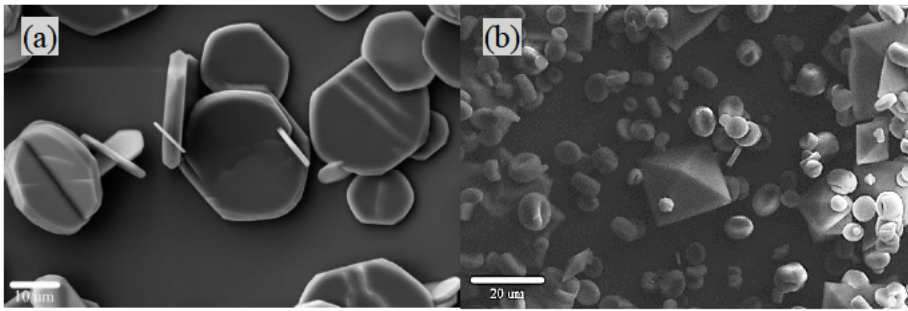


**Figure 25.** SEM micrographs of (a) Calcium oxalate Monohydrate and (b) Calcium Oxalate Dihydrate obtained in SUM

COD is less stable in physiological conditions thus, there was no formation at the standard temperature investigated (37 °C). So, to get an image of the COD in SUM, the temperature was significantly decreased (4 °C). As can be seen, the COD formed had a bipyramidal shape and the (100) face was not present. This means that the (101) face is growing so slowly it becomes the most visibly dominate face in the crystal.

### 3.4.2. Impact of sugar additives on Morphology

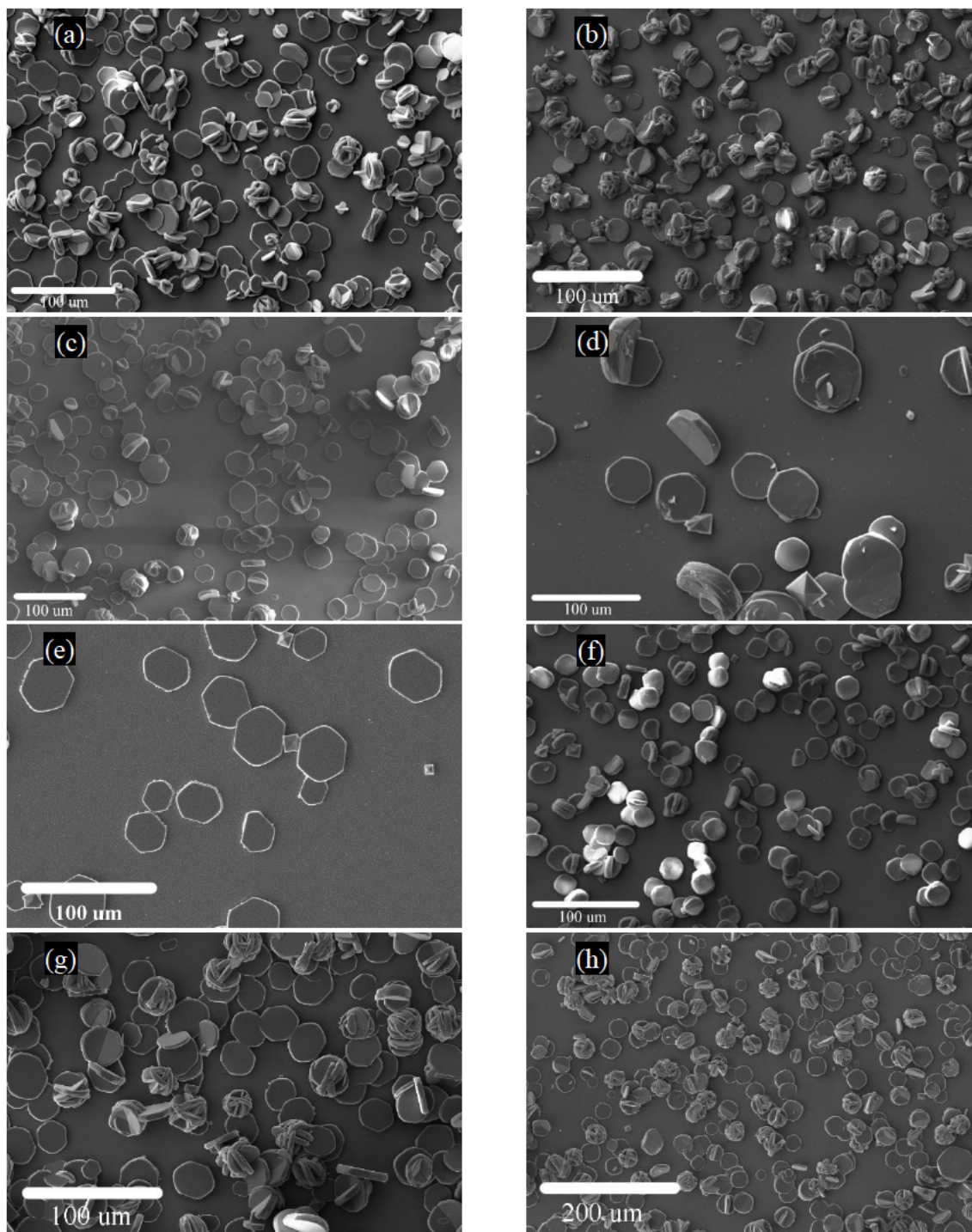


**Figure 26.** *CaOx morphology impacted by sugar additives; (a) pure SUM, (b) SUM+Zn<sup>2+</sup>, (c) Galactose (20 mM), (d) Galactose (10 mM)+Zn<sup>2+</sup>, (e) Fructose (20 mM), (f) fructose (10 mM)+Zn<sup>2+</sup>, (g) Glucose (20 mM), (h) glucose (10 mM)+Zn<sup>2+</sup>*

### 3.4.2.1. Galactose

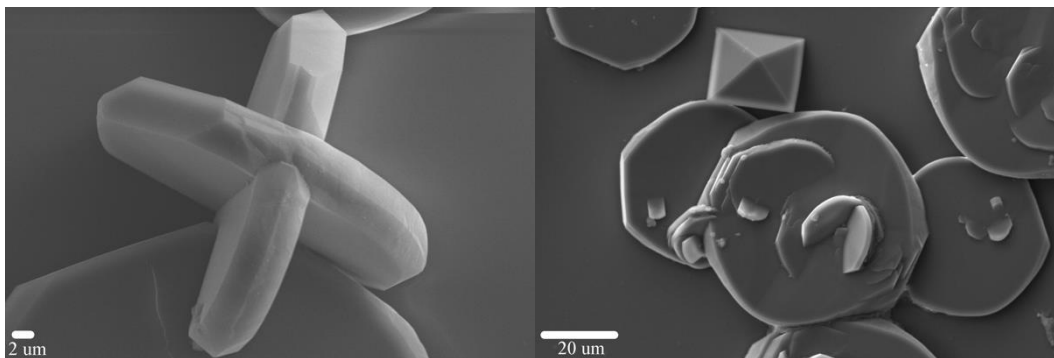


**Figure 27.** *CaOx morphology impacted by Galactose (20 mM) (left), Galactose (10 mM)+Zn<sup>2+</sup> (right)*

Overall, galactose did not greatly impact the crystal shape. Although there is a small impact as the crystal has a greater width, implying there is some slowing of the (021) and related faces making it more dominant. Also, the particles appear to be growing within other crystals with or without the presence of zinc ions. Something to note is that the presence of the sugar appears to make it more likely for crystals to grow inside of other crystals and in addition there appears to be the stabilisation of COD such that some COD particles are still observed when the galactose is present.

### 3.4.2.2. Fructose

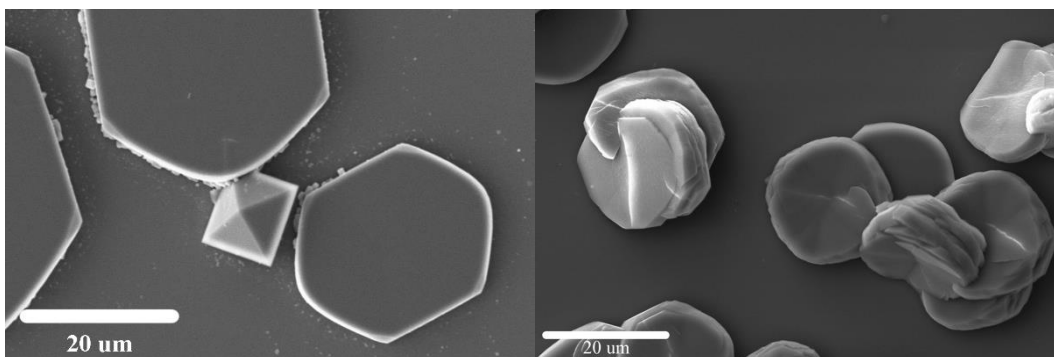


**Figure 28.** *CaOx morphology impacted by Fructose (20 mM) (left), Fructose (10 mM)+Zn<sup>2+</sup> (right)*

In the SUM the impact of Fru on the morphology of COM is minimal, the particles are very similar to the COM in SUM with a larger (010) face. However, of interest is the formation of the COD particles.

When Fru is present in the SUM+Zn<sup>2+</sup> the crystals seem to have a layering effect that appears to have some crystals growing on top of the already formed crystals. Additionally, the (010) face is barely noticeable so the (021) faces are more dominant in comparison. With the addition of the zinc ions to the medium, Fru becomes much more rounded and appear much smaller.

### 3.4.2.3. Glucose

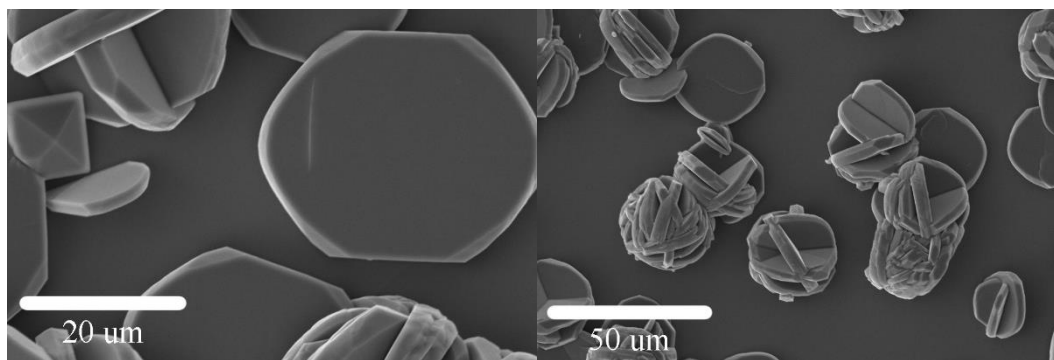


**Figure 29.** *CaOx morphology impacted by Glucose (20 mM) (left), Glucose (10 mM)+Zn<sup>2+</sup> (right)*

In figure 29 it can be seen that the crystals formed in the presence of Glu in SUM are very similar to that of the particles formed in SUM, this suggests there is little interaction between Glu and COM especially those involving the binding and slowing of face growth. Though, what can be seen is the presence of some COD again implying some connection between the sugar additives and the presence of the COD. Also, again, it is observed that crystals are growing inside the other crystals during the formation, resulting in many crystals that nearly form completely spherical crystals. It appears that the trends of the formation of crystals in others is greatly amplified when the zinc ions are also present in the SUM.

### 3.4.3. Impact of Single Carboxylic acid containing additives on Morphology

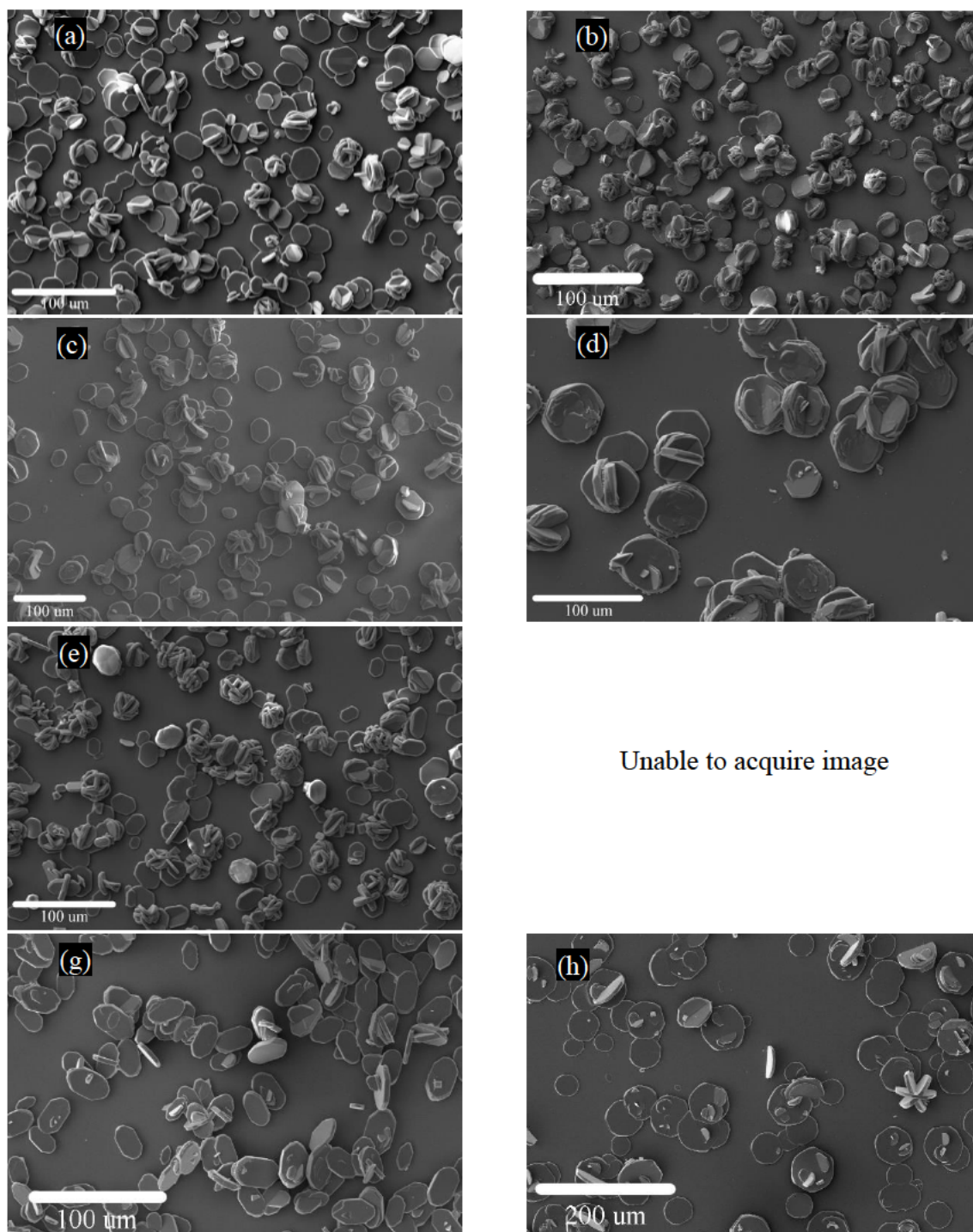


**Figure 30.** *CaOx impacted by SCAA; (a) pure SUM, (b) SUM+Zn<sup>2+</sup>, (c) Sodium Gluconate, (d) Sodium Gluconate+Zn<sup>2+</sup> (e) Acetylsalicylic Acid, (g) Lactic Acid, (h) Lactic Acid+Zn<sup>2+</sup>*

### 3.4.3.1. Sodium Gluconate

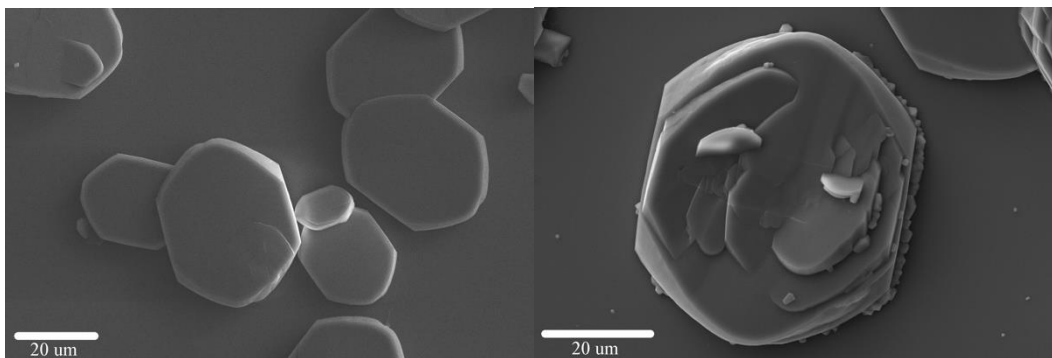


**Figure 31.** *CaOx morphology impacted by sodium gluconate (20 mM) (left), sodium gluconate (10 mM)+Zn<sup>2+</sup> (right)*

In the case of figure 31 the presence of NaG doesn't appear to have altered the shape of the COM significantly. While there is some evidence of the crystals forming in other crystals in SUM this is much more significant when zinc ions are present in the solution. This shows the smaller crystals forming just off angle to the basal face.

### 3.4.3.2. Acetyl Salicylic acid

There are clear effects on the sizes and the aggregation state of particles in the presence of acetyl salicylic acid (Figure 30e).

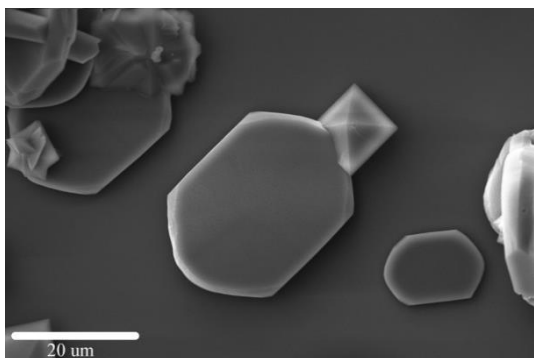


**Figure 32.** *CaOx morphology impacted by acetyl salicylic acid (20 mM)*

It is also seen that COD is more prevalent when ASA is in this solution than in SUM alone. There is also a significant amount of the formation of crystals inside other crystals. Even to the point that figure 32 has a COD crystal forming inside the edge of a COM crystal. It also appears that the (010) face has been elongated resulting in a slimmer appearance. This is interesting on comparison to the other additives as this is one of the few additives that appear have slowed the (010) face making it appear more dominant.

### 3.4.3.3. Lactic Acid

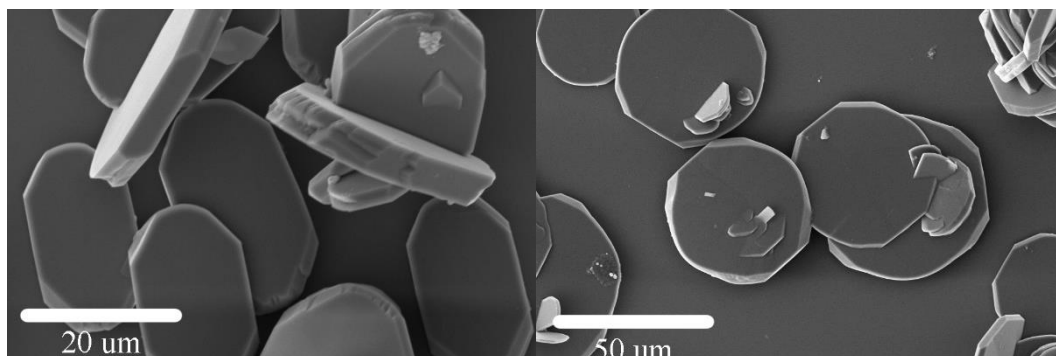


**Figure 33.** *CaOx morphology impacted by Lactic acid (20 mM) (left), Lactic acid (10 mM)+Zn<sup>2+</sup> (right)*  
The presence of LA in SUM results in particles that have more dominant (010) faces. Additionally, the (021) related faces are more rounded, particularly where those faces meet. Also, there is still a significant degree of crystals growing inside other crystals. This effect is not mirrored when zinc is present, the COM particles take on a more circular shape and the (010) faces are less prominent. This means that the interaction of LA with zinc ions slows down the (021) face.

### 3.4.4. Impact of Multiple Carboxylic acid containing additives on Morphology

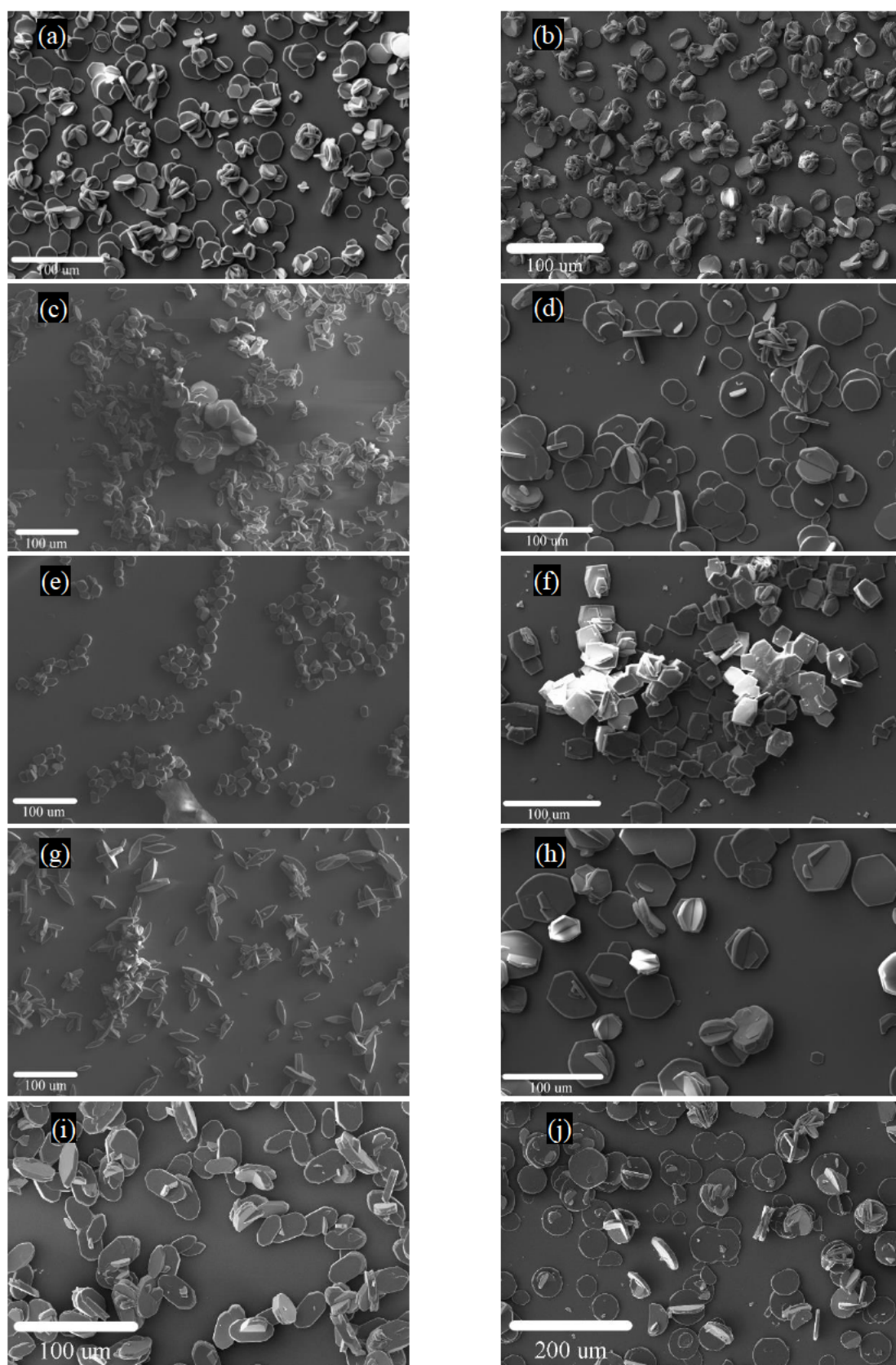


**Figure 34.** SEM micrographs of CaOx (40 mM) crystal morphology in SUM with: (a) pure SUM; (b) SUM+Zn<sup>2+</sup> (c) Maleic acid, 20 mM; (d) Maleic Acid+Zn<sup>2+</sup>; (e) tartaric acid, 20 mM; (f) tartaric acid+Zn<sup>2+</sup>; (g) EDTA, 1 mM; (h) EDTA+Zn<sup>2+</sup>; (i) Succinic Acid 20 mM; (j) Succinic Acid+Zn<sup>2+</sup>

#### 3.4.4.1. Maleic Acid

The MA impacted crystals (Figure 34c and Figure 35), for the most part, show a particle shape that is more pointed and similar to that of COM in water. The basal face appears narrower than that observed for COM in pure water, though the overall shape is similar. This implies that the presence of MA prevents interaction with citrate (the reason for the rounding shown in COM in SUM, Figure 25a) or its impact is greater than that of citrate (later data should help confirm which). There are larger crystal aggregates that are similar to the SUM impacted COM morphology seen in Figure 34a (though isolated and aggregated together), suggesting it is likely that the interaction is competitive.

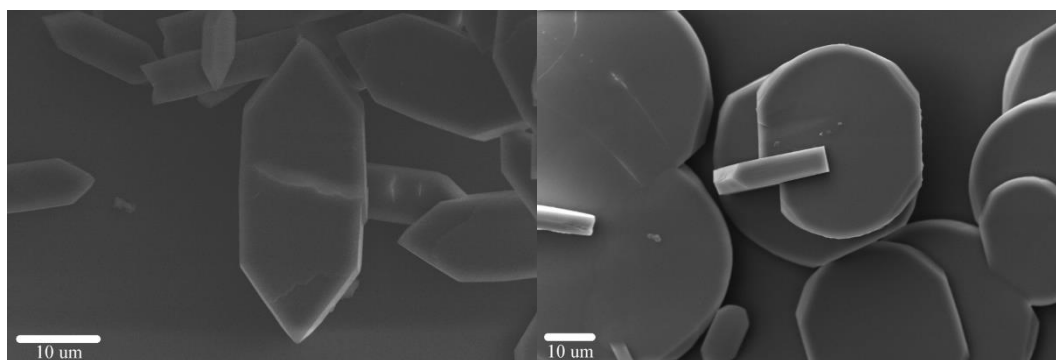


**Figure 35.** SEM micrograph of a MA impacted CaOx crystal in SUM (left) and SUM+Zn<sup>2+</sup> (right)

After the addition of zinc ions to the SUM the MA appears to have no impact on the morphology. When comparing Figure 25b and Figure 35 (right) it is observed that the COM crystals have returned to the citric acid impacted morphology of the typical standard SUM.

When zinc ions are present there is a significant variation in crystal size; but no other notable morphological differences from COM particles formed in SUM. It was noted that a substantial amount of aggregation was present in the SEM micrograph. It was found that the crystals with the MA (in SUM+Zn<sup>2+</sup>) additive appear to aggregate with a high frequency to the point where there are few crystals that aren't in contact with other crystals.

#### 3.4.4.2. Tartaric Acid

TA appears to inhibit and aggregate COM particles significantly (Figure 34e and Figure 36). However, TA also has some interesting morphological effects. The crystals formed have lost symmetry, though there are still aspects that can be identified from the standard crystalline morphology. For example, the COM (12-1) and (021) faces are more dominant, leading to an

angled appearance of the crystal. The (010) faces appear more dominant compared to the control. This suggests that there may be adsorption to those faces.

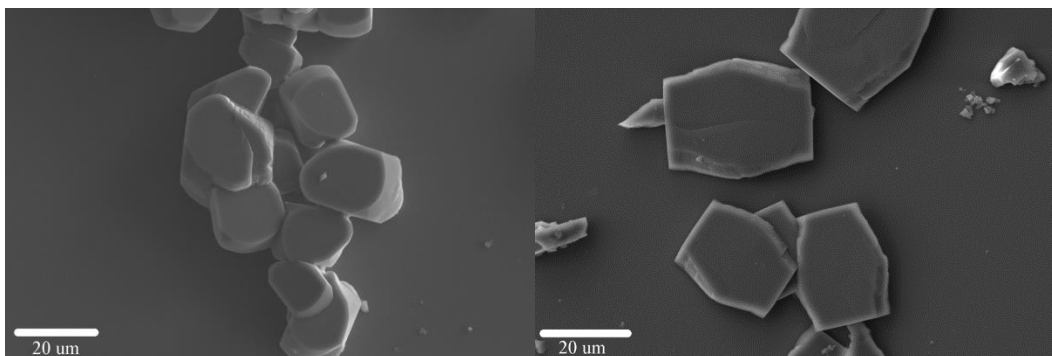


**Figure 36.** SEM micrograph of tartaric acid impacted CaOx crystals in SUM (left) and SUM+Zn<sup>2+</sup> (right)

In the presence of tartaric acid and zinc ions, the particles formed are more symmetrical than those in presence of tartaric acid in SUM (Figure 34f and 36 (right)). These particles appear to have less rounding than COM in SUM with the (021), (12-1) and (010) faces better defined. Though the shape of the crystals is wider and shorter than COM particles formed in the presence of other additives. There also appears to be the formation of possible (001) faces.

#### 3.4.4.3. EDTA

The morphology of COM in the presence of EDTA is shown in Figure 34g and Figure 37. There appears to be a large amount of aggregation, with crystals growing into other crystals.

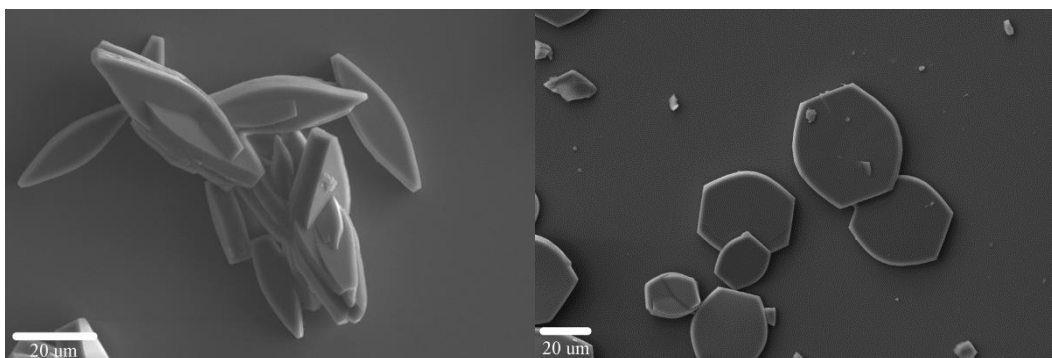


**Figure 37.** SEM micrograph of EDTA impacted CaOx crystals in SUM (left) and SUM+Zn<sup>2+</sup> (right)

The (010) face has almost disappeared when EDTA is present, and the points of the crystals seem to have formed a more angular shape than that of COM in SUM. The (12-1) and (021) faces are more dominant when EDTA is present. The crystals also seem very smooth, which is

not what is expected when leaching/dissolution occurs (the crystal typically has divots or etch pits) if the EDTA were removing the metal from a preformed solid. (93) Thus, this does not appear to be happening in this instance. The morphology is significantly different to that of the citric acid impacted crystals, which suggests that the EDTA is causing ongoing inhibition in the crystallisation process.

Similar to MA, the addition of zinc ions has resulted in the morphology appearing to resemble the morphology of COM in the SUM. As detailed in the Section 3.1, this is likely due to the EDTA binding to the zinc ions in preference to the calcium ions. (94) This is confirmed to some extent by the morphology returning to that of the control.

#### 3.4.4.4. Succinic Acid

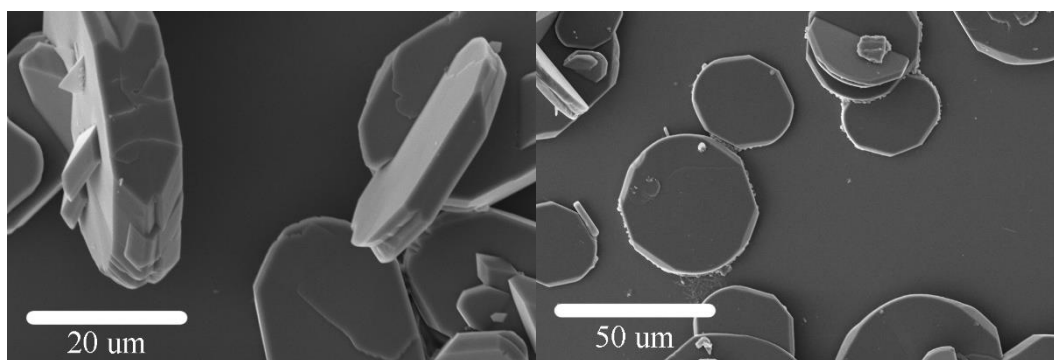


**Figure 38.** *CaOx morphology impacted by succinic acid (20 mM) (left) in SUM, and succinic acid (10 mM) in SUM+Zn<sup>2+</sup> (right)*

SA has a very similar observable effect to that of LA where in SUM the (021) face elongated and became rounded while the (010) face became shorter. Similarly, in the presence of Zn<sup>2+</sup>, the SA forms rounded crystals.

### 3.4.5. Impact of Macromolecular additives on Morphology

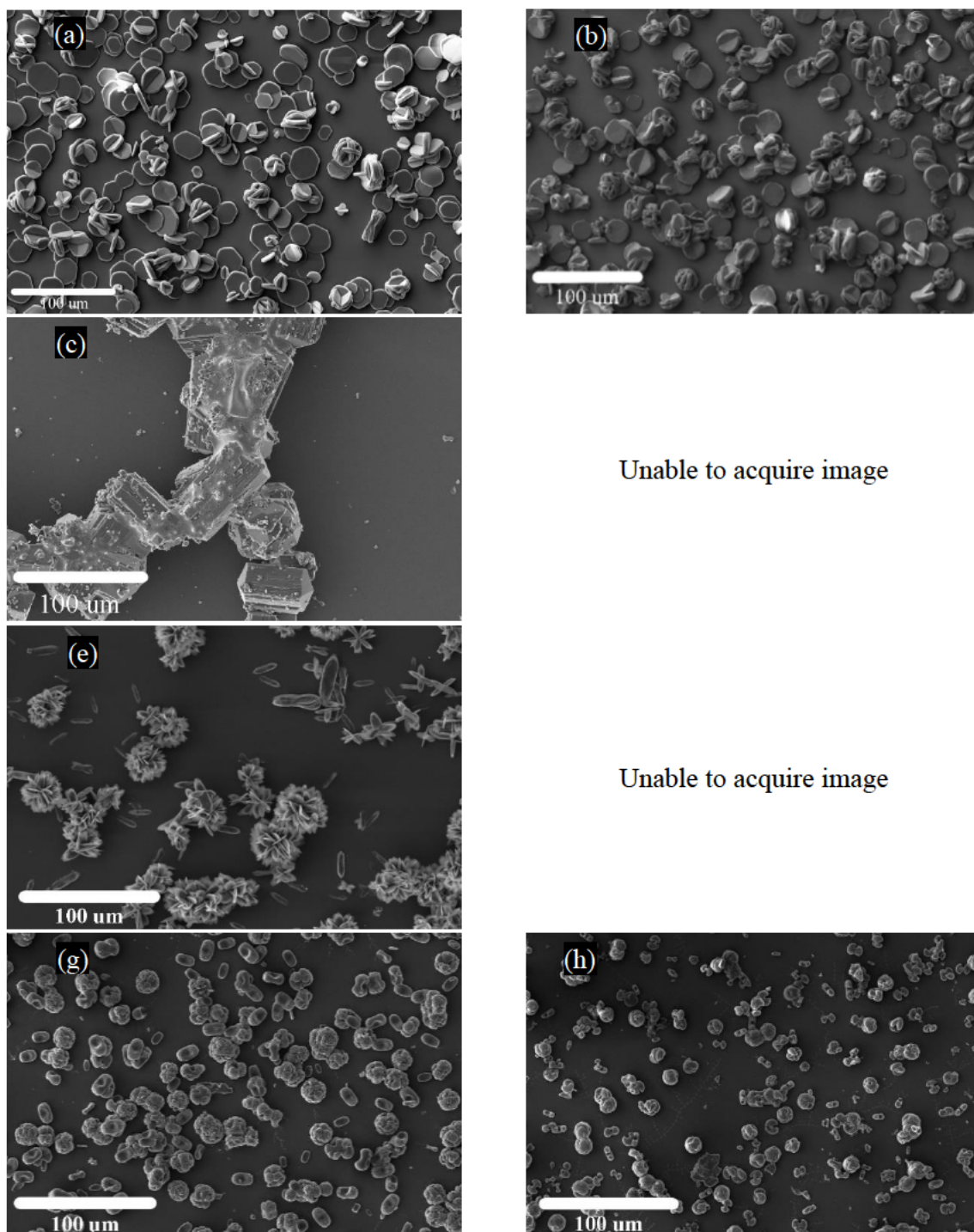


**Figure 39.** SEM micrographs of CaOx (40 mM) crystal morphology in SUM with: (a) pure SUM; (b) SUM+Zn<sup>2+</sup> (c) PRAA, 1 mM; (d) PRAA+Zn<sup>2+</sup>; (e) CPro, 1 mM; (f) CPro+Zn<sup>2+</sup>; (g) PCLys, 1 mM; (h) PCLys+Zn<sup>2+</sup>

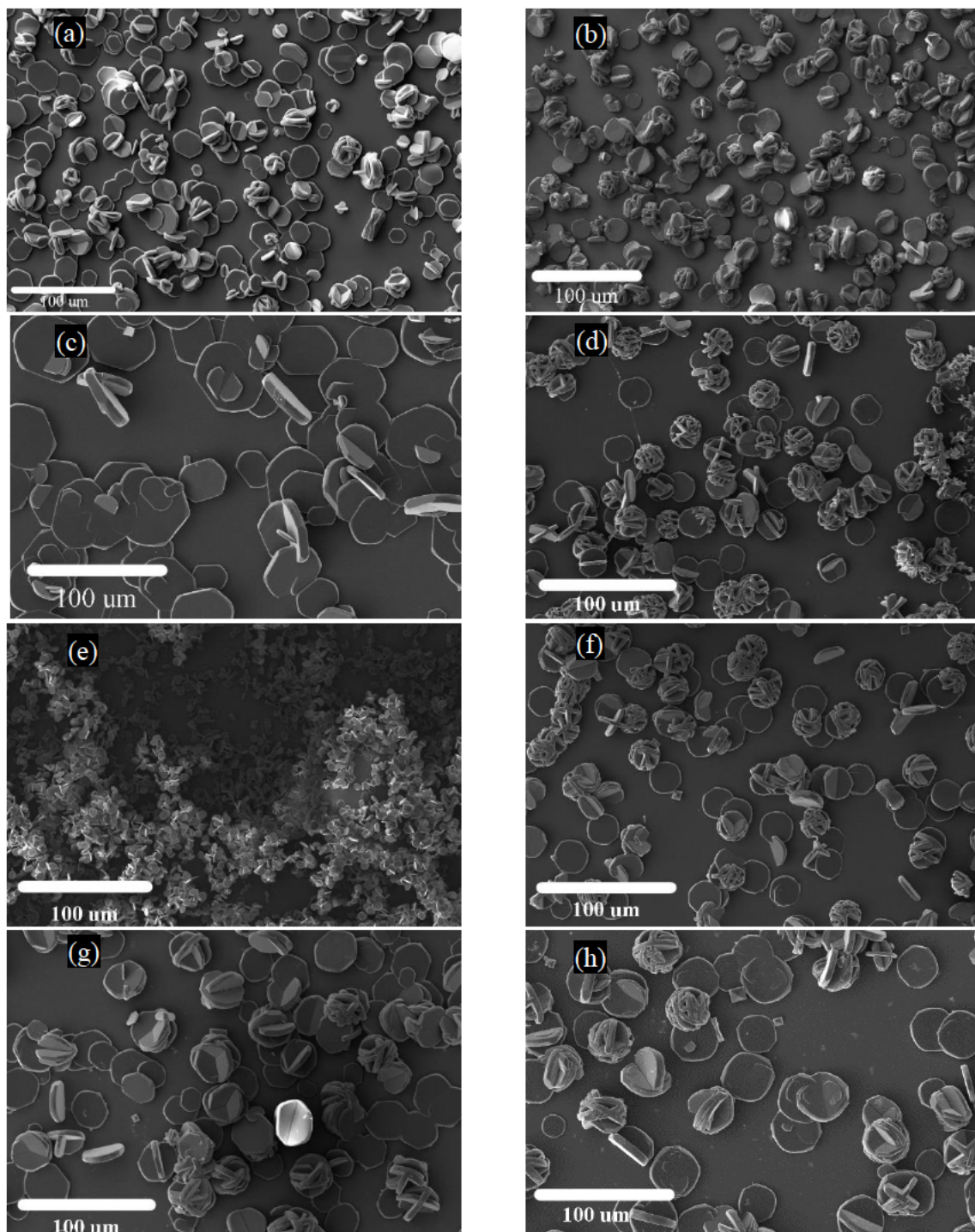


**Figure 40.** SEM micrographs of CaOx (40 mM) crystal morphology in SUM with: (a) pure SUM; (b) SUM+Zn<sup>2+</sup> (c) AA, 4 mM; (d) AA+Zn<sup>2+</sup>; (e) Pro, 4 mM; (f) Pro+Zn<sup>2+</sup>; (g) Lys, 4 mM; (h) Lys+Zn<sup>2+</sup>

### 3.4.5.1. Aspartic acid functionalised propyl resorcin[4]arene

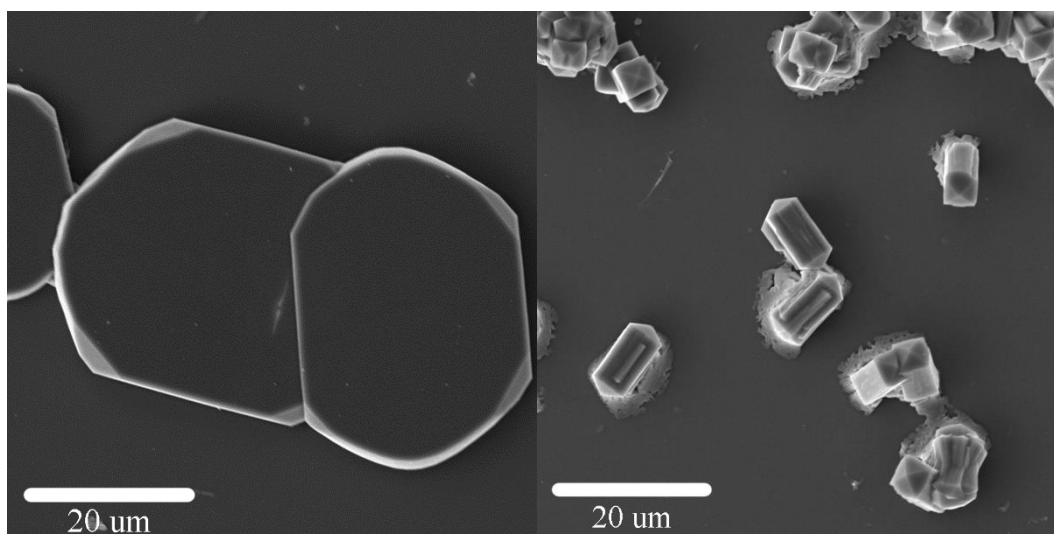


**Figure 41.** *CaOx morphology impacted by aspartic acid (4 mM) (left), aspartic acid functionalised resorcin[4]arene (1 mM) (right)*

In figure 41 is the comparison between the effect of the aspartic acid alone and the aspartic acid on the resorcin[4]arene. On the left it can be seen the crystals are very similar to the typical COM crystals found in the standard SUM. However, on the right it can be seen that the crystals are of a very different morphology, and in fact, COD, is exclusively present. The COD is also significantly elongated compared to the COD observed previously (either at low temperature or in the presence of other additives), having a very visible (100) face and also having a large number of crystals forming inside of other crystals. The process of collecting crystals was more difficult as they did not stick to the glass plate. Because of this the plate could not be rinsed off without losing all the crystals.

The formation of COD exclusively is of interest as this typically does not occur within our standard tests although it does occur in the presence of the PRAA. This means that the presence of PRAA stabilises the formation of COD. This means that either PRAA inhibits the transition from COD to COM or that the formation of COD is templated.

### 3.4.5.2. Proline functionalised Calix[4]arene

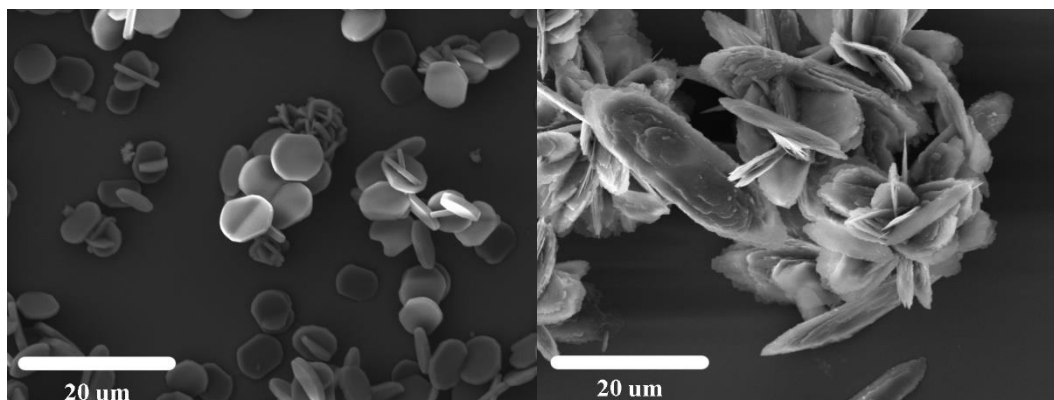


**Figure 42.** *CaOx morphology impacted by proline (4 mM) (left), proline functionalised calix[4]arene (1 mM) (right)*

Considering the morphology of the proline amino acid in SUM there is an impact on the size of the formed crystals as well as on aggregation. There is no significant impact on the morphology as the faces all seem quite similar to that of the SUM formed crystals. This implies that there is some interaction but that it is not face specific.

The crystals formed in the presence of CPro are very flat and much thinner than any of the crystals formed thus far in either SUM or in the presence of any of the additives. Additionally, there is some visible layering and a large amount of crystals growing inside of other crystals. The (010) face is the dominate face as the (021) and associated faces are not very noticeable in comparison.

### 3.4.5.3. Lysine functionalised propyl calix[4]arene

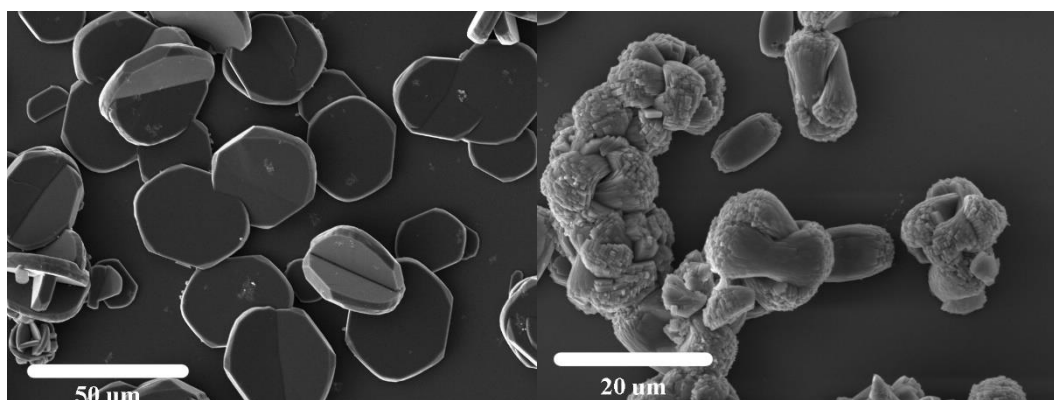


**Figure 43.** *CaOx morphology impacted by lysine (4 mM) (left), lysine functionalised calix[4]arene (1 mM) (right)*

In figure 43, the amino acid lysine is not found to have a significant impact on the COM crystals formed in SUM. Again, the amino acid seems to have very minor impact on the overall morphology of the crystals, reproducing the shape of the standard COM morphology in the SUM. However, when the Lys is functionalised onto a calix[4]arene with a propyl chain (PCLys) the crystals don't have very well-defined features, but the Raman spectrum confirms these are indeed COM particles. It is very hard to distinguish any faces with certainty on these crystals, the morphology is so altered compared to particles formed in both pure water and SUM. What can be seen is a roughness on the outside of the crystals and a large degree of aggregation. These crystals also seem to be a lot thicker and rounder than the standard crystals.

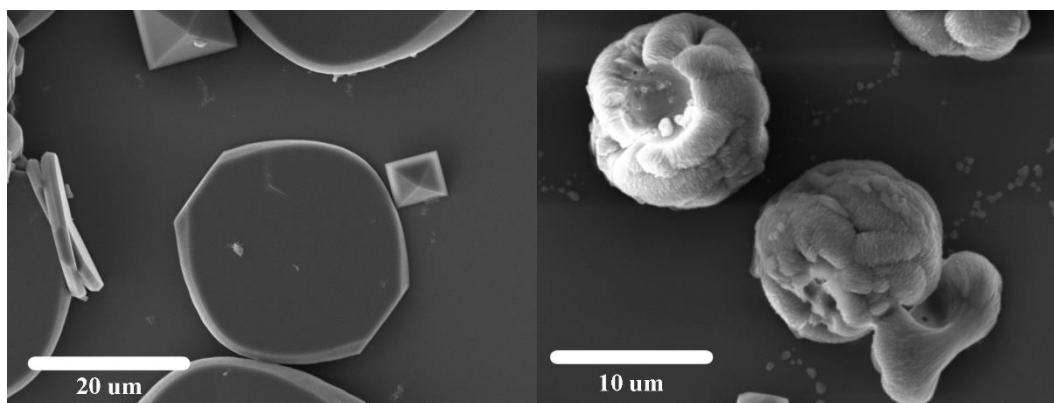


**Figure 44.** *CaOx morphology impacted by lysine (4 mM) in the presence of zinc ions (left), lysine functionalised calix[4]arene (1 mM) in the presence of zinc ions (right)*

When zinc ions are present in addition to the Lys there is not much of a change with respect to the lone amino acid except for the stabilisation of some COD that can be seen in figure 44. The minor change in the morphology is what's expected from the impact of zinc ions in the medium.

When viewing the particles formed in SUM+PCLys+Zn<sup>2+</sup>, the crystals have no well-defined faces from the typical COM shape. Again, these crystals were confirmed as COM by Raman and not another phase. The crystals also seem to either aggregate into or form almost spherical structures with a very roughened surface. With these structures it also seems that there is some sort of indent in the shape. This indented shape doesn't seem to be associated with a particular face, although this does appear to be reproduced in the crystals. This same sort of indent can be seen in the lower right of the image where what looks closer to a single particle is shown. It does seem there is some sort of lower surface to the crystal too. So, the presence of PCLys seems to greatly impact the crystal's morphology in some way such that there are no defined faces. It is difficult to tell which faces are inhibited or promoted based on these images. There was also a limit on the amount of PCLys available to test in the project and so it wasn't possible to do multiple tests to determine the interaction of this additive further.

### 3.4.6. Impact of additives on crystal size

In this section the sizes of the formed particles are assessed as this gives further information regarding the additive's inhibitory potency. This involved measuring the area and aspect ratio of particles using ImageJ. The aspect ratio is defined as being the length/width. There is a high value for the error associated with the area of these crystals, but the large number of crystals measured still give context for the overall trend of the additive's impact.

#### 3.4.6.1. Impact of sugar additives on crystal dimensions

Table 4 shows the impact the sugar additives had on the aspect ratio and size of the COM crystals observed. It can be seen that in SUM the additives tend to not change the overall relationship of the length and width significantly as the change in the aspect ratio is minimal. The largest impact is seen with the presence of Gal and Glu. Fru was observed to reduce the area of particles formed to a minor degree and then Gal and Glu by a more significant amount. This may suggest that the stereochemistry of the sugar ring may impact the size as rings as the Fru is a 5 membered ring in comparison to that of the other sugars which are both 6 membered in their chair confirmations.

**Table 4.** Recorded impact of the sugar additives in SUM (additives at 20 mM) and with the presence of zinc ions (additives at 10 mM) on the size and aspect ratio of CaOx

Chemical Present	SUM		SUM + Zn <sup>2+</sup>	
	Aspect Ratio	Area (um <sup>2</sup> )	Aspect Ratio	Area (um <sup>2</sup> )
Standard	1.23	910 ± 263	0.97	1102 ± 346
Fru	1.29	851 ± 479	0.98	3019 ± 1780
Gal	1.12	574 ± 222	1.09	925 ± 394
Glu	1.07	535 ± 135	0.97	635 ± 130

With the addition of zinc ions, Fru has a significant impact on the size of particles formed, increasing the area of the average crystal by almost 3 times compared to the standard with zinc ions. This interaction is interesting as the overall aspect ratio has not changed so this interaction must not be face specific. This is surprising given that Glu had the lowest particle counts recorded in the DLS investigation (lower nucleation rates can lead to larger particles in batch systems).

Both the Gal and Glu additives, when zinc ions are present, form particles with sizes less than compared to the pure SUM. Although the Glu impacts minimally, the presence of Gal has a much more noticeable impact with the addition of zinc ions to the medium (if both aspect ratio

and area is considered), this suggests there may be some additional interaction with Gal and zinc ions. Whilst there isn't a lot of variance with the other sugars in the recorded aspect ratios, Gal has the biggest change.

### 3.4.6.2. Impact of single carboxylic acid containing additive on crystal dimensions

In table 5 the impacts of the single carboxylic acid additives on the final sizes of the COM crystals can be observed. This shows that the presence of LA and ASA significantly reduce the average area of particles by half in the SUM. This is consistent with the nucleation promotion observed with DLS. When more nucleation occurs particles will grow to a smaller size in a batch system. There is a very minor impact of the NaG on the area of crystals formed. Additionally, ASA and NaG have very minor impacts on the aspect ratio despite the large impact that ASA has on the overall crystal area. In just the SUM, LA seems to have the largest overall impact, deviating from the standard in both size and aspect ratio significantly. Given that aspect ratio is length/width, it appears that LA is making the particles longer supporting that the (010) is more dominant.

**Table 5.** *Recorded impact of the additives containing one carboxylic acid group in SUM (additives at 20 mM) and with the presence of zinc (additives at 10 mM) on the size and aspect ratio of CaOx*

Chemical Present	SUM		SUM + Zinc	
	Aspect Ratio	Area ( $\mu\text{m}^2$ )	Aspect Ratio	Area ( $\mu\text{m}^2$ )
Standard	1.23	910 $\pm$ 263	0.97	1102 $\pm$ 346
ASA	1.34	429 $\pm$ 208	_____	_____
NaG	1.34	807 $\pm$ 368	1.12	1851 $\pm$ 574
LA	1.67	385 $\pm$ 116	0.92	2404 $\pm$ 574

Contrasting the impact when the additives are in the SUM with zinc ions present, it is observed that the overall area of each crystal is increased significantly compared to the standard. This implies that the interaction between the zinc ions and the carboxylic acid additives is causing some effect to promote the growth of the particles. When the additives are in the pure SUM smaller particles are formed due to the higher nucleation rate. There are notably larger particles when zinc ions with the additives is present which could be associated to the lower nucleation rate, but the sizes are larger than the SUM+Zn<sup>2+</sup> while the nucleation rates are higher, thus growth must be promoted.

The interaction between the organic and the zinc ions seems to result in the formation of larger CaOx particles. There is a more significant impact from the LA which may be due to the stereochemistry associated with the molecule.

### 3.4.6.3. Impact of additives containing multiple carboxylic acids on crystal dimensions

**Table 6.** *Recorded impact of the additives containing multiple carboxylic acid group in SUM (additives at 20 mM) and with the presence of zinc (additives at 10 mM) on the size and aspect ratio of CaOx. \*EDTA at 1 mM concentration*

Chemical Present	SUM		SUM + Zinc	
	Aspect Ratio	Area ( $\mu\text{m}^2$ )	Aspect Ratio	Area ( $\mu\text{m}^2$ )
Standard	1.23	910 $\pm$ 263	0.97	1102 $\pm$ 346
EDTA*	0.32	204 $\pm$ 116	0.95	1504 $\pm$ 841
MA	2.27	253 $\pm$ 96	1.20	1798 $\pm$ 984
TA	1.53	271 $\pm$ 102	0.78	579 $\pm$ 254
SA	1.90	504 $\pm$ 97	1.02	490 $\pm$ 111

Similar to the single carboxylic acid containing additives, the multiple carboxylic acid containing additives also generally decrease the size of the particles formed without zinc ions present.

Whilst with the MA and EDTA are present in the SUM they have both a significant impact on the size and aspect ratio of the COM particles, although the change is in the opposite direction. The length of the particles formed when EDTA is present is much smaller unlike the case with MA where the width of particles is much smaller, resulting in this change in the ratio. It does, however, seem that MA and EDTA seem to lose their inhibitory effect when zinc ions are present implying some interactions between them and the  $\text{Zn}^{2+}$ . Whilst EDTA is a known chelator as already discussed, E 1.8, MA is not, nor would it be expected to chelate zinc ions (this has a significantly lower complexation constant, Table 3, than that of oxalate or other species in the SUM). Despite this, there appears to be an interaction between MA and  $\text{Zn}^{2+}$  based both on the morphology and the size. When zinc ions are present there is still some deviation in the aspect ratio for MA, though to a lesser extent.

The impact of the additive on the size of the resultant particles can be understood for MA as being due to the increased nucleation rate observed previously. However, for TA and EDTA, nucleation was inhibited (in SUM) thus the smaller sizes must be due to growth inhibition.

The presence of TA seems to inhibit the COM growth overall and makes the formation of these crystals smaller in both the SUM and the SUM with zinc ions did not change the effect that TA had on nucleation rate. Whilst the COM size is still smaller in the presence of zinc ions the effect is notably lessened especially in comparison to the large effect on the COM size in SUM. The big change for the TA comes from the aspect ratio. The shape of the crystal changes to be much wider in the presence of zinc ions.

#### 3.4.6.4. Impact of macromolecule additive on crystal dimensions

In table 7 the comparison between the impact of the amino acid functionalised macrocycles and their associated amino acids on the particle sizes can be seen. It is noted that PRAA did not form any crystals when zinc ions were present. The presence of CPro and zinc ions was also unable to be assessed because the particles were not on the plate when analysed under SEM.

It is observed that within SUM that generally the macrocycles lead to smaller particles with higher aspect ratios compared to the single amino acid counterparts. Additionally, the single amino acids lead to smaller particles with higher aspect ratios compared to the standard, with the exception of Lys. The area of the formed crystals in the presence of aspartic acid is slightly higher than the standard, although the other amino acids lead to smaller particles. The particles formed in the presence of Lys being approximately half of those formed in SUM with those formed in the presence of Pro significantly smaller. The presence of the PRAA forms COD particles and so strictly speaking the size cannot be compared to the standard or to the AA system. The presence of Pro amino acid does form significantly smaller particles although the change between that and the Pro-containing macrocycle is that while there is a significant change in the aspect ratio, increasing from the 1.31 to 3.46, the resulting particle is larger when Pro is tethered to the macrocycle. Thus, these changes in size and aspect ratio of the particles formed cannot be rationalised by the presence of the amino acids alone.

**Table 7. Recorded impact of the macromolecule additives in SUM (additives at 20 mM) and with the presence of zinc (additives at 10 mM) on the size and aspect ratio of CaOx. \*\* PRAA recording the size and aspect ratio of COD**

Chemical Present	SUM		SUM + Zinc	
	Aspect Ratio	Area ( $\mu\text{m}^2$ )	Aspect Ratio	Area ( $\mu\text{m}^2$ )
Standard	1.23	910 $\pm$ 263	0.97	1102 $\pm$ 346
PRAA**	2.23	46 $\pm$ 14	—	—
AA	1.32	1214 $\pm$ 425	1.19	347 $\pm$ 67
CPro	3.46	142 $\pm$ 54	—	—
Pro	1.31	32 $\pm$ 9	0.98	420 $\pm$ 39
PCLys	1.81	111 $\pm$ 27	1.44	58 $\pm$ 12
Lys	1.16	583 $\pm$ 140	0.98	738 $\pm$ 242

The smaller particle size observed in the case of PRAA could also be due to the nucleation promotion observed, but nucleation promotion is also observed in the case of AA and the final particle sizes are larger than the standard particles. This suggests that the presence of AA promotes growth of COM. Similarly, when the Pro and CPro are present the particle counts are close to the standard but the sizes of COM particles is much smaller than the standard suggesting that growth of COM is inhibited.

While the PRAA and CPro weren't able to be investigated with zinc ions present their respective amino acids were. The change between the SUM and when zinc ions were present generally was that the particles in the presence of zinc ions have a lower aspect ratio (compared to SUM), stemming from the increase in the crystal width. When observing the impact on size (for the case of SUM+Zn<sup>2+</sup>) there are different effects, the presence of AA resulted in particles which were much smaller while in the presence of Pro particles formed were significantly larger. Overall, however, the amino acids lead to particles with similar areas and suggesting that the interaction of amino acids in SUM with zinc ions is the same for all these amino acids. It is also of note that while the particles formed in the presence of the amino acids started with similar aspect ratios the change in the aspect ratio is different, 0.13 for AA and 0.336 for Pro. The effect of the amino acids alone seems to be much closer to the standard in size, although the nucleation of these vary, with Pro being near standard and AA being a notable promoter.

When comparing the effect the presence of zinc ions have on Lys and PCLys the aspect ratio for both decreases compared to their SUM tests, but then the size effect is still very different to each other. When the Lys is in the SUM solution with zinc ions the particles' size increases

moderately. The presence of PCLys and zinc ions forms smaller particles which is different to the effect most molecules have, implying there is perhaps some interaction with the zinc ions that increase the impact of the PCLys in terms of growth. Unfortunately, due to limited amount of this additive there is no DLS data for this yet. Overall, the macromolecules have differing but very interesting impacts on the morphology which should be explored further.

### 3.5. Aggregation potential

Zeta potential measures the double layer around a particle and, at low ionic strength, is related to the surface charge. More importantly, the zeta potential can give information on the likelihood of aggregation, as particles in a solution with similar surface charges will repel each other. As a rule of thumb, particles with zeta potentials  $>\pm 30$  mV are not likely to aggregate. (95) Thus this can give information on the likelihood of larger stone formation through an aggregative process such as coagulation is unlikely.

It can be seen that in comparison to the standard, zinc ions increase the zeta potential in magnitude but make the particle more negative. This is despite the addition of the positive ions of zinc. One possible way in which this may occur is if the zinc ions adsorb to the surface and then attract the negative counter-ions from the SUM to the particle resulting in a more negative value.

### 3.5.1. Effect of sugar additives on zeta potential

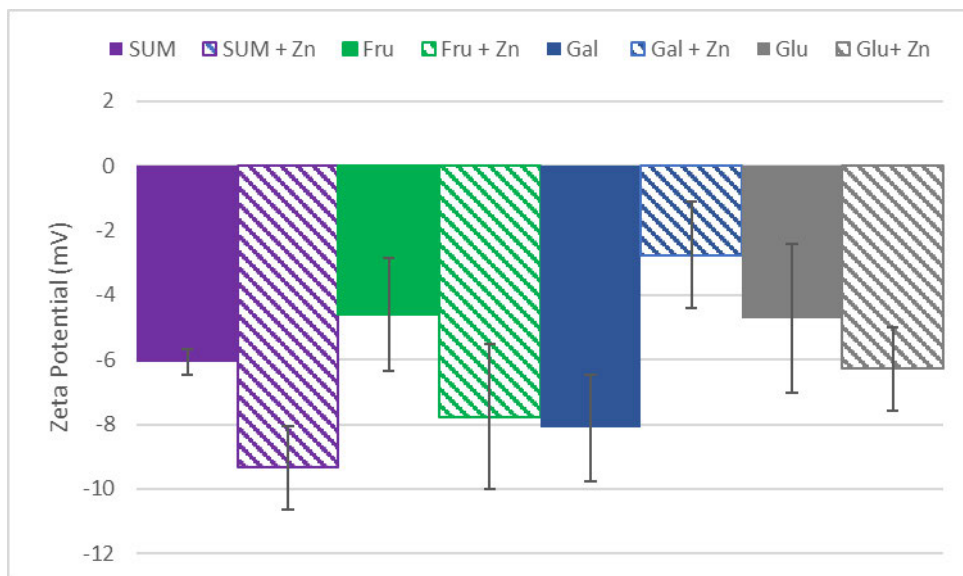


**Figure 45.** Effect of sugars in solution on the zeta potential of CaOx crystals; SUM (purple) and chemicals with zinc (Hashed), Fructose (20 mM) (Green), Galactose (20 mM) (blue), Glucose (20 mM) (Grey) While in SUM fructose and glucose have similar zeta potential values, the galactose result is significantly different with the signal being even greater in magnitude than that of just the standard in SUM. After the addition of zinc ions to the medium both Fru and Glu result in a decrease (more negative) in zeta potential whilst the galactose results in the opposite behaviour to the other sugars.

This suggests some major difference between Fru and Glu compared to that of Gal. While comparing the conformations of the cyclic compounds it can be seen that Glu has most of its hydroxyl groups equatorial which can make it hard for binding to a single zinc ion. What is seen is the effect of the zinc ions to lower the zeta potential (as per the standard in SUM) with a minor impact from the sugar. When considering the effect of galactose there has been some *in vivo* tests that have shown some unique interactions between galactose with small metals like zinc and calcium. (91) So it's likely some interaction with the calcium causes the difference in SUM compared to the standard while the interaction is with the zinc ions when they are present, resulting in the large change.

### 3.5.2. Effect of single carboxylic acid containing additives on zeta potential

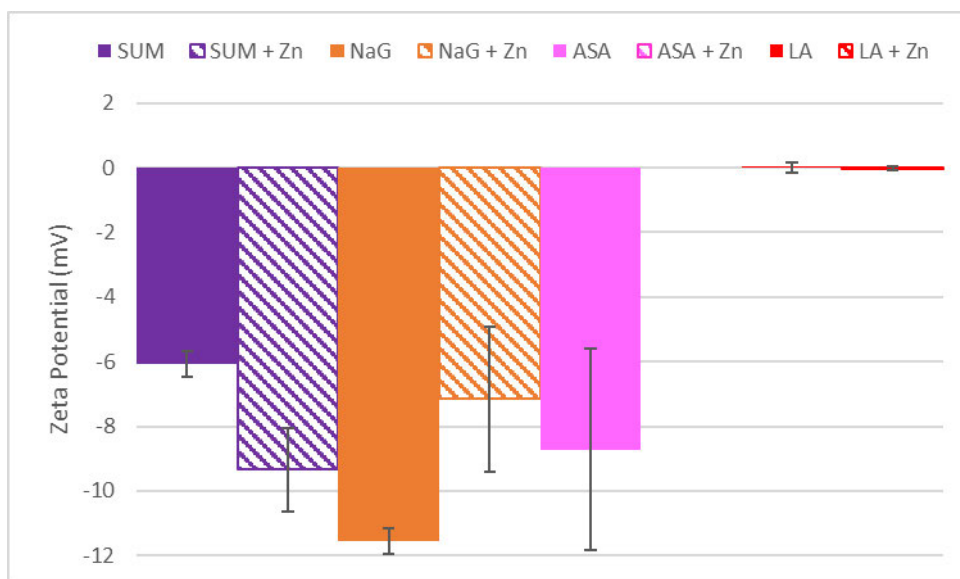


**Figure 46.** Effect of single carboxylic acid additives in solution on the zeta potential of CaOx crystals; SUM (purple) and chemicals with zinc (Hashed), Sodium Gluconate (20 mM) (orange), Acetylsalicylic acid (20 mM) (Pink), Lactic acid (20 mM) (Red)

The impact of ASA with zinc ions was left out of Figure 46 due to the production of non-calcium-based compounds as outlined in section 3.3.2, equation 1.9.

It can be seen that the presence of NaG produces some of the most negatively charged particles from the data set. This may be due to the numerous hydroxyl groups in the structure of NaG forming hydrogen bonds with other NaG molecules around the particle making a negative region.

When NaG is present there is a change in zeta potential on further addition of zinc ions to the SUM. This aligns with the significant increase in the aggregation of CaOx observed in the SEM images (Figure 30c). Additionally, this change may be due to the zinc ions complexing with NaG and removing it from interacting, resulting in a zeta potential closer to the standard in SUM. The presence of both causes the two effects to counter each other resulting in the near standard value.

ASA shows a very moderate effect on the charge around the particles, with high variation. This is interesting as the complexation constant would imply a stronger interaction with the COM particle.

LA has a very large impact on the magnitude of the zeta potential compared to the SUM or SUM + Zn<sup>2+</sup>. As the overall charge of the particle is very close to zero there is negligible repulsion of the particles resulting in a high likelihood of coagulation.

Of interest is the very different interactions from these additives despite all of them containing a single carboxylic acid which should be contributing to the majority of the effect. Even the comparison between the NaG and LA where they are structurally similar, leads to very different behaviour. This suggests that stereochemistry is critical for the interaction of the additive in these systems.

### 3.5.3. Effect of multiple carboxylic acid containing additives on zeta potential

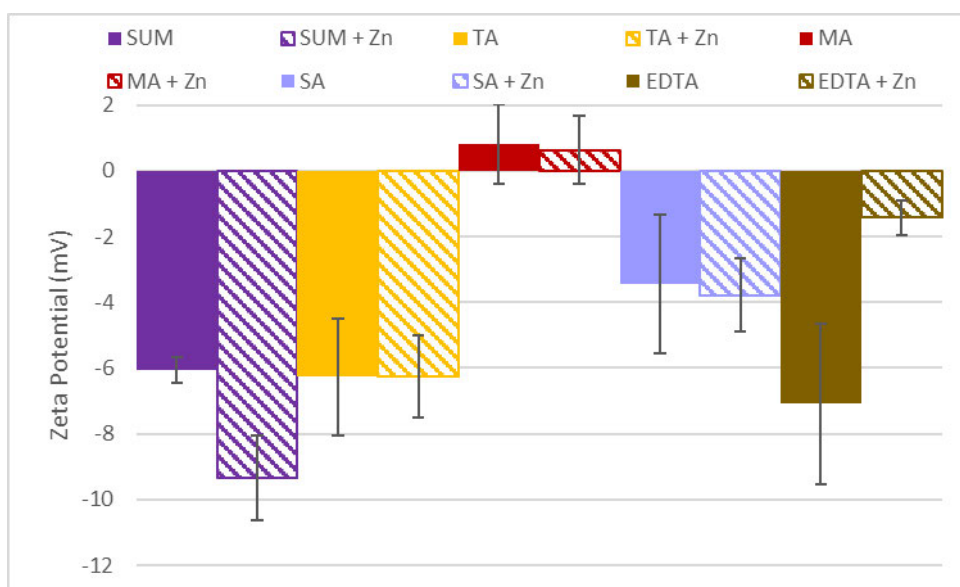


**Figure 47.** Effect of multiple carboxylic acid containing additives in solution on the zeta potential of CaOx crystals; SUM (purple) and chemicals with zinc (Hashed), Tartaric acid (20 mM) (Yellow), Maleic acid (20 mM) (Maroon), Succinic acid (20 mM) (Lilac), EDTA (1 mM) (Brown)

It can be observed that for most of the species with multiple carboxylic acids there is very minor difference between the zeta potential of particles with or without the zinc ions present. The only exception to this is the presence of EDTA, which has a significant change. That is likely due to the formation of the EDTA complex discussed in earlier sections. This complex must cause some further interaction than just the removal of zinc ions from the medium as this effect far exceeds the effect of the standard and the zinc ions. This means that the presence of EDTA with Zn<sup>2+</sup> should result in an increased likelihood of aggregation.

TA seems to have no overall change from the particles in SUM even when zinc ions are present. This may be due to TA interacting preferentially with the surface or perhaps the zinc ions and

TA interact in concert with no additional effect to the surface, resulting in no significant change to the zeta potential and no significant additional chance of aggregation.

MA shows a significant change from the trend of the multiple carboxylic acid containing additives whereby the particles formed have a near zero zeta potential. This effect may be due to the locked Cis position of the MA double bond, in the other molecules there is no bond locking the carboxylic acid groups in one position. This results in there being a neutral area around the particle as the negative regions of the carboxylic acids are locked into place. These results are however supported by the SEM images where in the presence of MA particles show a high tendency to aggregate (Figure 34c) compared to CaOx in the SUM (Figure 34a).

The effect that the SA has on the zeta potential is very minor, although the magnitude is decreased this value is not changed to a degree to give a significant alteration of the likelihood of aggregation.

The effects of the zeta potential on the remaining additives with the zinc ions added are not clearly supported by SEM images, which may be due to the fact that the morphology experiments are obtained in quiescent conditions and particle collisions are required to induce aggregation.

### 3.5.4. Effect of macromolecular additives on zeta potential

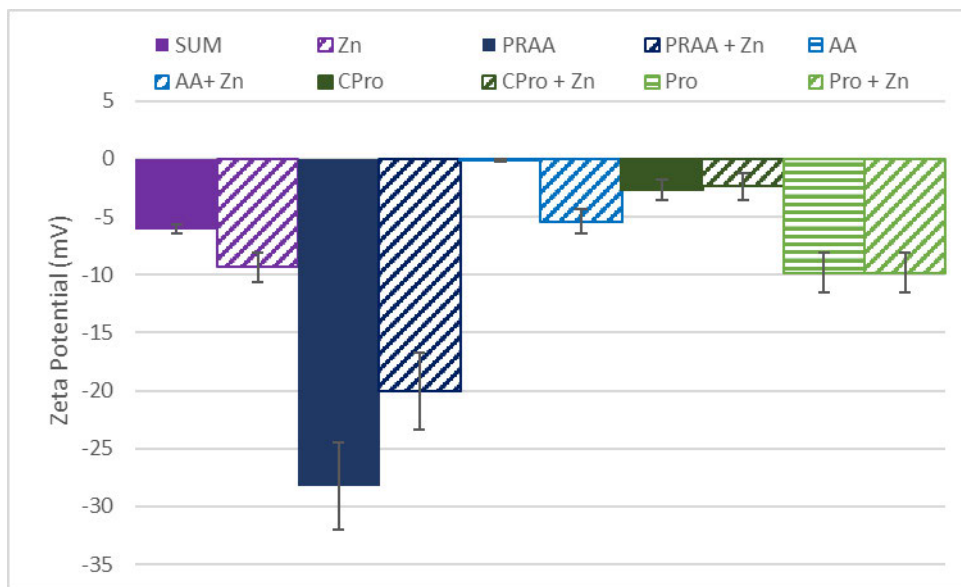


**Figure 48.** Effect of multiple carboxylic acid containing additives in solution on the zeta potential of CaOx crystals; SUM (purple) and chemicals with zinc (Hashed), PRAA (1 mM) (Navy), Aspartic acid (4 mM) (Blue line), CPro (1 mM) (Moss), Proline (4 mM) (green line)

The effect of PRAA on the resulting zeta potential (Figure 48) is significantly above the effect of the standard and any other additive recorded in these tests. The high absolute magnitude of the zeta potential reduces the likelihood of aggregation to form larger particles. This is likely due to the overwhelming large amount of electron sites for interacting with other species which leads to charge repulsion. When zinc ions are present the additive can also interact with the zinc ions which is likely why there is a reduction in the magnitude of the zeta potential. The high absolute magnitude will mean the lowest likelihood of aggregation of the particles in the presence of this molecule. In addition to charge stabilisation, these larger molecules may also sterically stabilise particles against aggregation, thus a lower zeta potential may not be as critical for these macrocyclic additives.

This is in stark contrast to the presence of AA which shows particles with a zeta potential close to zero. This is likely due to the tendency for the molecule to form a zwitterion at the experimental pH. This means that the molecule is able to interact with the metal ions in solution. This means that alone AA will likely increase the tendency of particles to aggregate. In contrast to the large impact shown on the resorcin[4]arene, the AA alone does not result in a similar effect. This shows that the interaction is being made by the combination of the base resorcin[4]arene structure and the functionalised chemical, which leads to a significant effect on the zeta potential that is much stronger than just the AA.

The particles formed in the presence of CPro show a zeta potential closer to zero. This could be due to the proline only containing four carboxylic acid groups as opposed to the 8 in the PRAA. Alternatively, the presence of a phenolic hydroxide at the lower rim of the structure causes some additional interaction resulting in this lower magnitude. As the phenolic hydroxyl is neutral the presence of these groups in the double layer may result in a smaller absolute value of the zeta potential. However, the Pro by itself seems to have an interaction similar in magnitude to that of the SUM with zinc ions present. In both situations with the calix[4]arene and the proline by itself it seems that the addition of zinc does not have a significant impact on the zeta potential.

## 3.6. Adsorption to the surface of COM

### 3.6.1. Adsorption tests in SUM

This test used AR grade COM to determine if there was adsorption of the additives to the surface of COM. Adsorption at growth sites is a mechanism that is known to inhibit the growth of the crystals. By performing these tests, the result should show minor signals from the additive on the surface, thus indicating whether adsorption has occurred. Further analysis could then confirm chemisorption versus physisorption.

The result of these tests showed minimal change to the signal by either FTIR or Raman analysis as that seen for pure COM. This could be due to the lack of adsorption or it may be because the adsorption occurs at a level below the detection limit of the technique.

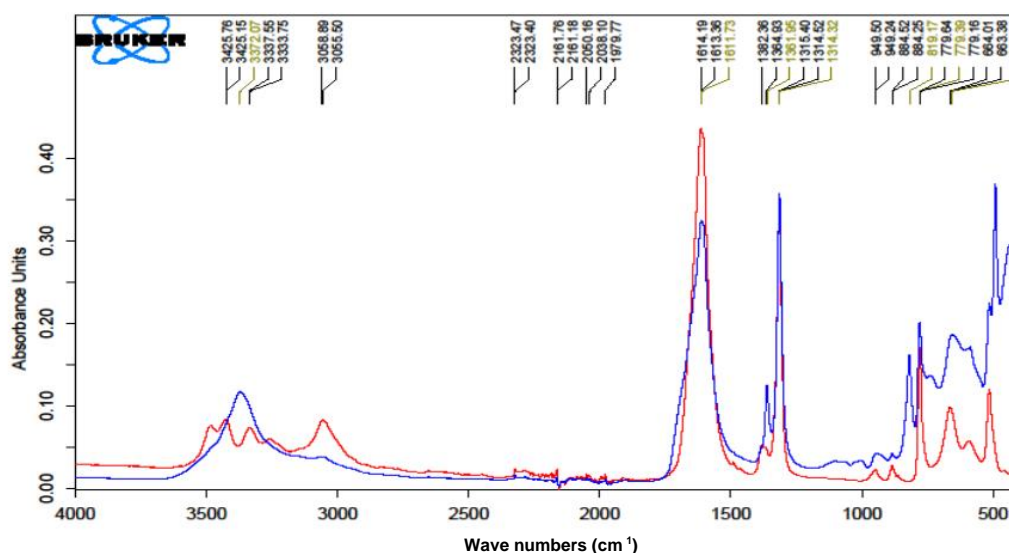


**Figure 49.** Adsorption analysis via FTIR spectroscopy comparing the standard (red) with the zinc ions additive test (blue)

Of the additives tested only one resulted in obvious signs of interaction at the COM surface. As seen in Figure 49, there was a stark difference in the signals present at 3372 cm<sup>-1</sup> in the spectrum, with the zinc ions as additive present (blue) compared to that of the standard spectrum. The sharp doublet signal at 1362 cm<sup>-1</sup> is indicative of a zinc oxalate bond where the signal change is due to the bond strength difference between calcium and zinc. (96) The signal at 3372 cm<sup>-1</sup> is indicative of the change between the monohydrate signal of the COM and the zinc oxalate existing as the dihydrate form. (96)

### 3.6.2. Adsorption tests in deionised water

Following the analysis in SUM the other additives were tested, and this resulted in little change from the control tests. Due to the complexity of the SUM solution and the results showing minor changes at best, the solution was changed to see if the impacts were noticeable in pure water (and using Raman rather than FTIR). Though it can not necessarily be related to the behaviour in SUM it is still of interest in the cases where the signal was at the limits of detection. As found previously, for many of the additives there was no variation in the spectrum, but there were some differences.

#### 3.6.2.1. Adsorption with zinc

To confirm that previous data was reproducible, the results of the complex medium and the zinc ions were tested to see if it would reproduce a similar response with the peaks on the Raman spectrum indicative of the zinc oxalate signal.

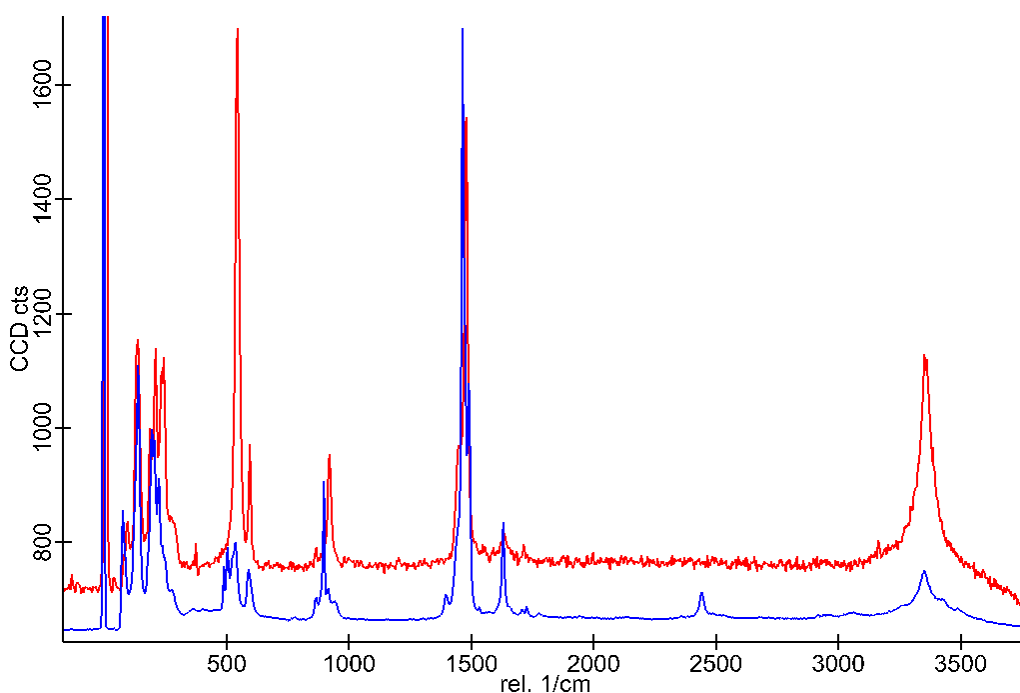


**Figure 50.** *Raman spectrum of COM testing the adsorption of zinc ions on the surface of COM comparing the pure water test (red) in the SUM (blue)*

In comparing the two spectra, the results in pure water show a stronger and clearer signal at approximately  $3200\text{ cm}^{-1}$  (Figure 50). Additionally, there is a peak at approximately  $2500\text{ cm}^{-1}$ , which may be due to some additional interaction in the SUM as it is absent in the water tests. Also, of note is the much higher singlet signal at  $500\text{ cm}^{-1}$  which shows the zinc oxalate peak even better. This is such a strong relationship there may be some substitution of the calcium ions with zinc ions in the actual solid.

### 3.6.2.2. Tartaric Acid adsorption

Tartaric acid has been one of the most interesting additives so far with a significant and noticeable effect on nucleation, morphology and size. So, there was some expectation that the additive would result in a large change to the oxalate spectrum. When testing in pure water there was a significant deviation compared to when TA was in the SUM, with multiple peaks being present between 1700 and 3000  $\text{cm}^{-1}$  (Figure 51).

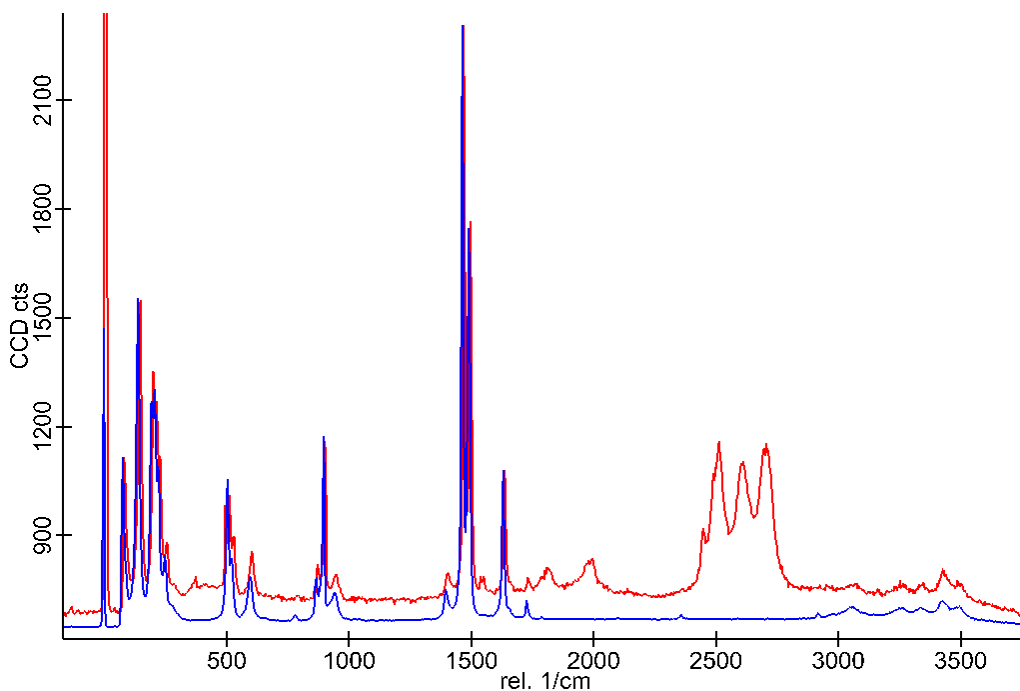


**Figure 51.** Raman spectrum of COM testing the adsorption of Tartaric Acid on the surface of COM comparing adsorption in deionised water (red) with the adsorption in SUM (blue)

Of interest is that while there are additional peaks in the adsorption spectrum these peaks don't line up with any peaks from the additive TA (appendix figure 1) or the control in SUM (appendix figure 2). There is some variation possibly due to the additive at around 1600  $\text{cm}^{-1}$ . This shows that there is some connection between the additive and the COM that is more than just coming close to the surface. This interaction has two stronger peaks along with two weaker peaks between 2500 and 2700  $\text{cm}^{-1}$  as well as a peak at 1950  $\text{cm}^{-1}$  as variations from the standard.

These results confirm that TA adsorbs strongly to the surface of COM and that adsorption interactions are important in the mechanism of how TA inhibits COM nucleation and growth.

### 3.7. Incorporation to the crystal

The depth analysis had a similar aim to that of the adsorption investigation (Section 3.6), though this assessment focuses on determining whether the additive is incorporated into the crystal solid and at which stage this occurs during crystallization. This data should also shed light on whether the method of inhibition is incorporation throughout crystal growth or only adsorption to the surface of the crystal. The stage of inhibition can be assessed by the spatial location of the signal within the crystal. If the signal of the additive is only present in the interior of the crystal the additive would have incorporated early in the growth of the crystal. In contrast, if the signal is on the exterior of the crystal the interaction is mainly through adsorption, which prevents further growth.

The incorporation is determined using a confocal Raman set-up where multiple spectra are collected as the laser scans through the crystal. This then translates into an image that can show peaks and signals at various depths within the crystal. The brighter the pixel in the scanned image the higher the Raman signal of that particular wavenumber band to create a 'heat-map'. By plotting where that signal appears and comparing it to a signal of the COM, one can determine when and where the additive is substituting into the crystal.

For many of the additives, there was little variation from the standard COM spectrum as discussed above. This may be due to the limit of detection of the machine, as adsorption or incorporation may be at a very low concentration. Alternatively, inhibition is not occurring *via* an adsorption mechanism (highly unlikely).

Both the signals at 2500 and 2700  $\text{cm}^{-1}$  (Figure 52) are only present when TA is in the SUM; this is regardless of whether zinc ions have been added to the SUM. The hydrate signal (3500  $\text{cm}^{-1}$ ) also appears stronger than in a standard COM spectrum, which may mean that the TA is interacting with the COM and/or other SUM components.

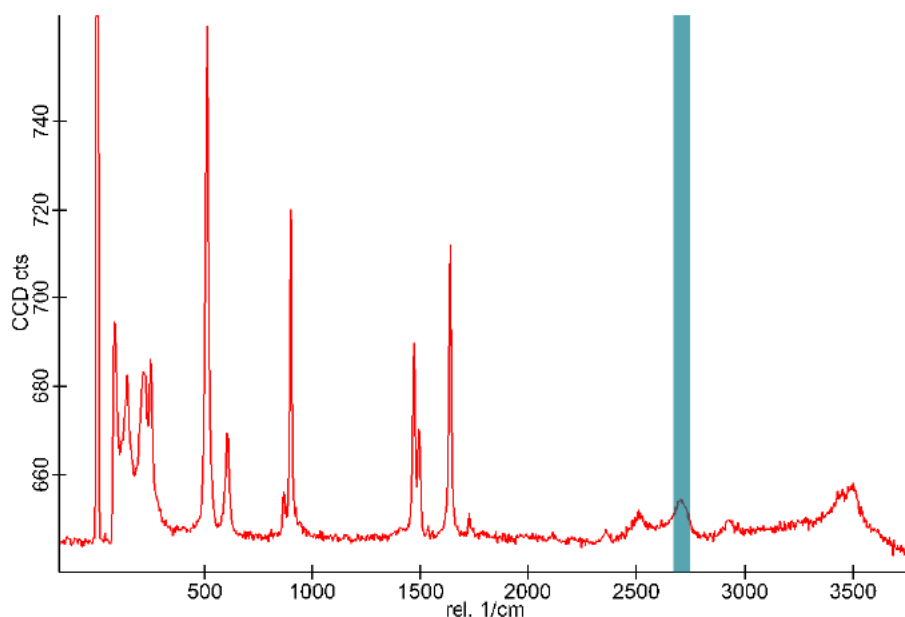


**Figure 52.** Raman spectrum from the internal signal of the tartaric acid impacted crystals

Figure 53 shows the depth analysis of the TA impacted CaOx crystal in SUM + Zn<sup>2+</sup> (similar data was collected for TA in SUM, see appendix figure 3); Figure 53 presents the ‘heat-map’ from the CaOx doublet signal at 1500 cm<sup>-1</sup>. This represents the response from the whole crystal, and Figure 53b shows where in the crystal the 2700 cm<sup>-1</sup> signal can be found. This signal is located exclusively towards the centre of the crystal, implying this interaction occurs early on in the nucleation and growth process. The 2500 and 2700 cm<sup>-1</sup> signals are also present in the adsorption data on the surface of the COM, implying a similar interaction occurring there. This means that the TA is likely interacting in the early stage of crystallisation incorporating most or all of the TA into these crystals. If this was not the case, the adsorption data suggests that the signal would appear in all areas of the crystal instead.

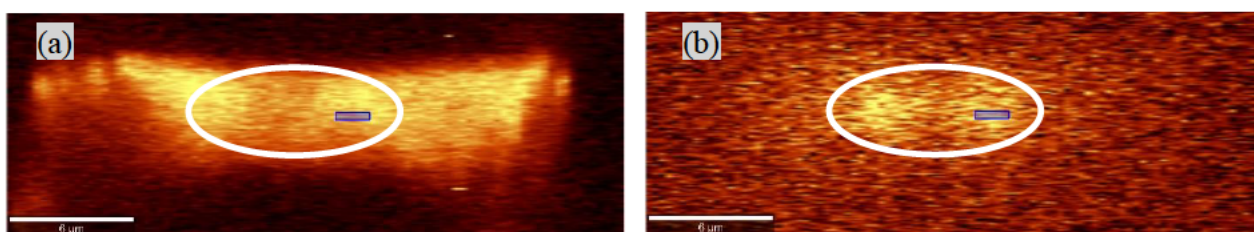


**Figure 53.** (a) CaOx signal (1500 cm<sup>-1</sup>) in the crystal with the presence of tartaric acid additive (20 mM). (b) Unknown signal (2700 cm<sup>-1</sup>) present in the crystal.

### 3.8. 2D Nucleation and Growth analysis

In this section the additives are tested to determine their impact on the rates of the  $\langle 001 \rangle$  and  $\langle 010 \rangle$  directions on the (100) face of COM through AFM (see Figure 54). This gives information on the impact these additives have on growth rates and can contribute to our understanding of the final morphology reached. This analysis also takes much longer and is more costly than other analyses, and because of the cost only the additives of greatest impact on the morphology were investigated which due to time constraints, the impact of some additives was not able to be assessed.

Generally, it is noted that slower faces become the more dominant face displayed in the morphology.



**Figure 54.** AFM images at different times ((a) followed by (b), followed by (c)) displaying the closing of etch pits and the assignment of growth directions. All images are  $5 \mu\text{m} \times 5 \mu\text{m}$

It is to be noted that the analysis was composed of measuring the closure of etch pits, that is that over time the etch pit becomes smaller due to growth and so while Figures 55 and 56 have the change in the etch pit widths, these give the negative relationship to growth. It is also worth noting that the EDTA in solution actually formed larger holes due to its chelating properties (i.e. the crystal was still dissolving). While this wasn't the intended response, it can still give an insight into the directions that the additive impacts the most.

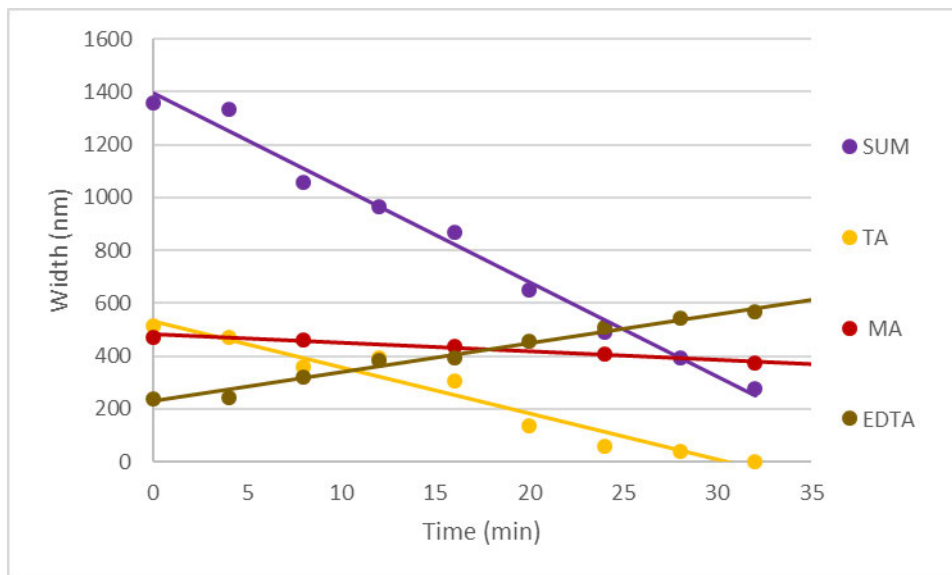


**Figure 55.** *Change in an etch pits width over time with respect to the <001> direction*

Considering the rate at which the pits close for MA, it is significantly slowed compared to the standard in both directions. This is likely the reason that in the Section 0 the morphology is closer to the pure water morphology, causing the faces to grow more slowly overall and become more dominant in the morphology. There is still a significant difference in the growth rate compared to the standard; the largest deviation from the control is that of the <001> which is why the MA SEM images display a more dominant (010) face on the crystals. Where the <010> change is much less compared to the standard. Which implies the (021) faces are less impacted by the presence of MA.

Looking at the TA there is a much greater variation in the directions of crystal growth rate. It is observed that with this additive present the <001> is slower, and thus the particle should be longer, compared to the <010>. This supports the crystals observed in the Section 0 but doesn't give enough information on the crystal growth to explain the asymmetric crystals we see form with TA. The crystals typically have more dominant (010) faces, which implies slower growth for this face.

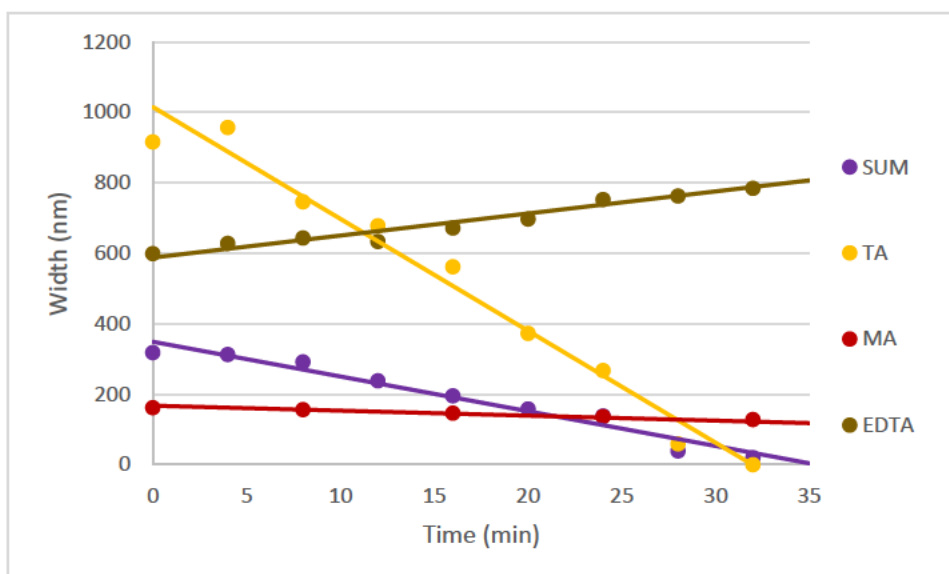


**Figure 56.** *Change in an etch pits width over time with respect to the <010> direction*

Finally, looking at EDTA, the <001> is the fastest dissolving, which is why the crystals are so wide in comparison to the standard. Although the difference between the <010> and <001> isn't significant it could be due to an interaction on the (021) face which results in those faces being so dominant with the (010). This supports the crystal formed being a lot narrower and has a significantly larger width as this direction is slowed. This means that the interaction is happening mainly on the (021) faces.

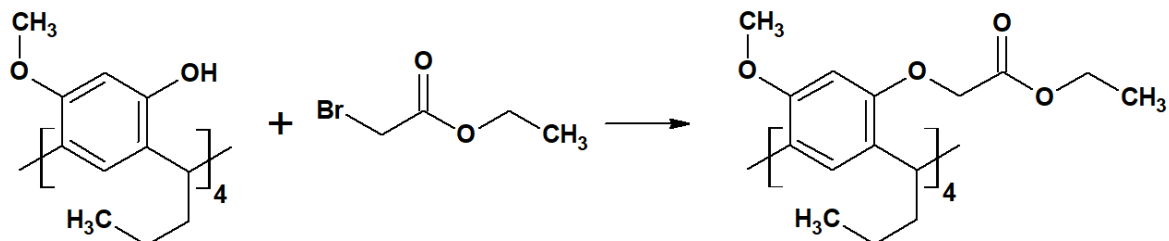
**Table 8.** *Summary of 2D nucleation rate by AFM analysis. EDTA\* caused the increasing of the etch pit width and so has a negative value*

Additive	<010> rate (nm/s)	<001> rate (nm/s)
Control	0.16	0.495
EDTA*	-0.099	-0.19
Tartaric Acid	0.57	0.31
Maleic Acid	0.023	0.055

While it can be seen that for most of the situations the <010> is the slow growing direction, TA is the exception. This further makes the TA interesting as it does not follow the trend observed by the other carboxylic additives. This is likely due to the hydroxyl on carbons 2 and 3 of TA suggesting hydrogen bonding may be important.

## 4. Synthesis Methods

### Synthesis of 1<sup>6</sup>,3<sup>6</sup>,5<sup>6</sup>,7<sup>6</sup>-tetra(ethoxycarbonylmethyleneoxy)-1<sup>4</sup>,3<sup>4</sup>,5<sup>4</sup>,7<sup>4</sup>-tetramethoxy-2,4,6,8-tetrapropylresorcin[4]arene



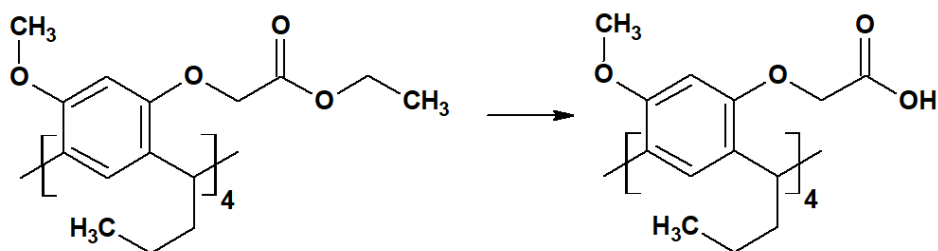
The tetrahydroxy tetramethoxyresorcin[4]arene (1.2 g, 1.68 mmol) was stirred with ethyl bromoacetate (1.5 mL, 13.5 mmol) in acetonitrile until the solid completely dissolved. Then potassium carbonate (1.8 g, 13.0 mmol) was added, forming a suspension as it stirred. This mixture was then heated to reflux for 40 hours. The solid was then filtered off and the solvent reduced under vacuum. The resulting oil was dissolved in diethyl ether (10 mL) and then washed in brine (2x20 mL). This was then dried with magnesium sulfate, filtered and final reduced under vacuum to give a white powder (1.256 g, 77%)

IR ( $\nu/\text{cm}^{-1}$ ): 2952 w (C-H), 1749 s (C=O), 1612 w (C-H aro), 1188 w (C-O).

$^1\text{H}$  NMR ( $\delta/\text{ppm}$ ,  $\text{CDCl}_3$ ): 0.92 (t, 12H,  $\text{CH}_2\text{CH}_3$ ,  $J = 7.4$  Hz), 1.28 - 1.31 (m, 12H,  $\text{OCH}_2\text{CH}_3$ ), 1.32 - 1.37 (m, 8H,  $\text{CH}_2\text{CH}_2\text{CH}$ ), 1.78 - 1.84 (m, 8H,  $\text{CH}_3\text{CH}_2\text{CH}_2$ ), 3.61 (s, 12H,  $\text{CH}_3\text{O}$ ), 4.10 - 4.16 (m, 8H,  $\text{CH}_3\text{CH}_2\text{O}$ ), 4.20 - 4.26 (m, 8H,  $\text{OCH}_2\text{C=O}$ ), 4.54 (t, 4H,  $\text{ArCHCH}_2$ ,  $J = 7.6$ ), 6.30 (s, 4H, H-Ar), 6.63 (s, 4H, H-Ar).

This matched that of the original work by M Bertata (76)

**1<sup>6</sup>,3<sup>6</sup>,5<sup>6</sup>,7<sup>6</sup>-tetra(carbonylmethyleneoxy)-1<sup>4</sup>,3<sup>4</sup>,5<sup>4</sup>,7<sup>4</sup>-tetramethoxy-2,4,6,8-tetrapropylresorcin[4]arene**



Sodium hydroxide pellets (0.15 g, 3.7 mmol) were dissolved in deionised water (4 mL), then added to tetra (ethoxycarbonylmethyleneoxy) tetramethoxyresorcin[4]arene (0.5 g, 0.47 mmol) in methanol (15 mL) and this was heated to reflux for 3 hours. The solvent was removed under vacuum and the resulting liquid was acidified with HCl and the solid which formed was then vacuum filtered to give a white powder (0.443 g, 88%).

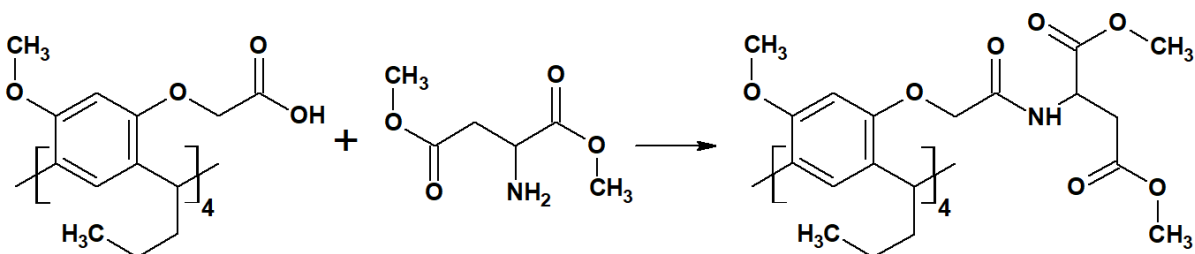
ATR-IR: ( $\nu/\text{cm}^{-1}$ ): = 3446 w (O-H), 1731 (C=O), 1609 w (C-H aro), 1176 w (C-O).

<sup>1</sup>H NMR ( $\delta/\text{ppm}$ , Acetone-*d*<sup>6</sup>): 0.93 (t, 12H, CH<sub>2</sub>CH<sub>3</sub>, *J* = 7.4 Hz), 1.32 - 1.34 (m, 8H, CH<sub>2</sub>CH<sub>2</sub>CH), 1.86 - 1.88 (m, 8H, CH<sub>3</sub>CH<sub>2</sub>CH<sub>2</sub>), 2.87 (s, 4H, OH), 3.68 (s, 12H, CH<sub>3</sub>O), 4.26 - 4.33 (m, 8H, OCH<sub>2</sub>C=O), 4.70 - 4.65 (m, ArCHCH<sub>2</sub>), 6.53 (s, 4H, H-Ar), 6.85 (s, 4H, H-Ar).

This matched that of the original work by M Bertata (76)

**1<sup>6</sup>,3<sup>6</sup>,5<sup>6</sup>,7<sup>6</sup>-tetra[(dimethyl-*L*-aspartyl)-*N*-carbonylmethyleneoxy]-1<sup>4</sup>,3<sup>4</sup>,5<sup>4</sup>,7<sup>4</sup>-tetramethoxy-2,4,6,8-**

**tetrapropylresorcin[4]arene**



The tetra(carbonylmethyleneoxy) tetramethoxy tetrapropylresorcin[4]arene (0.5 g, 0.5 mmol), aspartic acid dimethyl ester (1.65 g, 11.4 mmol) and triethylamine (1.15 mL, 8.25 mmol) was dissolved in dichloromethane (30 mL) at room temperature and then TBTU (2.81 g, 5 mmol) was added. This was stirred at room temperature for 4 hours before being quenched by HCl.

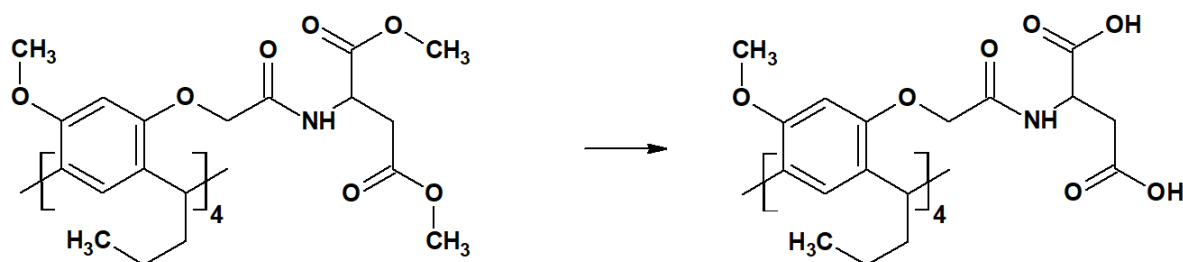
The organic layer was then extracted and washed with sodium bicarbonate (2 x 20 mL). The organic layer was then dried with magnesium sulfate, filter and finally the solvent was then reduced under vacuum to give a white powder (0.355 g, 45 %).

ATR-IR: ( $\nu/\text{cm}^{-1}$ ) = 3405 (N-H), 1731 (C=O), 1676 (NC=O), 1498 (C-O), 1193 (C-O)

$^1\text{H}$  NMR ( $\delta/\text{ppm}$ ,  $\text{CDCl}_3$ ): (Note: there is a 1:2 mixture of diastereoisomers) 0.91 – 0.95 (m, 12H,  $\text{CH}_2\text{CH}_3$ ), 1.32 - 1.34 (m, 8H,  $\text{CH}_2\text{CH}_2\text{CH}$ ), 1.82 - 1.85 (m, 8H,  $\text{CH}_3\text{CH}_2\text{CH}_2$ ), 2.23 (s, 4H, *NH*) 2.83 (s, 12H,  $\text{CH}_3\text{O}$ ), 3.63 – 3.64 (m, 8H,  $\text{OCH}_2\text{C=O}$ ), 3.70 – 3.71 m, 8H,  $\text{OCH}_2(\text{C=O})\text{NH}$ ), 4.50 - 4.57 (m, *CHNH*), 4.88 – 4.91 (m, Ar*CHCH*<sub>2</sub>), 6.30, 6.34, 6.72, 6.76 (4 s, 2 x 4H, *H-Ar*),

This matched that of the original work by M Bertata (76)

**1<sup>6</sup>,3<sup>6</sup>,5<sup>6</sup>,7<sup>6</sup>-tetra[(*L*-aspartyl)-*N*-carbonylmethyleneoxy]-1<sup>4</sup>,3<sup>4</sup>,5<sup>4</sup>,7<sup>4</sup>-tetramethoxy-2,4,6,8-tetrapropylresorcin[4]arene**



Sodium hydroxide pellets (0.1 g, 2.5 mmol) were dissolved in deionised water (4 mL), then added to tetra (dimethyl -*L*-aspartyl) tetramethoxyresorcin[4]arene (0.35 g, 0.23 mmol) in methanol (15 mL), this was heated to reflux for 3 hours. The solvent was removed under vacuum and the resulting liquid was acidified with HCl and the solid which formed was then vacuum filtered and then dried over  $\text{P}_2\text{O}_5$ . Yield was a light orange powder (0.316 g, 90%)

ATR-IR: ( $\nu/\text{cm}^{-1}$ ) = 3389 (N-H), 2931 (C-H), 1732 (C=O), 1635 (N-C=O), 1192 (C-O)

$^1\text{H}$  NMR ( $\delta/\text{ppm}$ ,  $\text{CDCl}_3$ ): (Note: there is a 1:2 mixture of diastereoisomers) 0.92 – 0.97 (m, 12H,  $\text{CH}_2\text{CH}_3$ ), 1.32 - 1.34 (m, 8H,  $\text{CH}_2\text{CH}_2\text{CH}$ ), 1.82 - 1.84 (m, 8H,  $\text{CH}_3\text{CH}_2\text{CH}_2$ ), 2.87 (s, 12H,  $\text{CH}_3\text{O}$ ), 3.63 – 3.64 (m, 8H,  $\text{OCH}_2\text{C=O}$ ), 3.70 – 3.71 m, 8H,  $\text{OCH}_2(\text{C=O})\text{NH}$ ), 4.50 - 4.57 (m, *CHNH*), 4.88 – 4.91 (m, Ar*CHCH*<sub>2</sub>), 6.30, 6.34, 6.72, 6.76 (4 s, 2 x 4H, *H-Ar*),

## 5. Overall conclusion and further work

Throughout this research several techniques have been used, these include SEM, DLS, AFM and confocal Raman spectroscopy in order to gain information on the various processes occurring during CaOx crystallization in the presence of many additives. In addition, the investigation sought to determine the effect of 16 different additives in a SUM rather than simply water, to better mimic a urinary environment, and looked at the impact of adding zinc(II) ions into the SUM. Those additives with the most interesting results with regard to nucleation and morphology then underwent additional tests to further elucidate their effect and the mechanism of interaction on calcium oxalate. This investigation looked at small molecules and functionalised scaffolds such as calix[4]arenes, and their comparison to the component amino acids, the results of which provided several prospective additives worthy of further investigation.

### 5.1. Sugars

Sugars are a class of molecules for which there has been limited research in literature and so spurred their inclusion into investigating their effects on calcium oxalate crystallisation. While the Fru and Glu additives both resulted in similar effects, having a minimal impact on the zeta potential measured or the number of particles formed (nucleation rate), of note was that Gal behaved differently, promoting the nucleation rate and resulting in particles with a more negative zeta potential. The more negative zeta potential may contribute to the greater particle count recorded as less aggregation may lead to higher final particle numbers. The addition of zinc ions resulted in particles with a slightly more negative zeta potential with the standard, Fru and Glu, but once again Gal had the opposite effect. This may be due to the positions of the hydroxyl groups and/or the stereochemistry of the molecule. Additionally, this gives further insight into the interaction that sugars have on the formation of kidney stones. In particular, the presence of these sugars may cause a higher nucleation rate or could promote the increased aggregation of COM particles, depending on which sugar is present and at what levels. When considering the size and form of particles formed from the addition of the sugars there are also some unique effects. When sugars are present there is more COD observed to be formed. Overall, the particles appear smaller when the sugar additive is present in the solution compared to the standard. However, when zinc ions are present with Fru the particles are significantly

larger than the standard. This effect may be due to the stereochemistry associated with the molecule as it is a 5 membered ring where the other structures formed will be the typically in the 6 membered ring confirmation.

## 5.2. Single Carboxylic acid containing additives

It was generally noted that when testing the nucleation rate of calcium oxalate in the presence of these additives, particle numbers were generally higher than the standard in SUM. With the addition of the zinc ions to the medium the trend of the LA and NaG changed to a more linear appearance, not reaching an observable maximum within 20 minutes. It is also of note that they were still observed to be nucleation promoters. The presence of ASA formed a zinc acetyl salicylate compound that was “gel-like” in appearance when zinc ions were present and so was not investigated further. Considering the particles formed, while there is a significant deviation in size for ASA and La, being much smaller than the standard particles, the presence of NaG resulted in particles with approximately the same size as the standard. When zinc ions were added both NaG and LA resulted in much larger particles than the standard. The zeta potential results were varied, NaG resulted in particles with the largest negative zeta potential recorded for the small molecular weight additives. This means that of all the small molecule additives the NaG results in the particle to be more negative, which in turn means there is more of a repulsion between the particles in solution. The presence of LA resulted in particles with a near zero zeta potential, which may be due to the stereochemistry of the molecule. The less negative zeta potential around the particle should make the repulsion lower. In any event, this small zeta potential means the likelihood of aggregation is higher. This means that LA is a very poor additive for the purposes of the inhibiting kidney stones. While NaG may be more useful as it inhibits aggregation but there is a promotion effect on the nucleation and an effect in the presence of zinc ions altering the size and zeta potential significantly.

## 5.3. Multi-Carboxylic Acid containing Additives

Increasing the number of carboxylic acids, and presumably the ability to interact with the calcium or zinc ions, the tested additives had varying impacts. As was expected, the EDTA had a significant impact on the size of particles formed and the nucleation rate. This was expected due to its known chelating properties. Also, when the zinc ions were present the EDTA would interact preferentially with these cations causing its inhibition effect to be lessened. Further

investigation showed that when zinc ions and EDTA were present together particles formed with a zeta potential much closer to zero, meaning that the particles are more likely to aggregate. So, while EDTA had a positive result in the SUM the effects when zinc ions are present at an equal or higher concentration are not desirable. TA is one of the most promising additives tested, as the addition of zinc ions did not significantly impact either the nucleation rate or zeta potential value. Although the addition of zinc ions did impact the morphology and size of the crystals formed, the impact on those other properties is more significant with respect to possible treatment of kidney stones. Additionally, the TA Raman signals found in the depth analysis of the crystal shows that TA is incorporated in the formed COM. While this signal has yet to be properly assigned, the presence of this signal in both the depth analysis and the adsorption test warrants further investigation. As stated before, the zeta potential was unchanged in the presence of TA + Zn<sup>2+</sup> and that result is approximately the same as the standard SUM value, meaning the propensity of particles to aggregate is not significantly different to the standard particles.

The presence of MA showed promising results for the morphology, causing particles to form that were similar to the expected morphology in pure water, with very defined faces and very slim crystals. However, when investigating the nucleation rate and zeta potential the results were not desirable, MA was found to be a mild promoter of the nucleation rate and the zeta potential of the particles formed were near zero. This effect also warrants further investigation as it appears that the MA may be preventing the influence of the citric acid in the SUM. This may be due to some interaction of the MA directly with the citric acid. It is also of note that when MA is present the growth rate of the faces is significantly slower than the standard's or the other additives tested for growth rate using AFM. Lastly there was SA, this additive did not have a major impact on the nucleation rate, though the zeta potential was found to be close to zero.

The addition of all of these additives caused significant morphological changes, with varying effects on the length and width of the particles formed. The TA and EDTA caused wide and short crystals where the other two produced very slim crystals. Some additives caused nucleation promotion while others caused nucleation inhibition. TA and EDTA were the most promising additives, although EDTA had its drawbacks with its tendency to interact with zinc ions preferentially.

## 5.4. Macromolecular additives

When investigating the large molecular weight additives, a comparison to the non-tethered amino acid at an equivalent concentration was used to determine the effect of having the amino acid on the scaffold. The isolated scaffold was not used to compare with due to its low solubility in aqueous solutions. Thus, functionalisation can be used to alter solubility and the functional group can interact with the crystal during formation/growth. The PRAA was very intriguing as its presence resulted in the exclusive formation of the COD form. This is interesting as in the standard solution the particles formed were predominately COM with some additives resulting in minor COD formation/stabilisation. The presence of PRAA does result in a higher recorded nucleation rate, but this is the nucleation of COD exclusively. Additionally, the presence of PRAA resulted in particles formed that had the highest recorded zeta potential, of -27 mV in the SUM, over double the next closest additive. When zinc ions were added, this effect is lowered but the recorded zeta potential of the particles formed was still significantly larger than the other additives. When considering the nucleation rate with zinc ions present the trend is altered, where before it reached its maximum within 5 minutes, this is slowed such that it doesn't appear to reach a maximum within the timeframe of the experiment. None of these effects are seen when the AA is present alone, which means that this effect is unique to the AA being on the resorcinarene. This effect could be due to the large number of carboxylic acids on this structure.

In the case of PCLys, there wasn't enough available of this substance for all the tests to be performed, therefore the only results obtained were morphological. The resulting morphology was of note where roughening around the edges of the crystals formed was observed and the faces were not clearly defined, even in comparison to the standard. Due to this, it will be interesting to investigate this additive further when more is available. The morphology of particles obtained when the Lys amino acid was present was not anywhere near the appearance of the PCLys, so again the effect on calcium oxalate was significant when the amino acid was tethered on these larger scaffolds.

Lastly, the CPro; this additive resulted in particles with a morphology that deviated from the standard COM appearance. The faces were still well defined, but the crystals were very thin and had a layering effect. Again, the amino acid alone did not have such a significant effect on the crystals formed, being significantly smaller but with a negligible effect on the overall appearance. Unfortunately, the presence of the CPro resulted in particles with the zeta potential much closer to zero than the PRAA and Pro. This result suggests the particles are more likely to aggregate, and this is reflected in the SEM images. This may be due to the chemistry of the

scaffold which has the amino acid functionalised to the top rim and the lower rim having a simple hydroxyl, which is a neutral component that will result in the zeta potential being closer to zero. When zinc ions are present in solution the nucleation rate is significantly lower than in the standard. When the Pro and CPro are in SUM the particle count is very close to the standard, however, when zinc(II) ions are added the particle count in the presence of Pro remains near to the standard where the particle count in the presence of CPro is much lower. For both the PRAA and CPro it was hard to obtain images of the morphology with the presence of zinc ions.

## 5.5. Further work

From this research it has become obvious that the investigation of functionalised calixarene molecules is a very interesting avenue for crystal growth modification. The amount of variation that can be observed when just investigating different amino acids is intriguing and opens up other options for functionalisation. It could be interesting to functionalise these scaffolds with small molecule additives that are already known to inhibit COM/COD. This may result in an even greater effect. There also needs to be more comparative analysis with the functional groups of the scaffold as well as completely different chemical species to be functionalised on the scaffold. Furthermore, a comparison of the effects of different scaffolds should be investigated to determine the most effective for inhibition.

Further investigation into the varying inhibition potency even though the structures of many molecules were similar, specifically MA, TA and SA, should be conducted in order to understand more fully the structure activity relationships. In addition, there are a large number of chemical functional groups that haven't been investigated, such as those containing nitrogen and aromatic compounds which can give new information about what groups will result in unique effects on the morphology or other impacts. Additionally, more tests could be performed to elucidate the mechanism of interaction further. The growth tests (AFM studies) were not performed for all of the additives of interest and as such the further use of the AFM to view the interaction the additives have on the different faces of COM would be of interest. This test could be very interesting to investigate the properties of PRAA as this resulted in only COD formation and so would be interesting to see what occurs when the PRAA is brought into contact with COM.

Also, there can be further investigation into utilising new techniques that may even further elucidate the effect that occurs between the additives and the calcium oxalate. One possible method is x-ray photoelectron spectroscopy (XPS), which might show the presence of any

organics and possibly indicate whether there is any change in bonding or interactions of the organics and metals in or on the crystal. (97) It is also of note that that the response from the adsorption tests were quite low and so further insight may be shown with thermogravimetric analysis. This will give a better detection of the adsorption of the additives onto the particles, though not showing the chemical changes.

Finally, the additives found to inhibit in some way through this research could be adapted into tests using real urine prior to toxicological, animal, and then human, tests to determine further inhibition efficiency.

## 6. References

1. Lowenstam HA, Weiner S. On biomineralization: Oxford University Press on Demand; 1989.
2. Bazylnski DA, Frankel RB. Biologically Controlled Mineralization in Prokaryotes. *Reviews in Mineralogy and Geochemistry*. 2003;54(1):217-47.
3. Sand KK, Pedersen CS, Matthiesen J, Dobberschütz S, Stipp SLS. Controlling biomineralisation with cations. *Nanoscale*. 2017;9(35):12925-33.
4. Alelign T, Petros B. Kidney Stone Disease: An Update on Current Concepts. *Adv Urol*. 2018;2018:3068365.
5. Lopez M, Hoppe B. History, epidemiology and regional diversities of urolithiasis. *Pediatr Nephrol*. 2010;25(1):49-59.
6. Tsujihata M. Mechanism of calcium oxalate renal stone formation and renal tubular cell injury. *International Journal of Urology*. 2008;15(2):115-20.
7. Alok S, Jain SK, Verma A, Kumar M, Sabharwal M. Pathophysiology of kidney, gallbladder and urinary stones treatment with herbal and allopathic medicine: A review. *Asian Pac J Trop Dis*. 2013;3(6):496-504.
8. Finkelstein VA, Goldfarb DS. Strategies for preventing calcium oxalate stones. *CMAJ*. 2006;174(10):1407-9.
9. Ziembra JB, Matlaga BR. Epidemiology and economics of nephrolithiasis. *Investig Clin Urol*. 2017;58(5):299-306.
10. Rule AD, Lieske JC, Li X, Melton LJ, 3rd, Krambeck AE, Bergstralh EJ. The ROKS nomogram for predicting a second symptomatic stone episode. *J Am Soc Nephrol*. 2014;25(12):2878-86.
11. Uribarri J, Oh MS, Carroll HJ. The First Kidney Stone. *Annals of Internal Medicine*. 1989;111(12):1006-9.
12. Sutherland JW, Parks JH, Coe FL. Recurrence after a single renal stone in a community practice. *Miner Electrolyte Metab*. 1985;11(4):267-9.
13. Johnson CM, Wilson DM, O'Fallon WM, Malek RS, Kurland LT. Renal stone epidemiology: a 25-year study in Rochester, Minnesota. *Kidney Int*. 1979;16(5):624-31.
14. Edvardsson VO, Indridason OS, Haraldsson G, Kjartansson O, Palsson R. Temporal trends in the incidence of kidney stone disease. *Kidney Int*. 2013;83(1):146-52.
15. Gutman AB, Yü Ta-F. Uric acid nephrolithiasis. *The American Journal of Medicine*. 1968;45(5):756-79.
16. Prien EL, Prien EL. Composition and structure of urinary stone. *The American Journal of Medicine*. 1968;45(5):654-72.
17. Boyce WH, Garvey FK. The amount and nature of the organic matrix in urinary calculi: a review. *J Urol*. 1956;76(3):213-27.
18. Howard JE, Thomas WC. Some Observations on Rachitic Rat Cartilage of Probable Significance in the Etiology of Renal Calculi. *Trans Am Clin Climatol Assoc*. 1959;70:94-102.
19. Ryall RL, Grover PK, Marshall VR. Urate and Calcium Stones &#x2014; Picking Up a Drop of Mercury With One's Fingers? *American Journal of Kidney Diseases*. 1991;17(4):426-30.
20. Moe OW. Kidney stones: pathophysiology and medical management. *The Lancet*. 2006;367(9507):333-44.
21. Le Dudal M, Huguet L, Perez J, Vandermeersch S, Boudierlique E, Tang E, et al. Stiripentol protects against calcium oxalate nephrolithiasis and ethylene glycol poisoning. *The Journal of Clinical Investigation*. 2019;129(6):2571-7.

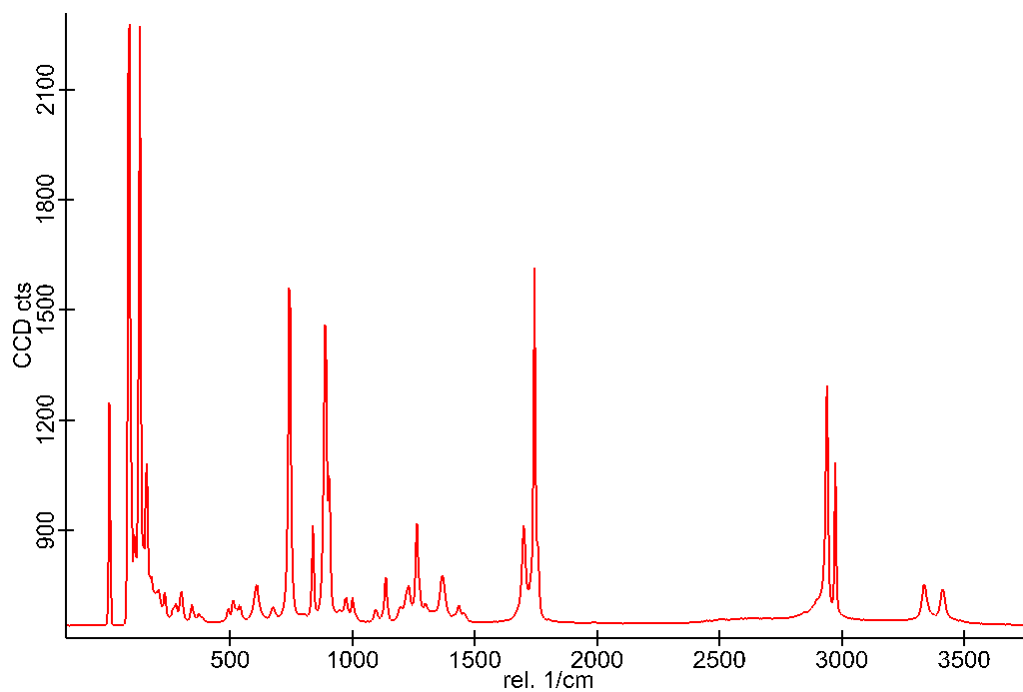
22. Rendina D, Mossetti G, De Filippo G, Benvenuto D, Vivona CL, Imbroinise A, et al. Association between metabolic syndrome and nephrolithiasis in an inpatient population in southern Italy: role of gender, hypertension and abdominal obesity. *Nephrology Dialysis Transplantation*. 2008;24(3):900-6.
23. Gorbachinsky I, Akpinar H, Assimos DG. Metabolic syndrome and urologic diseases. *Rev Urol*. 2010;12(4):e157-e80.
24. Amin R, Asplin J, Jung D, Bashir M, Alshaikh A, Ratakonda S, et al. Reduced active transcellular intestinal oxalate secretion contributes to the pathogenesis of obesity-associated hyperoxaluria. *Kidney international*. 2018;93(5):1098-107.
25. Sofia HN, Manickavasakam.K, Walter TM. PREVALENCE AND RISK FACTORS OF KIDNEY STONE. *Global journal for Research Analysis*. 2016;volume 5:page 183-7.
26. Soucie JM, Coates RJ, McClellan W, Austin H, Thun M. Relation between geographic variability in kidney stones prevalence and risk factors for stones. *Am J Epidemiol*. 1996;143(5):487-95.
27. Nimmannit S, Malasit P, Susaengrat W, Ong-Aj-Yooth S, Vasuvattakul S, Pidetcha P, et al. Prevalence of Endemic Distal Renal Tubular Acidosis and Renal Stone in the Northeast of Thailand. *Nephron*. 1996;72(4):604-10.
28. Soucie JM, Coates RJ, McClellan W, Austin H, Thun M. Relation between Geographic Variability in Kidney Stones Prevalence and Risk Factors for Stones. *American Journal of Epidemiology*. 1996;143(5):487-95.
29. Tefekli A, Cezayirli F. The history of urinary stones: in parallel with civilization. *ScientificWorldJournal*. 2013;2013:423964-.
30. Miller NL, Lingeman JE. Management of kidney stones. *BMJ*. 2007;334(7591):468-72.
31. Rubin JI, Arger PH, Pollack HM, Banner MP, Coleman BG, Mintz MC, et al. Kidney changes after extracorporeal shock wave lithotripsy: CT evaluation. *Radiology*. 1987;162(1):21-4.
32. Pearle Margaret S, Calhoun Elizabeth A, Curhan Gary C, null n. UROLOGIC DISEASES IN AMERICA PROJECT: UROLITHIASIS. *Journal of Urology*. 2005;173(3):848-57.
33. Antonelli JA, Maalouf NM, Pearle MS, Lotan Y. Use of the National Health and Nutrition Examination Survey to Calculate the Impact of Obesity and Diabetes on Cost and Prevalence of Urolithiasis in 2030. *European Urology*. 2014;66(4):724-9.
34. Hodgkinson A, Nordin BE. Physical chemistry of calcium stone formation. *Biochem J*. 1971;122(1):5P-6P.
35. Brar T, France P, Smirniotis PG. Heterogeneous versus homogeneous nucleation and growth of zeolite A. *The Journal of Physical Chemistry B*. 2001;105(23):5383-90.
36. Gibbs JW. On the equilibrium of heterogeneous substances. *American Journal of Science*. 1878(96):441-58.
37. Meyer JL, Thomas WC. Trace Metal-Citric Acid Complexes as Inhibitors of Calcification and Crystal Growth: II. Effects of Fe(III), Cr(III) and Al(III) Complexes on Calcium Oxalate Crystal Growth. *The Journal of Urology*. 1982;128(6):1376-8.
38. Evan AP, Coe FL, Lingeman JE, Shao Y, Sommer AJ, Bledsoe SB, et al. Mechanism of Formation of Human Calcium Oxalate Renal Stones on Randall's Plaque. *The Anatomical Record*. 2007;290(10):1315-23.
39. Brečević L, Škrtić D, Garside J. Transformation of calcium oxalate hydrates. *Journal of Crystal Growth*. 1986;74(2):399-408.
40. Yoreo J, Vekilov P. Principles of Crystal Nucleation and Growth. *Reviews in Mineralogy & Geochemistry - REV MINERAL GEOCHEM*. 2003;54:57-93.
41. Bramley AS, Hounslow MJ, Ryall RL. Aggregation during precipitation from solution. Kinetics for calcium oxalate monohydrate. *Chemical Engineering Science*. 1997;52(5):747-57.
42. Christmas KG, Gower LB, Khan SR, El-Shall H. Aggregation and Dispersion Characteristics of Calcium Oxalate Monohydrate: Effect of Urinary Species. *Journal of Colloid and Interface Science*. 2002;256(1):168-74.

43. Ratkalkar VN, Kleinman JG. Mechanisms of Stone Formation. *Clin Rev Bone Miner Metab.* 2011;9(3-4):187-97.
44. Martin X, Smith LH, Werness PG. Calcium oxalate dihydrate formation in urine. *Kidney Int.* 1984;25(6):948-52.
45. Fleming DE, Van Bronswijk W, Ryall RL. A comparative study of the adsorption of amino acids on to calcium minerals found in renal calculi. *Clinical Science.* 2001;101(2):159.
46. Fleming DE, Van Riessen A, Chauvet MC, Grover PK, Hunter B, Van Bronswijk W, et al. Intracrystalline Proteins and Urolithiasis: A Synchrotron X-ray Diffraction Study of Calcium Oxalate Monohydrate. *Journal of Bone and Mineral Research.* 2003;18(7):1282-91.
47. Sayan P, Sargut ST, Kiran B. Calcium oxalate crystallization in the presence of amino acids, proteins and carboxylic acids. *Crystal Research and Technology.* 2009;44(8):807-17.
48. Lyons Ryall R, Fleming DE, Doyle IR, Evans NA, Dean CJ, Marshall VR. Intracrystalline Proteins and the Hidden Ultrastructure of Calcium Oxalate Urinary Crystals: Implications for Kidney Stone Formation. *Journal of Structural Biology.* 2001;134(1):5-14.
49. Aggarwal KP, Narula S, Kakkar M, Tandon C. Nephrolithiasis: molecular mechanism of renal stone formation and the critical role played by modulators. *Biomed Res Int.* 2013;2013:292953-.
50. Farmanesh S, Alamani BG, Rimer JD. Identifying alkali metal inhibitors of crystal growth: a selection criterion based on ion pair hydration energy. *Chemical Communications.* 2015;51(73):13964-7.
51. Raistrick B. The influence of foreign ions on crystal growth from solution. 1. The stabilization of the supersaturation of calcium carbonate solutions by anions possessing O-P-O-P-O chains. *Discussions of the Faraday Society.* 1949;5(0):234-7.
52. Elliot MN. Scale control by threshold treatment. *Desalination.* 1970;8(2):221-36.
53. Mpelwa M, Tang S-F. State of the art of synthetic threshold scale inhibitors for mineral scaling in the petroleum industry: a review. *Petroleum Science.* 2019;16(4):830-49.
54. Cooper KG, Hanlon LG, Smart GM, Talbot RE. The threshold scale inhibition phenomenon. *Desalination.* 1979;31(1):257-66.
55. Grases F, Millán A, Conte A. Production of calcium oxalate monohydrate, dihydrate or trihydrate. *Urological Research - UROL RES.* 1990;18:17-20.
56. Tomaz'ic' B, Nancollas GH. The kinetics of dissolution of calcium oxalate hydrates. *Journal of Crystal Growth.* 1979;46(3):355-61.
57. Whewellite: Mineralienatlas - Fossilienatlas 2019 [Available from: <https://www.mineralienatlas.de/lexikon/index.php/MineralData?lang=en&language=english&mineral=Whewellite>].
58. Romero V, Akpınar H, Assimos DG. Kidney stones: a global picture of prevalence, incidence, and associated risk factors. *Rev Urol.* 2010;12(2-3):e86-e96.
59. Barker T, Boon M, Jones F. The role of zinc ions in calcium oxalate monohydrate crystallization. *Journal of Crystal Growth.* 2020;546:125777.
60. Cody AM, Cody RD. Contact and penetration twinning of calcium oxalate monohydrate (CaC<sub>2</sub>O<sub>4</sub>·H<sub>2</sub>O). *Journal of Crystal Growth.* 1987;83(4):485-98.
61. Qiu SR, Wierzbicki A, Orme CA, Cody AM, Hoyer JR, Nancollas GH, et al. Molecular modulation of calcium oxalate crystallization by osteopontin and citrate. *Proc Natl Acad Sci U S A.* 2004;101(7):1811-5.
62. Hartl W, Klapper H, Barbier B, Ensikat H, Dronskowski R, Müller P, et al. Diversity of calcium oxalate crystals in Cactaceae. *Canadian Journal of Botany.* 2007;85:501-17.
63. Duan X, Qu M, Wang J, Trevathan J, Vrtiska T, Williams JC, Jr., et al. Differentiation of calcium oxalate monohydrate and calcium oxalate dihydrate stones using quantitative morphological information from micro-computerized and clinical computerized tomography. *The Journal of urology.* 2013;189(6):2350-6.
64. Fleisch H, Bisaz S. The inhibitory effect of pyrophosphate on calcium oxalate precipitation and its relation to urolithiasis. *Experientia.* 1964;20(5):276-7.

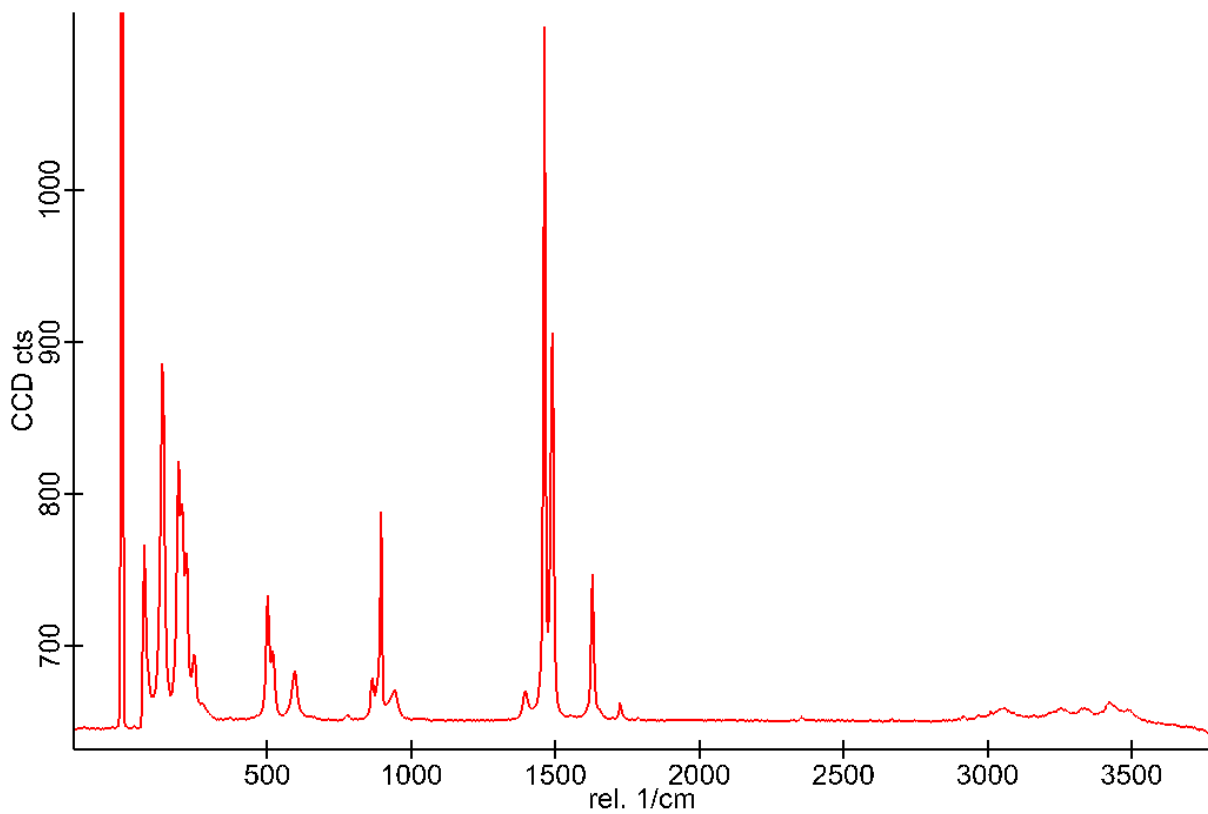
65. Dyer R, Nordin BEC. Urinary Crystals and their Relation to Stone Formation. *Nature*. 1967;215(5102):751-2.
66. Robertson WG, Peacock M, Nordin BEC. CALCIUM CRYSTALLURIA IN RECURRENT RENAL-STONE FORMERS. *The Lancet*. 1969;294(7610):21-4.
67. Letavernier E, Daudon M. Vitamin D, hypercalciuria and kidney stones. *Nutrients*. 2018;10(3):366.
68. Ferraro PM, Taylor EN, Gambaro G, Curhan GC. Vitamin D Intake and the Risk of Incident Kidney Stones. *The Journal of Urology*. 2017;197(2):405-10.
69. Singh GV, Hampson G, Thomas K, Bultitude M, Willis S. Vitamin D and kidney stones – is there an association? *BJU International*. 2019;123(5):751-2.
70. Fleisch H. Inhibitors and promoters of stone formation. *Kidney International*. 1978;13(5):361-71.
71. Barker T. Crystallisation of calcium oxalate in the presence of growth modifiers [Dissertation]: Curtin University; 2018.
72. He J, Lin R, Li H, Long H, Xuan J, He C, et al. Adsorption of EDTA onto calcium oxalate monohydrate. *RSC Advances*. 2015;5(105):86795-802.
73. Rose GA, Sulaiman S. Tamm-Horsfall Mucoproteins Promote Calcium Oxalate Crystal Formation in Urine: Quantitative Studies. *Journal of Urology*. 1982;127(1):177-9.
74. Muthukrishnan R, Gutsche CD. Calixarenes. 3. Preparation of the 2, 4-dinitrophenyl and camphorsulfonyl derivatives of the calix [8] arene from p-tert-butylphenol. *The Journal of Organic Chemistry*. 1979;44(22):3962-4.
75. D.M. Curtis A. Simple Calix[n]arenes and Calix[4]resorcinarenes as Drug Solubilizing Agents. *Journal of Nanomedicine Research*. 2015;2(3).
76. Bertata MAM. The Application of Chiral Resorcinarenes as Modifiers of Crystallization and Inhibitors of Corrosion 2018.
77. Rose GA. Biochemical aspects of urinary stones. *Proc R Soc Med*. 1977;70(8):517-20.
78. Grover PK, Ryall RL, Marshall VR. Does Tamm-Horsfall mucoprotein inhibit or promote calcium oxalate crystallization in human urine? *Clinica Chimica Acta*. 1990;190(3):223-38.
79. Goh CYJ, Franca; Mocerino, Mauro. Amino acid functionalised calixarenes: crystal growth modifiers and low molecular weight gelators: Curtin University 2012.
80. Worcester Em Fau - Nakagawa Y, Nakagawa Y Fau - Coe FL, Coe FL. Glycoprotein calcium oxalate crystal growth inhibitor in urine. (0378-0392 (Print)).
81. Brown P, Ackermann D, Finlayson B. Calcium oxalate dihydrate (weddelite) precipitation. *Journal of Crystal Growth*. 1989;98(3):285-92.
82. Sandström B. Diagnosis of Zinc Deficiency and Excess in Individuals and Populations. *Food and Nutrition Bulletin*. 2001;22(2):133-7.
83. Nečas D, Klapetek P. Gwyddion: an open-source software for SPM data analysis. *Open Physics*. 2012;10(1):181-8.
84. Bottrill O, Boon M, Barker T, Jones F. Calcium oxalate crystallization in synthetic urinary medium: The impact of a more complex solution medium, organic molecules and zinc ions. *Journal of Crystal Growth*. 2021;553:125940.
85. May PM, Muray K. Jess, a joint expert speciation system—II. The thermodynamic database. *Talanta*. 1991;38(12):1419-26.
86. Frost RL. An infrared and Raman spectroscopic study of natural zinc phosphates. *Spectrochimica Acta Part A: Molecular and Biomolecular Spectroscopy*. 2004;60(7):1439-45.
87. Weaver ML, Qiu SR, Hoyer JR, Casey WH, Nancollas GH, De Yoreo JJ. Surface aggregation of urinary proteins and aspartic Acid-rich peptides on the faces of calcium oxalate monohydrate investigated by in situ force microscopy. *Calcif Tissue Int*. 2009;84(6):462-73.
88. Piana S, Jones F, Gale JD. Assisted Desolvation as a Key Kinetic Step for Crystal Growth. *Journal of the American Chemical Society*. 2006;128(41):13568-74.
89. Piana S, Jones F, Gale JD. Aspartic acid as a crystal growth catalyst. *CrystEngComm*. 2007;9(12):1187-91.

90. Cook WJ, Bugg CE. Calcium interactions with d-glucans: crystal structure of  $\alpha,\alpha$ -Trehalose-calcium bromide monohydrate. *Carbohydrate Research*. 1973;31(2):265-75.
91. Rodríguez-Yoldi M-C, Mesonero J-E, Rodríguez-Yoldi M-J. Study of interaction between calcium and zinc and galactose intestinal transport. *Biological Trace Element Research*. 1995;50(1):1-11.
92. Antinozzi PA, Brown CM, Purich DL. Calcium oxalate monohydrate crystallization: citrate inhibition of nucleation and growth steps. *Journal of Crystal Growth*. 1992;125(1):215-22.
93. Karagöç Z, Alkan M, Kocakerim MM. Leaching kinetics of colemanite by aqueous EDTA solutions. *Metallurgical Transactions B*. 1992;23(4):409-13.
94. Sun B, Zhao FJ, Lombi E, McGrath SP. Leaching of heavy metals from contaminated soils using EDTA. *Environmental Pollution*. 2001;113(2):111-20.
95. Maurer T, Kraushaar-Czarnetzki B. Effect of electrolyte addition on the colloidal stability of aqueous zeolite sols. *Helvetica Chimica Acta*. 2001;84:2550-6.
96. Ni L, Wang L, Shao B, Wang Y, Zhang W, Jiang Y. Synthesis of Flower-like Zinc Oxalate Microspheres in Ether-water Bilayer Refluxing Systems and Their Conversion to Zinc Oxide Microspheres. *Journal of Materials Science & Technology*. 2011;27(6):563-9.
97. Bagus PS, Ilton E, Nelin CJ. Extracting Chemical Information from XPS Spectra: A Perspective. *Catalysis Letters*. 2018;148(7):1785-802.

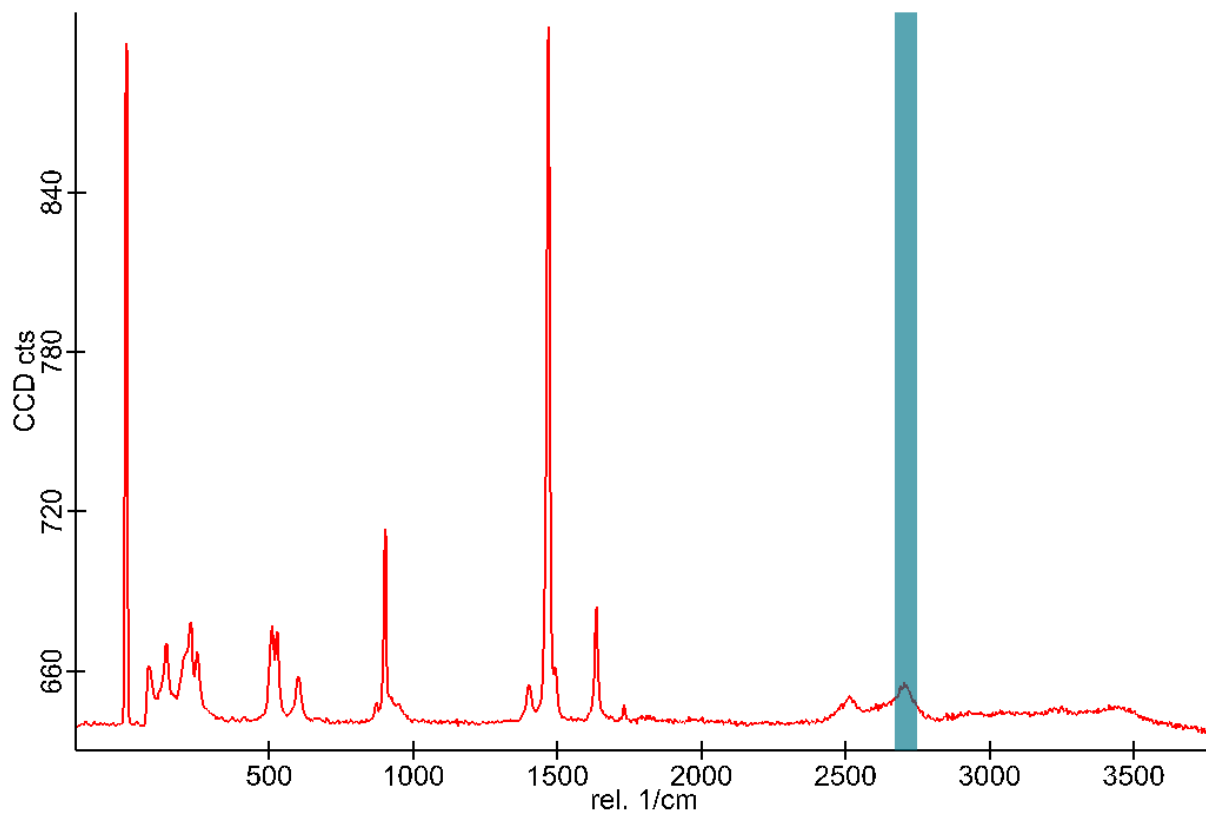
# 7. Appendix



*Appendix Figure 1. Pure tartaric acid Raman Spectrum*



**Appendix Figure 2. Raman spectrum of the control test of COM in SUM**



**Appendix Figure 3. Depth scan for the TA in pure SUM resulting in peaks in 2500 1/cm and 2700 1/cm**

*Appendix Table 1.*

*Attribution statement for reference (84)*

	Conception and Design	Acquisition of Data and Method	Data Conditioning and manipulation	Interpretation and discussion	Final approval	Total % contribution
<b>Odin Bottrill</b>	40	50	50	30	25	195 (39%)
Co Author 1 Acknowledgment: I acknowledge that these represent my contribution to the above research output Signed: [REDACTED]						
<b>Franca Jones</b>	50	15	20	30	25	140 (28%)
Co Author 1 Acknowledgment: I acknowledge that these represent my contribution to the above research output Signed: [REDACTED]						
<b>Matthew Boon</b>	0	15	20	30	25	90 (18%)
Co Author 1 Acknowledgment: I acknowledge that these represent my contribution to the above research output Signed: [REDACTED]						
<b>Timothy Barker</b>	10	20	10	10	25	75 (15%)
Co Author 1 Acknowledgment: I acknowledge that these represent my contribution to the above research output Signed: [REDACTED]						
<b>Total</b>	100	100	100	100	100	

**Appendix Table 2.**  
**involving this research**

**Attribution statement for future publication of papers**

	Conception and Design	Acquisition of data and method	Data analysis	Interpretation and discussion	Final approval	Total contribution
<b>Odin Bottrill</b>	50	80	80	60	50	64
Co Author acknowledgement:  I acknowledge that these represent my contribution to the above research output  Signed: 						
<b>Franca Jones</b>	50	20	20	40	50	36
Co Author acknowledgement:  I acknowledge that these represent my contribution to the above research output  Signed: 						
	100	100	100	100	100	100